CR-137721

Application Of Trajectory Optimization Techniques To Upper Atmosphere Sampling Flights Using The F4-C Phantom Aircraft

May 1975

(NASA-CR-137721) APPLICATION OF TRAJECTORY OPTIMIZATION TECHNIQUES TO UPPER ATMOSPHERE SAMPLING FLIGHTS USING THE F4-C PHANTOM AIRCRAFT (Aerophysics Research Corp., Bellevue, Wash.) 38 p HC $3.75 CSCL 13B G3/45

N76-10580

Unclas 03461

D. S. Hague

A. W. Merz

Prepared under Purchase Order No. A11416-B

for

NASA AMES RESEARCH CENTER

AEROPHYSICS RESEARCH CORPORATION

Box 187, Bellevue, Washington 98009

TABLE OF CONTENTS

TABLE OF CONTENTS (cont'd)

SUMMARY

Possible contamination of the upper atmosphere from the by-products of an industrial society has created the need for regular sampling of high-altitude atmospheric components. Atmospheric sampling has been carried out by NASA for a number of years using U2 aircraft. These aircraft have insufficient flight altitude capability for monitoring the growth of some potential contaminants which may be generated by aerosol container usage. This report examines the increase in sampling altitude which could be obtained if the U2 flights were supplemented by flights using an available high-performance supersonic aircraft, the Phantom F4-C.

Altitude potential of an off-the-shelf F4-C aircraft is examined in this report. It is shown that the standard F4-C has a maximum altitude capability in the region from 85000 to 95000 ft, depending on the minimum dynamic pressures deemed acceptable for adequate flight control. By using engine overspeed capability and by making use of prevailing winds in the stratosphere, it is suggested that the maximum altitude achievable by an F4-C should be in the vicinity of 95000 ft for routine flight operation by NASA personnel. This altitude is well in excess of the minimum altitudes which must be achieved for monitoring the possible growth of suspected aerosol contaminants.

INTRODUCTION

There have been recent suggestions that use of freon powered aerosol pressure containers can lead to significant modifications in upper atmospheric constituents over an extended period of time. If this happens one of the more serious consequences would be degradation in the ultra-violet radiation shielding properties of the upper atmosphere. It is thought that aerosol container atmospheric degradation can be detected by monitoring the relative density of a variety of chemical specie over a period of several years. A prime candidate for such a monitoring process is the chlorine radical $C_{\ell}0$. Figure 1 prepared by NASA's Ames Research Center provides a prediction of the anticipated density increase of this atmospheric component over the next sixty years.

Ames Research Center has now been engaged in upper atmosphere sampling for several years. Samples are collected by U2 aircraft. This vehicle has a cruise altitude capability of about 70000 feet. Predicted increases in $C_{\ell}0$ concentrations at this altitude during the next sixty years, Figure 1, are small. Therefore, if the growth of this upper atmospheric constituent is to be effectively monitored an aircraft having considerably higher altitude potential is required. Ideally this aircraft would be an existing vehicle, easily maintained, and having an altitude potential on the order of 90000 feet. Several modern military fighter aircraft have the potential for this altitude if a zoom climb maneuver is employed. The zoom climb maneuver concept is based on a kinetic potential energy exchange in which the vehicle is accelerated to high speed and then exchanges velocity for altitude. An extreme form of this maneuver is typically employed when establishing aircraft time-to-climb records. For example, the F4 Phantom fighter has an altitude potential in excess of 100000 feet if the day, location, and vehicle weight are carefully selected. The Phantom is a prime candidate for use in upper atmospheric sampling. It has

a) Wide distribution and availability, over 4000 built in several variants.

b) Demonstrated high altitude capability.

c) In certain versions, notably the RF4-C, an equipment bay large enough to contain the sampling equipment.

This report defines the altitude potential of standard F4-C aircraft using zoom climb maneuvers. Maximum altitude sensitivity to various parameters is presented. The parameter variations considered are

1) Zoom climb initial weight.

2) Minimum flight dynamic pressure.

3) Thrust improvements (available from engine overspeed or cold day operations).

4) Stratospheric wind distributions.

Trajectories are optimized by small perturbation techniques using the variational calculus procedure described in the following section. A nominal control history, Figure 2, is used to generate a nominal flight path. This path supplies the altitude history, Figure 3. The control history is then perturbed by a given amount represented by the shaded area in Figure 2. Of all control perturbations of given magnitude that producing the largest altitude gain, Δh, is employed to generate a new trajectory and the process is repeated until further altitude gains are impossible.

The aircraft and planetary representations and simplifications for this study are summarized in Figure 3. All trajectory computations in the present study were performed using the Atmospheric Trajectory Optimization Program, ATOP. This program has been developed with both NASA and USAF funding over a period of many years. The program, its past applications, and its derivatives are discussed in References 1 through 12. Program details are given in a later section. For those interested in results and not methodology the next two sections should be passed over.

FIGURE 1. EXAMPLE OF ALTITUDE DEPENDENCE - FREON EFFECTS, 1-D MODEL

(Terminate in 10 years, 30 year life in troposphere)

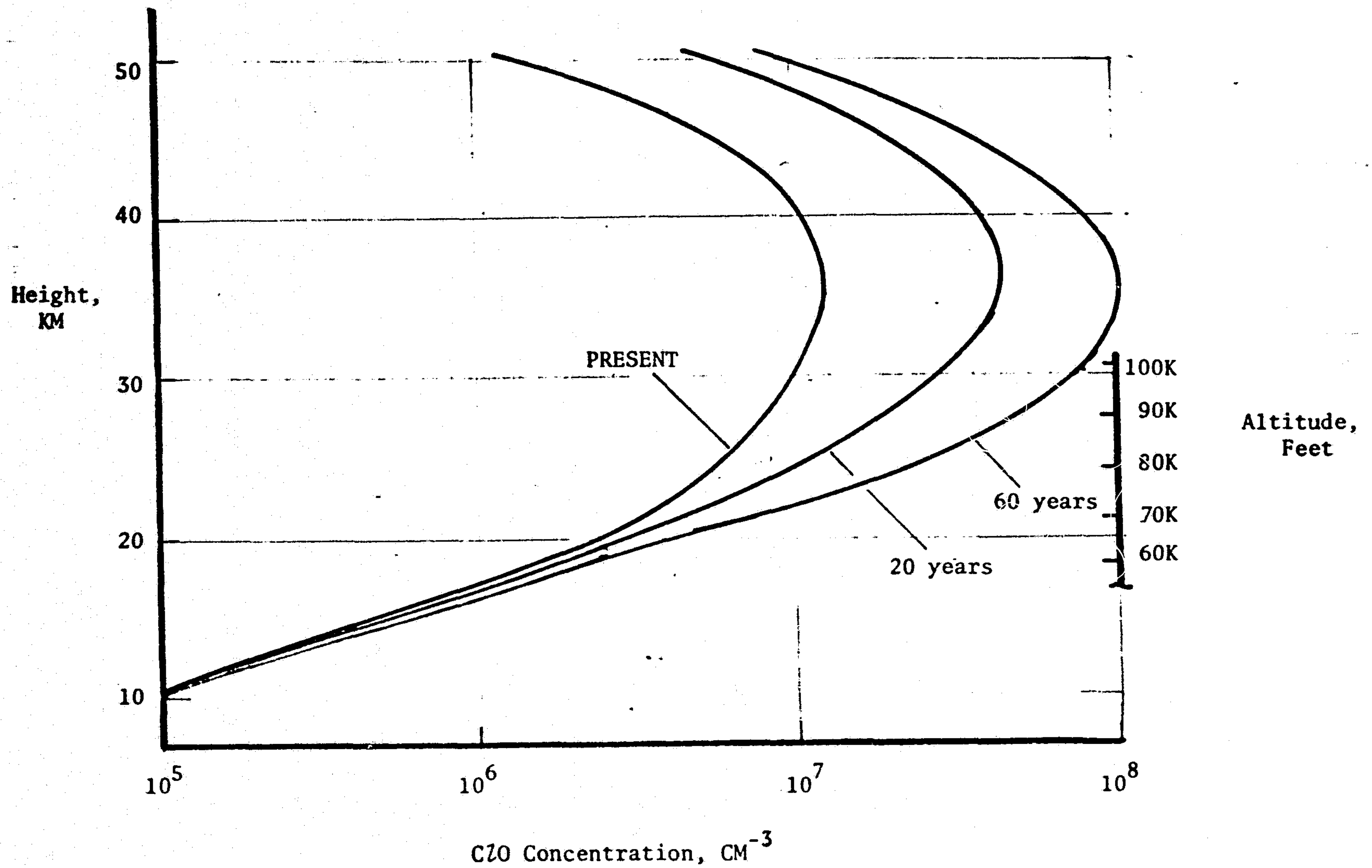

FIGURE 2.
SMALL PERTURBATION METHOD OF VARIATIONAL CALCULUS

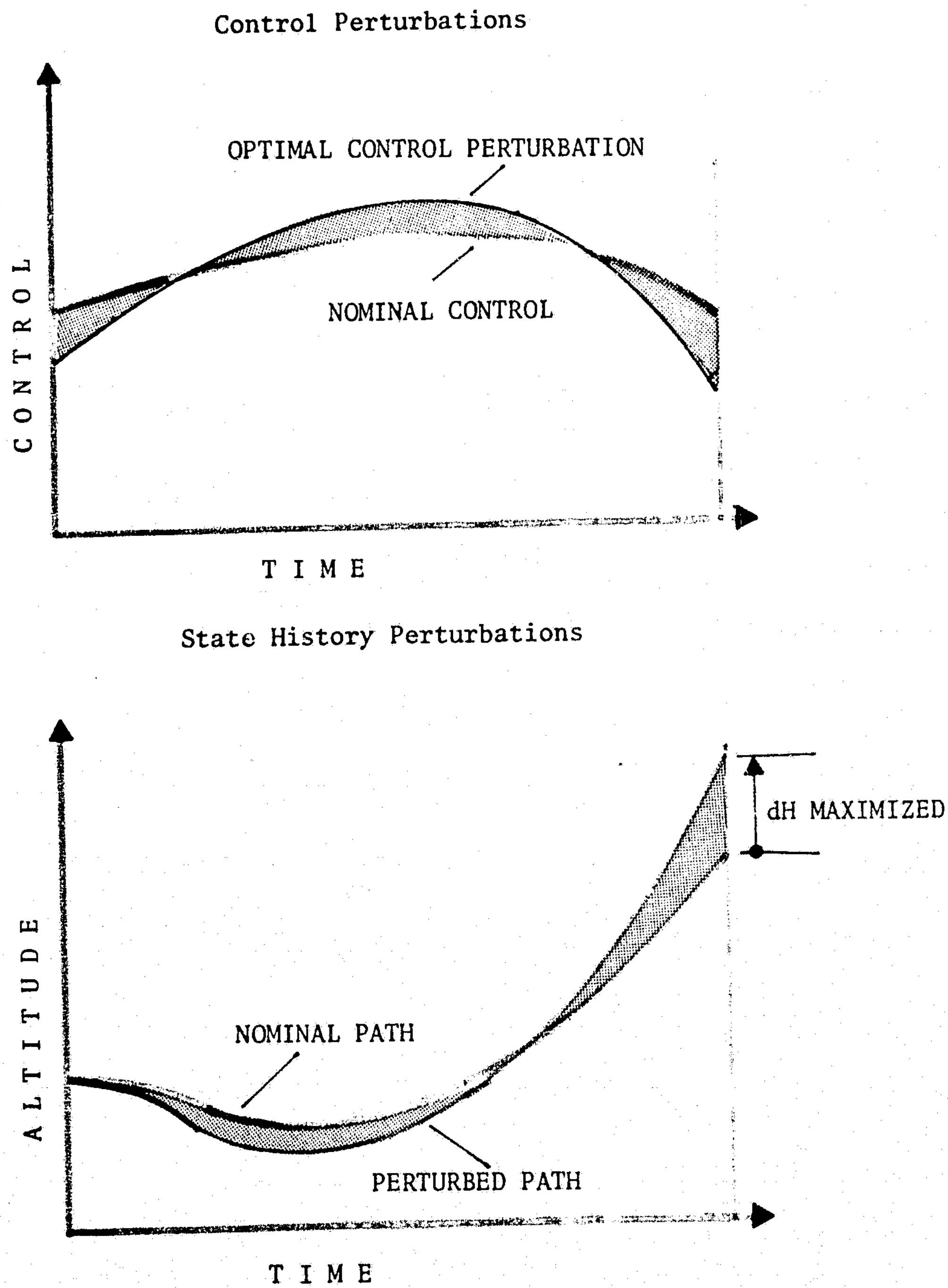

FIGURE 3. AIRCRAFT AND PLANETARY MODELS

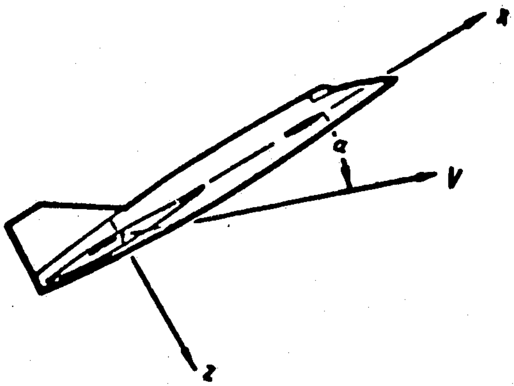

$T=T(M,h,N)$; $N=1$

$\dot{W}_F=\dot{W}_F(M,h,N)$; $N=1$

$C_L=C_L(M,h,\alpha)$

$C_D=C_D(M,h,\alpha)$

PLANAR PROBLEM- ANGLE OF ATTACK CONTROL

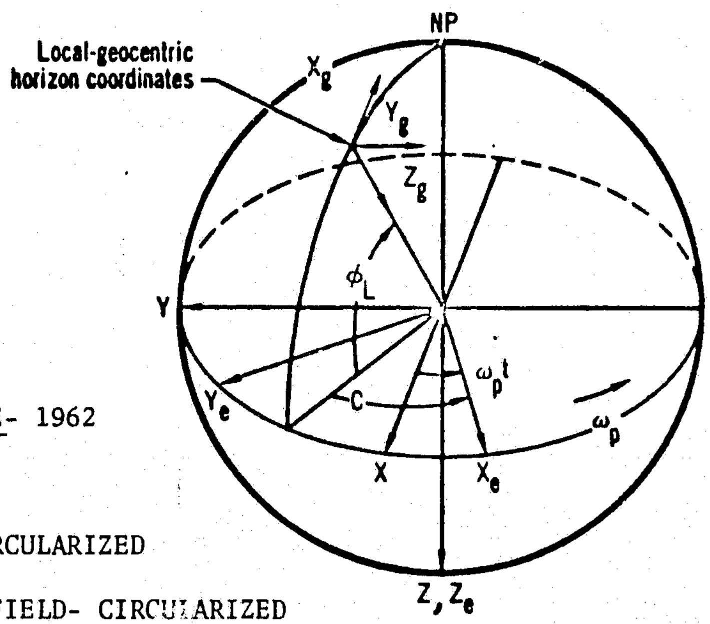

LAYERED ATMOSPHERE- 1962

WINDS- FUNCTION(h)

OBLATE PLANET- CIRCULARIZED

4 HARMONICS IN g FIELD- CIRCULARIZED

ROTATING PLANET- ROTATION ELIMINATED

THREE DEGREE OF FREEDOM- EQUATORIAL PLANE

PLANETARY CHARACTERISTICS

THE STEEPEST DESCENT METHOD

Problem Statement

Point mass motion is governed by three second order differential equations of position together with a first order differential equation governing the mass. By suitably defining additional state variables, it is possible to reduce these equations to a set of first order differential equations. Point mass motion is, therefore, governed by a set of first order differential equations. The form of these equations is

$$\left\{\dot{x}_n(t)\right\} = \left\{f\left(x_n(t),\ \alpha_m(t),\ t\right)\right\} \qquad \begin{matrix} n = 1,2 \ldots\ldots\ldots N \\ m = 1,2 \ldots\ldots\ldots M \end{matrix} \tag{1}$$

That is, there are N state variables whose derivatives $\dot{x}_n(t)$ are defined by N first order differential equations involving the state variables, together with M control variables, $\alpha_m(t)$, and t, the independent variable itself.

Constraints may be imposed on a set of functions of the state variables and time at the end of the trajectory. In this case, a set of constraint functions of the form

$$\left\{\psi_p\right\} = \left\{\psi_p\left(x_n(T),\ T\right)\right\} = 0 \qquad p = 1,2 \ldots\ldots\ldots P \tag{2}$$

can be constructed which the final trajectory must satisfy. Any one of the constraints may be used as a cut-off function which, when satisfied, will terminate a particular trajectory. The cut-off function can, therefore, be written in the form

$$\Omega = \Omega\left(x_n(T),\ T\right) = 0 \tag{3}$$

and determines the trajectory termination time T. In all, then, when the cut-off function is included, there are (P + 1) end constraints.

Finally, it may be that some other function of the state variables and time at the end of the trajectory is to be optimized. Hence, a pay-off function

$$\phi = \phi\left(x_n(T),\ T\right) \tag{4}$$

which is to be maximized or minimized, can be constructed.

Now, suppose that a nominal trajectory is available. The requirements of this trajectory are modest; it must satisfy the cut-off condition, Equation (3), but it need not optimize the pay-off function or satisfy the constraint equations. To generate this nominal trajectory by integrating Equations (1), the vehicle characteristics, the initial state variable values, and a nominal control variable history must be known. Once this nominal trajectory is available, the steepest descent process can be applied. To do this, the trajectory showing the greatest improvement in the pay-off function, while at the same time eliminating a given amount of the end point errors as measured by Equations (2) for a given size of control variable perturbation, is obtained by application of the Variational Calculus.

Equations (2) provide an end point error measure, for they will only be satisfied if the end points have been achieved. Therefore, any non-zero ψ_p represents an end point error which must be corrected. A convenient measure of the control variable perturbation can be defined by the scalar quantity,

$$DP^2 = \int_{t_0}^{T} \left\lfloor \delta\alpha(t) \right\rfloor \left[W(t) \right] \left\{ \delta\alpha(t) \right\} dt \tag{5}$$

where W is any arbitrary symmetric matrix. In the case where all control variables have a similar ability to affect the trajectory, W is taken equal to the unit matrix, and DP^2 becomes the integrated square of the control variable perturbations $\delta\alpha(t)$. It might be noted that if Equation 5 is to have meaning, it is essential that all control variables have the same dimensions. To meet this condition, the control variables can be expressed in non-dimensional form.

The constraint on control variable perturbation size represented by Equation (5) is an essential element of the steepest descent process; for the optimum perturbation will be found by local linearization of the non-linear trajectory equations about the nominal path. To insure validity of the linearized approximation, the analysis must be limited to small control variable perturbations by means of Equation (5) which provides an integral measure of the local perturbation magnitudes.

Single Stage Analysis

The steepest descent process has been outlined above. To implement this method, an analysis of all perturbations about the nominal trajectory must be undertaken. In the present report, all perturbations will be linearized; only first order perturbations in the control and state variables will be considered. The objective of the linearized analysis is

determination of the optimum control variable perturbation in the sense discussed in the previous section.

Denoting variables on the nominal trajectory by a bar

$$\left\{\alpha_m(t)\right\} \text{nominal} = \left\{\bar{\alpha}_m(t)\right\} \tag{6}$$

and

$$\left\{x_n(t)\right\} \text{nominal} = \left\{\bar{x}_n(t)\right\} \tag{7}$$

where there are M control variables and N state variables.

Now consider a small perturbation to the control variable history, $\delta\alpha(t)$; this in turn will cause a small perturbation in the state variable history, $\delta x(t)$. The new values of the variables become

$$\left\{\alpha(t)\right\} = \left\{\bar{\alpha}(t)\right\} + \left\{\delta\alpha(t)\right\} \tag{8}$$

and

$$\left\{x(t)\right\} = \left\{\bar{x}(t)\right\} + \left\{\delta x(t)\right\} \tag{9}$$

The nominal state variable and perturbed state variable histories can also be written as

$$\left\{\bar{x}(t)\right\} = \left\{x(t_o)\right\} + \int_{t_o}^{t} \left\{f\left(\bar{x}(t), \bar{\alpha}(t), t\right)\right\} dt \tag{10}$$

$$\left\{x(t)\right\} = \left\{x(t_o)\right\} + \int_{t_o}^{t} \left\{f\left(\bar{x} + \delta x, \bar{\alpha} + \delta\alpha, t\right)\right\} dt \tag{11}$$

Subtracting Equation (10) from Equation (11) and using Taylor's expansion to first order,

$$\left\{x(t)\right\} - \left\{\bar{x}(t)\right\} = \int_{t_o}^{t} \left\{\frac{\partial \bar{f}}{\partial x_n} \cdot \delta x^n + \frac{\partial \bar{f}}{\partial \alpha_m} \cdot \delta\alpha^m\right\} dt = \left\{\delta x(t)\right\} \tag{12}$$

where

$$\bar{f} = f\left(\bar{x}(t), \bar{\alpha}(t), t\right) \tag{13}$$

and where the repeated index indicates a summation over all possible values. Differentiation leads to

$$\frac{d}{dt}\left\{\delta x(t)\right\} = \left\{\frac{\partial \bar{f}}{\partial x_n} \delta x^n + \frac{\partial \bar{f}}{\partial \alpha_m} \delta\alpha^m\right\} \tag{14a}$$

or in matrix form

$$\frac{d}{dt}\left\{\delta x(t)\right\} = \left[F\right]\left\{\delta x\right\} + \left[G\right]\left\{\delta\alpha\right\} \tag{14b}$$

where

$$F_{ij} = \frac{\partial \bar{f}_i}{\partial x_j} \text{ and } G_{ij} = \frac{\partial \bar{f}_i}{\partial \alpha_j} \tag{15}$$

Here the $(i,j)^{th}$ element lies in the i^{th} row and j^{th} column of the matrices; F is an N x N matrix and G is an N x M matrix.

The effect of these perturbations on pay-off, cut-off, and constraint functions must now be determined. A general method for obtaining these effects, known as the 'adjoint method,' Reference 13,is to define a new set of variables by the equations

$$\left[\dot{\lambda}(t)\right] = -\left[F(t)\right]'\left[\lambda(t)\right] \tag{16}$$

By specifying various boundary conditions on the λ, the changes in all functions of interest can be found in turn. To show this pre-multiply Equation (14) by λ' and Equation (16) by $\delta x'$, transpose the second of these equations and sum with the first giving

$$\left[\lambda\right]'\cdot\left\{\frac{d}{dt}(\delta x)\right\} + \left[\dot{\lambda}\right]'\left\{\delta x\right\} = \left[\lambda\right]'\left[F\right]\left\{\delta x\right\} + \left[\lambda\right]'\left[G\right]\left\{\delta\alpha\right\} - \left[\lambda\right]'\left[F\right]\left\{\delta x\right\} \tag{17}$$

which may be written as

$$\left\{\frac{d}{dt}(\lambda'\delta x)\right\} = \left[\lambda\right]'\left[G\right]\left\{\delta\alpha\right\} \tag{18}$$

Integrating Equation (18) over the trajectory

$$\left\{\lambda'\delta x\right\}_T - \left\{\lambda'\delta x\right\}_{t_o} = \int_{t_o}^{T}\left[\lambda\right]'\left[G\right]\left\{\delta\alpha\right\}dt \tag{19}$$

Now define three distinct sets of λ functions by applying the following boundary conditions at t = T:

$$\left\{\lambda(T)\right\} = \left\{\frac{\partial\phi}{\partial x_i}\right\}_T = \left\{\lambda_\phi(T)\right\} \tag{20a}$$

$$\left\{\lambda(T)\right\} = \left\{\frac{\partial\Omega}{\partial x_i}\right\}_T = \left\{\lambda_\Omega(T)\right\} \tag{20b}$$

$$\left[\lambda(T)\right] = \left[\frac{\partial\psi_j}{\partial x_i}\right]_T = \left[\lambda_\psi(T)\right] \tag{20c}$$

Equation (16) may now be integrated in the reverse direction (i.e., from T to t_o) to obtain the functions, $\{\lambda_\phi(t)\}$, $\{\lambda_\Omega(t)\}$, and $\{\lambda_\psi(t)\}$.

Substituting each of these functions into Equation (19) in turn and noting that

$$\lfloor \lambda_\phi(T) \rfloor \{\delta x\} = \left\lfloor \frac{\partial \phi}{\partial x} \right\rfloor \{\delta x\} = \delta\phi_{t=T} \tag{21a}$$

$$\lfloor \lambda_\Omega(T) \rfloor \{\delta x\} = \left\lfloor \frac{\partial \Omega}{\partial x} \right\rfloor \{\delta x\} = \delta\Omega_{t=T} \tag{21b}$$

$$\left[\lambda_\psi(T) \right]' \{\delta x\} = \left[\frac{\partial \psi_i}{\partial x_j} \right] \{\delta x\} = \{\delta\psi_{t=T}\} \tag{21c}$$

It follows that

$$\delta\phi_{t=T} = \int_{t_o}^{T} \lfloor \lambda_\phi \rfloor [G] \{\delta\alpha\} dt + \lfloor \lambda_\phi(t_o) \rfloor \{\delta x(t_o)\} \tag{22a}$$

$$\delta\Omega_{t=T} = \int_{t_o}^{T} \lfloor \lambda_\Omega \rfloor [G] \{\delta\alpha\} dt + \lfloor \lambda_\Omega(t_o) \rfloor \{\delta x(t_o)\} \tag{22b}$$

$$\{\delta\psi\}_{t=T} = \int_{t_o}^{T} [\lambda_\psi]' [G] \{\delta\alpha\} dt + [\lambda_\psi(t_o)]' \{\delta x(t_o)\} \tag{22c}$$

Now, Equations (22) give the changes in pay-off function, cut-off function and constraint functions at the terminal time of the nominal trajectory; however, on the perturbed trajectory, the cut-off will usually occur at some perturbed time, T + ΔT. In this case, the total change in the above quantities becomes

$$d\phi = \int_{t_o}^{T} \lfloor \lambda_\phi \rfloor [G] \{\delta\alpha\} dt + \lfloor \lambda_\phi(t_o) \rfloor \{\delta x(t_o)\} + \dot{\phi}(T)\,\Delta T \tag{23a}$$

$$d\Omega = \int_{t_o}^{T} \lfloor \lambda_\Omega \rfloor [G] \{\delta\alpha\} dt + \lfloor \lambda_\Omega(t_o) \rfloor \{\delta x(t_o)\} + \dot{\Omega}(T)\,\Delta T \tag{23b}$$

$$\{d\psi\} = \int_{t_o}^{T} [\lambda_\psi]' [G] \{\delta\alpha\} dt + [\lambda_\psi(t_o)]' \{\delta x(t_o)\} + \{\dot{\psi}(T)\}\Delta T \tag{23c}$$

Equations (23) supply the change in pay-off, cut-off, and constraint functions on the perturbed trajectory.

The time perturbation in Equations (23a) and (23c) may be eliminated by noting that, by definition of the cut-off function, Equation (23b) must be zero.

$$\therefore \Delta T = -\frac{1}{\dot{\Omega}(T)}\left(\int_{t_o}^{T}\lfloor\lambda_\Omega\rfloor\left[G\right]\left\{\delta\alpha\right\}dt + \lfloor\lambda_\Omega(t_o)\rfloor\left\{\delta x(t_o)\right\}\right) \tag{24}$$

Substituting Equation (24) into Equations (23a) and (23c)

$$d\phi = \int_{t_o}^{T}\lfloor\lambda_{\phi\Omega}\rfloor\left[G\right]\left\{\delta\alpha\right\}dt + \lfloor\lambda_{\phi\Omega}(t_o)\rfloor\left\{\delta x(t_o)\right\} \tag{25a}$$

$$\left\{d\psi\right\} = \int_{t_o}^{T}\left[\lambda_{\psi\Omega}\right]'\left[G\right]\left\{\delta\alpha\right\}dt + \left[\lambda_{\psi\Omega}(t_o)\right]'\left\{\delta x(t_o)\right\} \tag{25b}$$

where

$$\left\{\lambda_{\phi\Omega}\right\} = \left\{\lambda_\phi\right\} - \frac{\dot{\phi}(T)}{\dot{\Omega}(T)}\left\{\lambda_\Omega\right\} \tag{26a}$$

$$\left[\lambda_{\psi\Omega}\right]' = \left[\lambda_\psi\right]' - \frac{\left\{\dot{\psi}(T)\right\}\lfloor\lambda_\Omega\rfloor}{\dot{\Omega}(T)} \tag{26b}$$

Equations (25) reveal the significance of the λ functions, originally defined by Equations (16) and (20). At time t_o, $\lambda_{\phi\Omega}$ gives the sensitivity of $\phi(T)$ to small perturbations in the state variables at t_o. Similarly, $\lambda_{\phi\Omega}(t)$ measures the sensitivity of $\phi(T)$ to small perturbations in the state variables at any time t. The sensitivity of the constraints $d\psi$ to small state variable perturbations at any time is likewise defined by each row of the function $\lambda_{\psi\Omega}(t)$.

A measure of the sensitivity of a trajectory to control variable perturbations can be obtained from the quantities $\lambda_\phi{}'_\Omega G$ and $\lambda_\psi{}'_\Omega G$. Consider a pulse control variable perturbation at time t', that is, $\delta(t-t')$, where δ is the Dirac delta function. With this type of control variable perturbation, it can be seen from Equations (25) that the changes in pay-off and constraint functions will be $\lambda_{\phi\Omega}(t')'G(t')$ and $\lambda_{\psi\Omega}(t')'G(t')$, respectively, for fixed initial conditions.

In order to apply the steepest-descent process, the performance function change, Equation (20a), must be maximized; subject to specified changes in the constraints, Equation (25b); and a

given size perturbation to the control variables, Equation (5). This can be achieved by constructing an augmented function in the manner of Lagrange which is to be maximized instead of $d\phi$. For the present problem, the augmented function is

$$U = \int_{t_o}^{T} \lfloor \lambda_{\phi\Omega} \rfloor [G] \{\delta\alpha\} dt + \lfloor \lambda_{\phi\Omega}(t_o) \rfloor \{\delta x(t_o)\}$$
$$+ \lfloor \nu \rfloor \left\{ \int_{t_o}^{T} [\lambda_{\psi\Omega}]' [G] \{\delta\alpha\} dt + [\lambda_{\psi\Omega}(t_o)]' \{\delta x(t_o)\} \right\}$$
$$+ \mu \int_{t_o}^{T} \lfloor \delta\alpha \rfloor [W] \{\delta\alpha\} dt \tag{27}$$

where the ν are P undetermined Lagrangian multipliers, and μ is a single undetermined Lagrangian multiplier. The objective now is to find that variation of the control variable history which will maximize U.

Consider a variation of $\delta\alpha$, that is a $\delta(\delta\alpha)$. Then, it is always possible to write any $\delta\alpha$ distribution in the form

$$\{\delta\alpha\} = \{A(t)\} k, \text{ or } \quad \lfloor \delta\alpha \rfloor = \lfloor A(t) \rfloor k \tag{28}$$

where A(t) prescribes the perturbation shape; and k, its magnitude. Now that part of Equation (27) which depends on $\delta\alpha$, the perturbation in the control variable, can be written in the form

$$\bar{U} = k \int_{t_o}^{T} \lfloor \lambda_{\phi\Omega} \rfloor [G] \{A(t)\} dt + k \lfloor \nu \rfloor \int_{t_o}^{T} [\lambda_{\psi\Omega}]' [G] \{A(t)\} dt$$
$$+ k^2 \mu \int_{t_o}^{T} \lfloor A(t) \rfloor [W] \{A(t)\} dt \tag{29}$$

So that

$$\frac{\partial \bar{U}}{\partial k} = \int_{t_o}^{T} \lfloor \lambda_{\phi\Omega} \rfloor [G] \{A(t)\} dt + \lfloor \nu \rfloor \int_{t_o}^{T} [\lambda_{\psi\Omega}]' [G] \{A(t)\} dt$$
$$+ 2k\mu \int_{t_o}^{T} \lfloor A(t) \rfloor [W] \{A(t)\} dt \tag{30}$$

or

$$\delta\bar{U} = \int_{t_o}^{T} \left(\lfloor \lambda_{\phi\Omega} \rfloor [G] \{\delta k \cdot A(t)\} + \lfloor \nu \rfloor [\lambda_{\psi\Omega}]' [G] \{\delta k \cdot A(t)\} + 2\mu \lfloor k \cdot A(t) \rfloor [W] \{\delta k \cdot A(t)\} \right) dt$$

$$= \int_{t_o}^{T} \left[\lfloor \lambda_{\phi\Omega} \rfloor [G] + \lfloor \nu \rfloor [\lambda_{\psi\Omega}]' [G] + 2\mu \lfloor \delta\alpha \rfloor [W] \right] \{\delta(\delta\alpha)\} \, dt \tag{31}$$

where it has been noted from Equation (28) that

$$\delta(\delta\alpha) = A(t)\ \delta k \tag{32}$$

Now, since Equation (31) holds for any A(t), it follows that it is a general relationship. Further, for $\bar{U}$ to be an extremal, $\delta\bar{U}$ must be zero.

If $\bar{U}$ has been maximized by means of a control variable perturbation $\delta\alpha$, $\delta\bar{U}$ must be stationary for all small perturbations to the $\delta\alpha$, that is, for all $\delta(\delta\alpha)$. The only way in which Equation (31) can be zero for all $\delta(\delta\alpha)$ is for the coefficient of $\delta(\delta\alpha)$ to be identically zero. That this last statement is true follows from considering the case where, over some finite time interval between t_o and T, the coefficient of $\delta(\delta\alpha)$ is, say, positive. If this were the case, we could choose a $\delta(\delta\alpha)$ distribution that was also positive in this same interval and zero elsewhere between t_o and T. It would follow that $\bar{U}$ was also positive, and, hence, $\bar{U}$ could not be maximum. A similar argument holds when $\delta(\delta\alpha)$ is negative over any interval in t_o to T. Hence, the coefficient of $\delta(\delta\alpha)$ must be identically zero in the whole interval $t_o \le t \le T$. This argument is essentially based on that presented by Goldstein, Reference 14. It follows that

$$\left[\lfloor \lambda_{\phi\Omega} \rfloor + \lfloor \nu \rfloor [\lambda_{\psi\Omega}]' \right] [G] = -2\mu \lfloor \delta\alpha \rfloor [W] \tag{33}$$

Transposing, noting that W is symmetric, and solving for $\delta\alpha$,

$$\left\{\delta\alpha\right\} = -\frac{1}{2\mu}\left[W\right]^{-1}\left[G\right]'\left\{\left\{\lambda_{\phi\Omega}\right\}+\left[\lambda_{\psi\Omega}\right]\left\{\nu\right\}\right\} \tag{34}$$

Substituting Equation (34) into Equation (25b)

$$\left\{d\beta\right\} = -\frac{1}{2\mu}\left\{\left\{I_{\psi\phi}\right\}+\left[I_{\psi\psi}\right]\left\{\nu\right\}\right\} \tag{35a}$$

where

$$\left\{d\beta\right\} = \left\{d\psi\right\} - \left[\lambda_{\psi\Omega}(t_o)\right]'\left\{\delta x(t_o)\right\} \tag{35b}$$

and

$$\left[I_{\psi\psi}\right] = \int_{t_o}^{T}\left[\lambda_{\psi\Omega}\right]'\left[G\right]\left[W\right]^{-1}\left[G\right]'\left[\lambda_{\psi\Omega}\right]dt \tag{36a}$$

$$\left\{I_{\psi\phi}\right\} = \int_{t_o}^{T}\left[\lambda_{\psi\Omega}\right]'\left[G\right]\left[W\right]^{-1}\left[G\right]'\left\{\lambda_{\phi\Omega}\right\}dt \tag{36b}$$

For subsequent use define the integral

$$I_{\phi\phi} = \int_{t_o}^{T}\left\lfloor\lambda_{\phi\Omega}\right\rfloor\left[G\right]\left[W\right]^{-1}\left[G\right]'\left\{\lambda_{\phi\Omega}\right\}dt \tag{36c}$$

The multipliers ν can be expressed in terms of the multipliers μ by Equation (35a)

$$\left\{\nu\right\} = -\left[I_{\psi\psi}\right]^{-1}\left\{2\mu\left\{d\beta\right\}+\left\{I_{\psi\phi}\right\}\right\} \tag{37}$$

Substituting Equation (34) into Equation (5)

$$DP^2 = \frac{1}{4\mu^2}\left(I_{\phi\phi} + \left\lfloor I_{\psi\phi}\right\rfloor\left\{\nu\right\} + \left\lfloor\nu\right\rfloor\left\{I_{\psi\phi}\right\} + \left\lfloor\nu\right\rfloor\left[I_{\psi\psi}\right]\left\{\nu\right\}\right) \tag{38}$$

Transposing the second term in the right hand side bracket

$$DP^2 = \frac{1}{4\mu^2}\left(I_{\phi\phi} + 2\left\lfloor\nu\right\rfloor\left\{I_{\psi\phi}\right\} + \left\lfloor\nu\right\rfloor\left[I_{\psi\psi}\right]\left\{\nu\right\}\right) \tag{39}$$

Substituting Equation (37) in Equation (39)

and noting that $\left[I_{\psi\psi}\right]^{-1}$ is symmetrical gives

$$4\mu^2 DP^2 = I_{\phi\phi} - \left\lfloor I_{\psi\phi} \right\rfloor \left[I_{\psi\psi}\right]^{-1} \left\{I_{\psi\phi}\right\} + 4\mu^2 \left\lfloor d\beta \right\rfloor \left[I_{\psi\psi}\right]^{-1} \left\{d\beta\right\} \tag{40}$$

So that

$$2\mu = \pm\sqrt{\frac{I_{\phi\phi} - \lfloor I_{\psi\phi} \rfloor \left[I_{\psi\psi}\right]^{-1} \left\{I_{\psi\phi}\right\}}{DP^2 - \lfloor d\beta \rfloor \left[I_{\psi\psi}\right]^{-1} \left\{d\beta\right\}}} \tag{41}$$

Substituting Equation (41) into Equation (37), the remaining Lagrangian multipliers are obtained in the form

$$\left\{\nu\right\} = -\left[I_{\psi\psi}\right]^{-1} \left\{\left\{I_{\psi\phi}\right\} \pm \sqrt{\frac{I_{\phi\phi} - \lfloor I_{\psi\phi} \rfloor \left[I_{\psi\psi}\right]^{-1} \left\{I_{\psi\phi}\right\}}{DP^2 - \lfloor d\beta \rfloor \left[I_{\psi\psi}\right]^{-1} \left\{d\beta\right\}}} \left\{d\beta\right\}\right\} \tag{42}$$

The optimum control perturbation is found by substituting Equations (41) and (42) back into Equation (34) and is

$$\left\{\delta\alpha\right\} = \mp \left[W\right]^{-1} \left[G\right]' \left\{\left\{\lambda_{\phi\Omega}\right\} - \left[\lambda_{\psi\Omega}\right] \left[I_{\psi\psi}\right]^{-1} \left\{I_{\psi\phi}\right\}\right\}$$

$$\times \sqrt{\frac{DP^2 - \lfloor d\beta \rfloor \left[I_{\psi\psi}\right]^{-1} \left\{d\beta\right\}}{I_{\phi\phi} - \lfloor I_{\psi\phi} \rfloor \left[I_{\psi\psi}\right]^{-1} \left\{I_{\psi\phi}\right\}}}$$

$$+ \left[W\right]^{-1} \left[G\right]' \left[\lambda_{\psi\Omega}\right] \left[I_{\psi\psi}\right]^{-1} \left\{d\beta\right\} \tag{43}$$

With this equation the steepest-descent control perturbation has been determined. Perturbing the control variables according to Equation (43) gives the optimum change in the trajectory as discussed in the section entitled, "Problem Statement," with the added effect of changes in the initial value of the state variables included through the term in $d\beta$. The appropriate sign to use on the first term of equation (43) can be determined by evaluating $d\phi$. Substituting the optimum control perturbation into Equation (25a) results in the equation shown on the following page.

$$d\phi = \pm\sqrt{\left(I_{\phi\phi} - \lfloor I_{\psi\phi} \rfloor \left[I_{\psi\psi} \right]^{-1} \left\{ I_{\psi\phi} \right\}\right)\left(DP^2 - \lfloor d\beta \rfloor \left[I_{\psi\psi} \right]^{-1} \left\{ d\beta \right\}\right)}$$
$$+ \lfloor I_{\psi\phi} \rfloor \left[I_{\psi\psi} \right]^{-1} \left\{ d\beta \right\} + \lfloor \lambda_{\phi\Omega}(t_o) \rfloor \left\{ \delta x(t_o) \right\} \tag{44}$$

As the quantity in the radical must be positive to assure the change in ϕ is real, it follows that the negative sign must be taken when minimizing the payoff function and the positive sign when maximizing the payoff function.

An Alternative Analysis Using the Independent Variable for Cut-Off

In the analysis of the previous section, it is implied that any function of the form

$$\Omega(x_n(T), T) = 0 \tag{45}$$

will suffice to terminate the trajectory. While this is true in an analytic sense, in practice any function passing through zero more than once in the cut-off region may be difficult to employ for cut-off purposes.

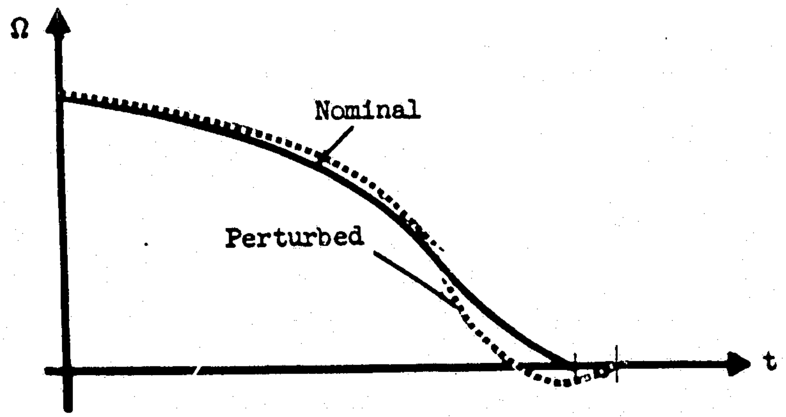

Figure 1.-- Double Valued Cut-Off Function

Figure 1 presents a nominal cut-off function history which decreases monotonically. The perturbed cut-off function history, shown dotted, behaves in a different manner in that it passes through zero twice in the cut-off region. As the trajectory must be integrated numerically, there is a danger that cut-off will occur the first time Ω passes through zero instead of the second, thereby introducing both errors in the linearized perturbations and preventing the build-up of the anticipated cut-off function history.

$$d\phi = \mp\sqrt{\left(I_{\phi\phi} - \lfloor I_{\psi\phi}\rfloor \left[I_{\psi\psi}\right]^{-1}\left\{I_{\psi\phi}\right\}\right)\left(DP^2 - \lfloor d\beta\rfloor\left[I_{\psi\psi}\right]^{-1}\left\{d\beta\right\}\right)}$$

$$+ \lfloor I_{\psi\phi}\rfloor\left[I_{\psi\psi}\right]^{-1}\left\{d\beta\right\} + \lfloor \lambda_{\phi\Omega}(t_o)\rfloor \left\{\delta x(t_o)\right\} \tag{44}$$

As the quantity in the radical must be positive to assure the change in ϕ is real, it follows that the negative sign must be taken when minimizing the payoff function and the positive sign when maximizing the payoff function.

POINT MASS TRAJECTORY EQUATIONS

Basic State Variables

Preceding portions of this report derived a successive approximation scheme for computation of optimum trajectories generated by a set of first order differential equations. The analysis is quite general and holds for trajectories generated by any set of first order differential equations. The object of the present section is to specialize the analysis to point mass vehicle trajectory problems. This will be accomplished when a suitable set of state variables, together with their derivatives, the control variables, and the forces associated with the control variables has been specified. First, a suitable coordinate system is selected, and Newton's Laws in this system are used to define the vehicle's motion.

Several suitable coordinate systems are available for point mass trajectory computations. The basic set of coordinates used in the present analysis is a rectangular set rotating with the earth, (X_e, Y_e, Z_e). This coordinate system is illustrated in Figure 4.

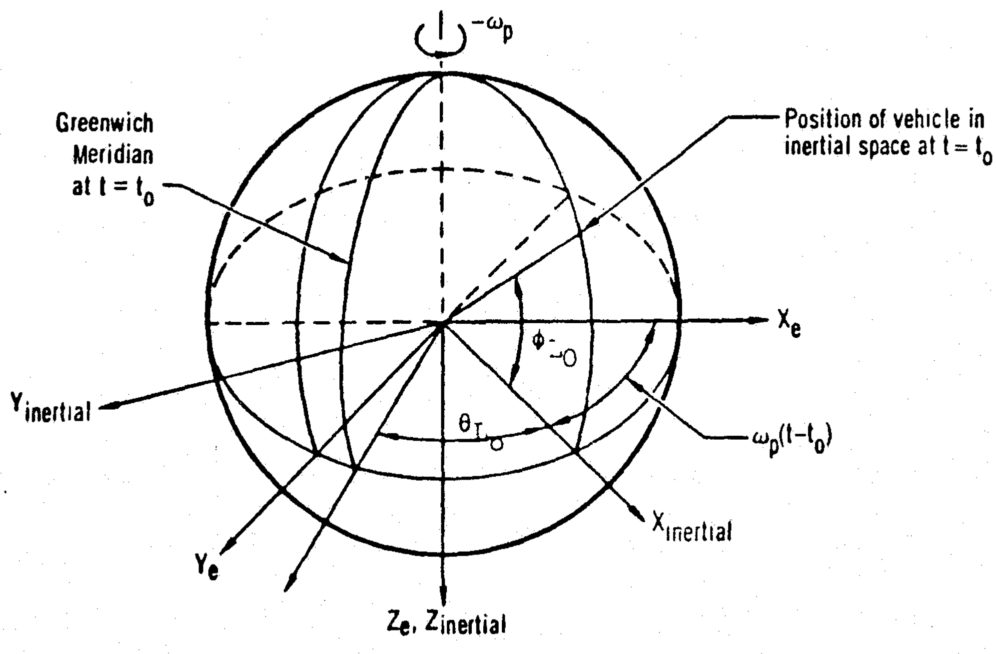

Figure 4.— Basic Coordinate System

The X_e and Y_e axes lie in the equatorial plane, the positive X_e axis being initially chosen as the intersection of this plane with the vehicle longitudinal plane at $t = t_o$. Y_e is 90° to the west of X_e, and Z_e is positive through the South Pole. Denoting the radius vector from the center of the earth to the point mass vehicle by $\mathbf{R}$, its magnitude is given by,

$$|\mathbf{R}| = \sqrt{X_e^2 + Y_e^2 + Z_e^2} \tag{45}$$

The angle between $\mathbf{R}$ and the North Pole is given by

$$\phi' = 90 - \phi_L \tag{46}$$

where ϕ_L is the latitude of the vehicle. As a result of the earth's rotation, an observer in the (X_e, Y_e, Z_e) system would detect an apparent motion of the point mass if it were at rest in inertial space. In time Δt the apparent displacement of such a vehicle would be

$$\delta R_{apparent} = R \sin \phi' . \ \omega_p \ \Delta t \tag{47}$$

to the west. In vector notation

$$\delta \mathbf{R}_{apparent} = \mathbf{R} \times \boldsymbol{\omega}_p \Delta t = -\boldsymbol{\omega}_p \times \mathbf{R} \Delta t \tag{48}$$

This apparent displacement is independent of the vehicle's motion and exists whether or not the vehicle is at rest in inertial space. In general, then, to an observer in the rotating coordinate system,

$$(\delta \mathbf{R})_e = (\delta \mathbf{R})_{inertial} + (\delta \mathbf{R})_{apparent} \tag{49}$$

$$\therefore \ (\delta \mathbf{R})_{inertial} = (\delta \mathbf{R})_e + \boldsymbol{\omega}_p \times \mathbf{R} \Delta t \tag{50}$$

Dividing Equation (50) by ΔT and taking the limit, it follows that

$$\left(\frac{d\mathbf{R}}{dt}\right)_{inertial} = \left(\frac{d\mathbf{R}}{dt}\right)_e + \boldsymbol{\omega}_p \times \mathbf{R} \tag{51}$$

or

$$\mathbf{V}_{inertial} = \mathbf{V}_e + \boldsymbol{\omega}_p \times \mathbf{R} \tag{52}$$

The vector $\mathbf{R}$ in Equation (51) could equally well be taken as any vector; the arguments of Equations (45) to (52) still hold. Therefore, in general, for any vector quantity the operational equality

$$\left(\frac{d}{dt}\right)_{inertial} = \left(\frac{d}{dt}\right)_e + \omega_p \times \qquad (53)$$

can be defined. Applying Equation (142) to Equation (141), the inertial acceleration is given by

$$\left(\frac{dV}{dt}\right)_{inertial} = \left(\left(\frac{d}{dt}\right)_e + \omega_p \times\right)\left(\left(\frac{dR}{dt}\right)_e + \omega_p \times R\right)$$

$$= \left(\frac{d^2R}{dt^2}\right)_e + \omega_p \times \left(\frac{dR}{dt}\right)_e + \omega_p \times \omega_p \times R \qquad (54)$$

Now Newton's Law applies in inertial space so that in the rotating system

$$\frac{F}{m} = \left(\frac{d^2R}{dt^2}\right)_e + 2\omega_p \times \left(\frac{dR}{dt}\right)_e + \omega_p \times \omega_p \times R \qquad (55)$$

Here $\mathbf{F}$ is the total force acting on the vehicle. This vector equation can be expressed in component form using the relationships

$$\mathbf{R} = X_e \cdot \mathbf{i} + Y_e \cdot \mathbf{j} + Z_e \cdot \mathbf{k} \qquad (56)$$

$$\omega_p = -\omega_p \cdot \mathbf{k} \qquad (57)$$

$$\mathbf{F} = F_{x_e} \cdot \mathbf{i} + F_{y_e} \cdot \mathbf{j} + F_{z_e} \cdot \mathbf{k} \qquad (58)$$

Here $\mathbf{i}$, $\mathbf{j}$, and $\mathbf{k}$ are unit vectors aligned along the X_e, Y_e, and Z_e axes, respectively. Equating components on either side of Equation (55)

$$\frac{F_{x_e}}{m} = \ddot{X}_e + 2\omega_p\dot{Y}_e - \omega_p^2 X_e \tag{59}$$

$$\frac{F_{y_e}}{m} = \ddot{Y}_e - 2\omega_p\dot{X}_e - \omega_p^2 Y_e \tag{60}$$

$$\frac{F_{z_e}}{m} = \ddot{Z}_e \tag{61}$$

These equations are not yet in a suitable form for the steepest descent analysis to be applied, for they are not in first order form. The transformation of Equations (59) to (61) into first order form is immediately accomplished if the following quantities are defined as state variables:

$$\{x\} = \begin{Bmatrix} X_e \\ Y_e \\ Z_e \\ u_e \\ v_e \\ w_e \end{Bmatrix} \tag{62}$$

where

$$\mathbf{V_e} = \frac{d\mathbf{R_e}}{dt} = u_e.\mathbf{i} + v_e.\mathbf{j} + w_e.\mathbf{k} \tag{63}$$

With this set of state variables the following expressions for the state variable derivatives are obtained from Equations (59) to (63).

$$\dot{X}_e = u_e \tag{64}$$

$$\dot{Y}_e = v_e \tag{65}$$

$$\dot{Z}_e = w_e \tag{66}$$

$$\dot{u}_e = \frac{F_{x_e}}{m} - 2\omega_p v_e + \omega_p^2 X_e \tag{67}$$

$$\dot{v}_e = \frac{F_{y_e}}{m} + 2\omega_p u_e + \omega_p^2 Y_e \tag{68}$$

$$\dot{w}_e = \frac{F_{z_e}}{m} \tag{69}$$

These equations are in the same form as Equation (1) provided the total force is a function of the state variables, a set of control variables, and time. When the mass is variable, it too must be introduced as a state variable. Any expression for the rate of change of mass of the form

$$\dot{m} = \dot{m}\left(x_n(t),\ \alpha_m(t),\ t\right) \tag{70}$$

may be used in the analysis. The above state variables, X_e, Y_e, Z_e, u_e, v_e, w_e, and m will be referred to as the basic state variables. In certain problems it becomes necessary to specify additional state variables; these will be discussed later in this section of the report.

Control Variables

The total force acting on the vehicle has three distinct sources: first, aerodynamic force as a result of interaction between the vehicle surfaces and the planetary atmosphere; second, gravitational force as a result of vehicle and planetary mass interaction; and finally, thrust forces introduced by the vehicle propulsion system.

Before aerodynamic forces can be computed, the atmospheric properties, vehicle velocity relative to the atmosphere, and vehicle attitude must be specified. Atmospheric properties can usually be specified as a function of altitude which, in turn, is a function of the state variables X_e, Y_e, Z_e. Vehicle velocity relative to the atmosphere is also a function of the state variables, for u_e, v_e, and w_e are the vehicle velocity components in a rotating system. The first and second factors determining aerodynamic forces are, therefore, functions of the basic state variables.

The remaining factor entering into aerodynamic force determination, the vehicle attitude, is clearly not a function of the basic state variables. For, given the vehicle's position and velocity, we are still quite free to specify its angular orientation in space. The angles which determine vehicle orientation may, therefore, be utilized as control variables by which aerodynamic forces may be modulated. Any set of three independent angles could be utilized for this purpose. Convention suggests use of the vehicle angle-of-attack and angle-of-sideslip to orient the vehicle reference axis with respect to the velocity vector. Angle-of-attack, (α), is the angle between the velocity vector and the vehicle reference axis when viewed in the vehicle side elevation. That is in a rectangular coordinate system, x, y, z with x along the vehicle reference axis, positive forward, y perpendicular to the vehicle plane of

symmetry, positive to starboard, and z completing a right hand system, a view normal to the x-z plane is considered. If u, v, w are the components of the vehicle velocity with respect to the atmosphere in this body axis system

$$\alpha = \tan^{-1}\left(\frac{w}{u}\right) \tag{71}$$

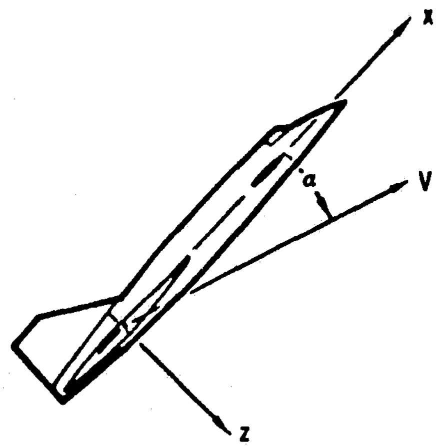

Figure 5.—Angle of Attack

Sideslip angle (β) is the angle between the velocity vector and the reference axis when looking down on the vehicle planform, that is along the z axis. In this case,

$$\beta = \tan^{-1}\left(\frac{v}{u}\right) \tag{72}$$

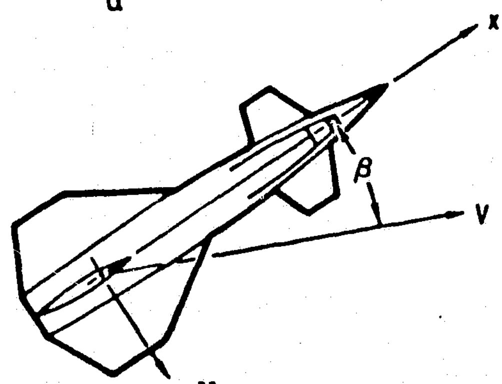

Figure 6.— Sideslip Angle

Angle of attack and sideslip completely define the attitude of the vehicle with respect to the velocity vector. The third angle required to establish vehicle orientation in space is a rotation about the velocity vector. This last angle, bank angle

(B_A), will be taken as zero when the vehicle plane of symmetry is vertical and the vehicle upright. Positive bank angle will be taken as a positive rotation about the velocity vector, as in Figure 7.

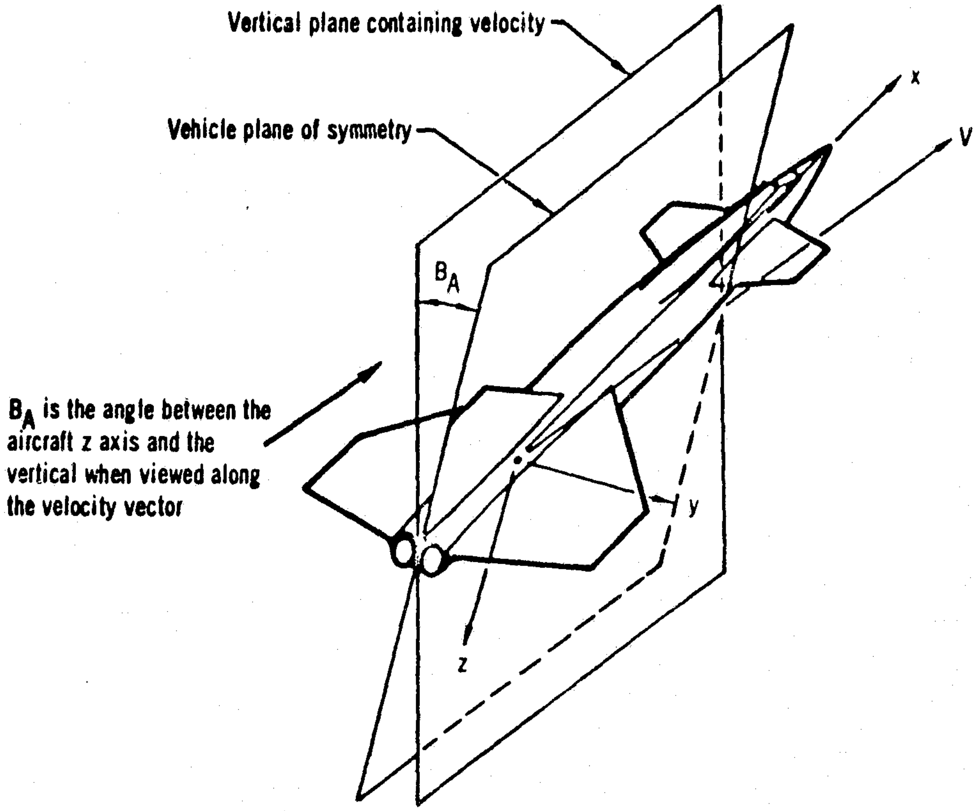

Figure 7.— Bank Angle

With the above set of angles to describe vehicle attitude, the velocity vector known and a given atmosphere, the aerodynamic forces can be completely specified.

Returning to the second source of vehicle force, gravitation, from Newton's Laws, this is merely a function of position and mass. It is, therefore, completely defined in terms of the state variables and, hence, introduces no new control variable.

The final source of vehicle force, thrust from the propulsion system, involves the atmospheric properties, either due to the atmospheric back pressure degrading the vacuum thrust or by virtue of the atmospheric fluid used in the combustion process which creates thrust. The propulsion unit efficiency may be

affected by Mach number and, hence, velocity so that thrust forces depend on the basic state variables of position and velocity in a similar manner to aerodynamic forces. If the propulsion system has a fixed orientation within the vehicle, the control variables introduced to describe aerodynamic forces suffice to describe thrust forces also. It may be, however, that the propulsion unit has a variable orientation within the vehicle. In this case, additional control variables to describe the relative position of the propulsion unit with respect to the vehicle are required. With vehicle attitude already specified by α, β and B_A, two additional angles are sufficient to orient the thrust. These may conveniently be taken as the cone angle from the reference axis, λ_T, and the inclination about the reference axis, ϕ_T. This latter angle will be measured positively about the reference axis and be zero when the thrust force is perpendicular to the port side of the vehicle plane of symmetry, as illustrated in Figure 8.

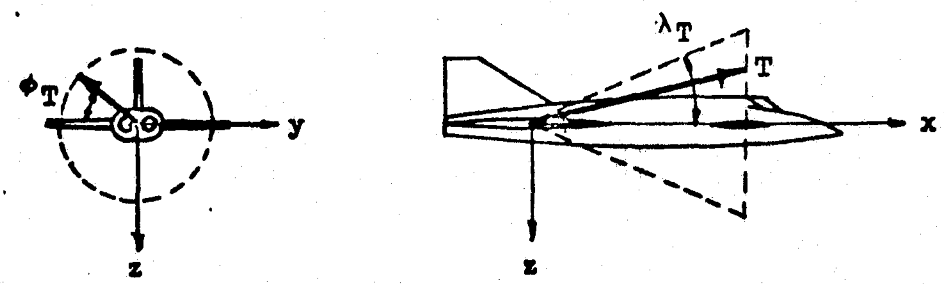

Figure 8.— Thrust Angles

One other control variable for thrust remains to be specified; this is the throttle setting, N, which serves to determine the propulsion unit power setting on variable thrust engines.

In all then, to specify the forces acting on a point mass vehicle with a single propulsion unit, six control variables, α, β, B_A, λ_T, ϕ_T, and N are required. If there is more than one independently controllable propulsion unit, additional λ_T, ϕ_T, and N must be defined.

Local geocentric-horizon coordinates.— Components of the planet-referenced acceleration are integrated to obtain the planet-referenced velocity components ($\dot{X}_e$, $\dot{Y}_e$, $\dot{Z}_e$). Vehicle position in this coordinate system is determined by integration of these velocities. Vehicle position in the planet-referenced spherical coordinate system will now be determined. The spherical coordinates are longitude, geocentric latitude, and distance from the center of the planet. Angle "C" represents the change in vehicle longitude and may be written

$$C = \theta_{L_0} - \theta_L \tag{73}$$

Angle C is related to the vehicle position by the expression

$$C = \mathrm{Tan}^{-1} \left(\frac{Y_e}{X_e}\right) \tag{74}$$

The relationships are illustrated in Figure 9.

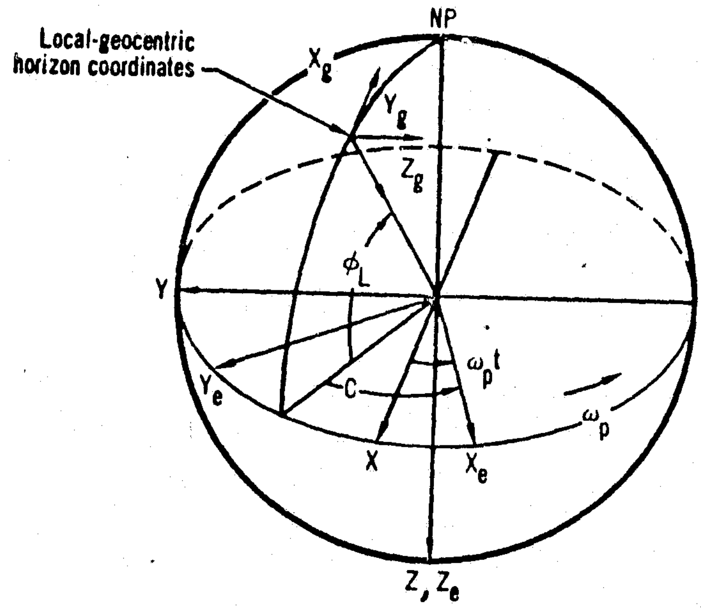

Figure 9.—Relation between Local-Geocentric, Inertial and Earth-Referenced Coordinates for Point-Mass Problems

To describe body motion relative to the planet, a local-geocentric-horizon coordinate system is employed. The Z_g-axis of this system is along a radial line passing through the body center of gravity and is positive toward the center planet. The X_g-axis of this system is normal to the Z_g-axis and is positive northward; Y_g forms a right-handed system. Figure 9 shows the relation of this coordinate system to the other systems employed.

To locate the X_g-Y_g-Z_g axes with respect to the X_e-Y_e-Z_e axes, first rotate about Z_e by an angle (180° + C) and then rotate about Y_g through the angle (90° - ϕ_L). The first rotation defines the intermediate coordinate system shown in Figure 10. The transformation is given by

$$\begin{vmatrix} \bar{1}_{X'} \\ \bar{1}_{Y_g} \\ \bar{1}_{Z_e} \end{vmatrix} = \begin{vmatrix} \text{Cos } (180^\circ + C) & \text{Sin } (180^\circ + C) & 0 \\ -\text{Sin } (180^\circ + C) & \text{Cos } (180^\circ + C) & 0 \\ 0 & 0 & 1 \end{vmatrix} \begin{vmatrix} \bar{1}_{X_e} \\ \bar{1}_{Y_e} \\ \bar{1}_{Z_e} \end{vmatrix}$$

or

$$\begin{vmatrix} \bar{1}_{X'} \\ \bar{1}_{Y_g} \\ \bar{1}_{Z_e} \end{vmatrix} = \begin{vmatrix} -\text{Cos } C & -\text{Sin } C & 0 \\ \text{Sin } C & -\text{Cos } C & 0 \\ 0 & 0 & 1 \end{vmatrix} \begin{vmatrix} \bar{1}_{X_e} \\ \bar{1}_{Y_e} \\ \bar{1}_{Z_e} \end{vmatrix} \tag{75}$$

The second rotation is shown in Figure 11. The transformation matrix for the second rotation is given by

$$\begin{vmatrix} \bar{1}_{X_g} \\ \bar{1}_{Y_g} \\ \bar{1}_{Z_g} \end{vmatrix} = \begin{vmatrix} \text{Cos } (90^\circ - \phi_L) & 0 & -\text{Sin } (90^\circ - \phi_L) \\ 0 & 1 & 0 \\ \text{Sin } (90^\circ - \phi_L) & 0 & \text{Cos } (90^\circ - \phi_L) \end{vmatrix} \begin{vmatrix} \bar{1}_{X'} \\ \bar{1}_{Y_g} \\ \bar{1}_{Z_e} \end{vmatrix}$$

or

$$\begin{vmatrix} \bar{1}_{X_g} \\ \bar{1}_{Y_g} \\ \bar{1}_{Z_g} \end{vmatrix} = \begin{vmatrix} \text{Sin } \phi_L & 0 & -\text{Cos } \phi_L \\ 0 & 1 & 0 \\ \text{Cos } \phi_L & 0 & \text{Sin } \phi_L \end{vmatrix} \begin{vmatrix} \bar{1}_{X'} \\ \bar{1}_{Y_g} \\ \bar{1}_{Z_e} \end{vmatrix} \tag{76}$$

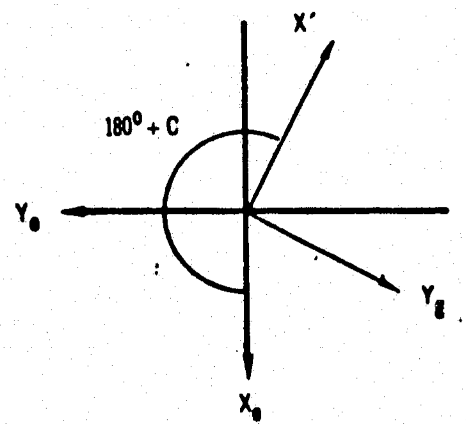

Figure 10– Intermediate Coordinate System Transformation from Earth Referenced to Local-Geocentric Coordinates

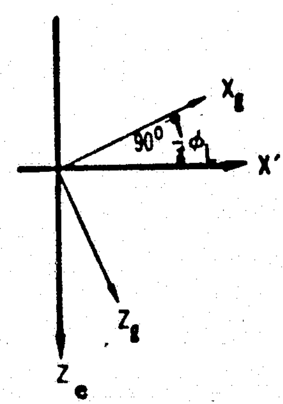

Figure 11– Final Rotation in Transformation from Earth-Referenced to Local-Geocentric Coordinates

In this analysis, a positive rotation is defined in the sense adopted for vector cross products in a right-handed system. That is, a positive rotation about the z-axis occurs when the x-axis rotates into the y-axis; positive rotation about the x-axis when y-axis rotates into the z-axis; and positive rotation about the y-axis when the z-axis rotates into the x-axis. The intermediate coordinate system (X', Y_g, Z_e) is eliminated by the method of successive rotation. The complete transformation is given by

$$\begin{vmatrix} \bar{1}_{X_g} \\ \bar{1}_{Y_g} \\ \bar{1}_{Z_g} \end{vmatrix} = \begin{vmatrix} \sin\phi_L & 0 & -\cos\phi_L \\ 0 & 1 & 0 \\ \cos\phi_L & 0 & \sin\phi_L \end{vmatrix} \begin{vmatrix} -\cos C & -\sin C & 0 \\ \sin C & -\cos C & 0 \\ 0 & 0 & 1 \end{vmatrix} \begin{vmatrix} \bar{1}_{X_e} \\ \bar{1}_{Y_e} \\ \bar{1}_{Z_e} \end{vmatrix} \qquad (77)$$

This can be reduced to the single transformation matrix

$$\begin{vmatrix} \bar{1}_{X_g} \\ \bar{1}_{Y_g} \\ \bar{1}_{Z_g} \end{vmatrix} = \begin{vmatrix} -\sin\phi_L \cos C & -\sin\phi_L \sin C & -\cos\phi_L \\ \sin C & -\cos C & 0 \\ -\cos\phi_L \cos C & -\cos\phi_L \sin C & \sin\phi_L \end{vmatrix} \begin{vmatrix} \bar{1}_{X_e} \\ \bar{1}_{Y_e} \\ \bar{1}_{Z_e} \end{vmatrix} \qquad (78)$$

which defines a direction cosine set (i, j, k) by the equation

$$\begin{vmatrix} \bar{1}_{X_g} \\ \bar{1}_{Y_g} \\ \bar{1}_{Z_g} \end{vmatrix} = \begin{vmatrix} i_1 & j_1 & k_1 \\ i_2 & j_2 & k_2 \\ i_3 & j_3 & k_3 \end{vmatrix} \begin{vmatrix} \bar{1}_{X_e} \\ \bar{1}_{Y_e} \\ \bar{1}_{Z_e} \end{vmatrix} \qquad (79)$$

Planet referenced velocity in the local-geocentric coordinate system is given by

$$\begin{vmatrix} \dot{X}_g \\ \dot{Y}_g \\ \dot{Z}_g \end{vmatrix} = \begin{vmatrix} i_1 & j_1 & k_1 \\ i_2 & j_2 & k_2 \\ i_3 & j_3 & k_3 \end{vmatrix} \begin{vmatrix} \dot{X}_e \\ \dot{Y}_e \\ \dot{Z}_e \end{vmatrix} \qquad (80)$$

and

$$V_g = \sqrt{\dot{X}^2_g + \dot{Y}^2_g + \dot{Z}^2_g}. \qquad (81)$$

Flight path angles are computed by

$$\sigma = \tan^{-1}\left(\frac{\dot{Y}_g}{\dot{X}_g}\right) \qquad (82)$$

and

$$\gamma = \sin^{-1}\left(\frac{-\dot{Z}_g}{V_g}\right) \tag{83}$$

Here σ is the heading angle and λ is the flight path angle.

Wind Axis Coordinates.— Aerodynamic and thrust forces for point-mass problems are conveniently summed in a wind-axis coordinate system, (X_A, Y_A, Z_A). Since the equations of motion are solved in (X_e, Y_e, Z_e) coordinates, the wind-axis components of force must then be resolved into this basic system.

When winds exist, defined by atmospheric velocity components along the local geocentric axes, vehicle velocity relative to the atmosphere is the vector difference of vehicle geocentric velocity and wind velocity. The wind axis system is then determined by the vehicle airspeed, V_A, and the flight path angles relative to the atmosphere λ_A and σ_A. If wind velocity is zero, $V_A = V_g$, $\lambda_A = \lambda$ and $\sigma_A = \sigma$. If there is a wind, with velocity components (X_{gw}, Y_{gw}, Z_{gw}), then

$$V_A = \sqrt{(\dot{X}_g-\dot{X}_{gw})^2 + (\dot{Y}_g-\dot{Y}_{gw})^2 + (\dot{Z}_g-\dot{Z}_{gw})^2} \tag{84}$$

$$\gamma_A = \sin^{-1}\left[-(\dot{X}_g-\dot{X}_{gw})/V_A\right] \tag{85}$$

$$\sigma_A = \tan^{-1}\left[(\dot{Y}_g-\dot{Y}_{gw})/(\dot{X}_g-\dot{X}_{gw})\right] \tag{86}$$

Forces are first resolved from wind axes to the local geocentric coordinates. The wind axes are defined relative to the local geocentric axes by three angles: heading, σ_A; flight path attitude, λ_A, defined above; together with angle, B_A.

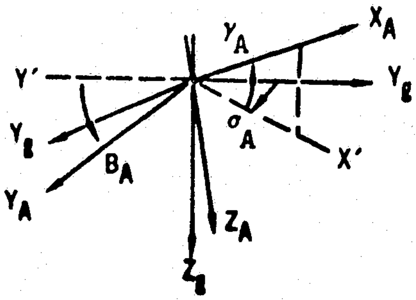

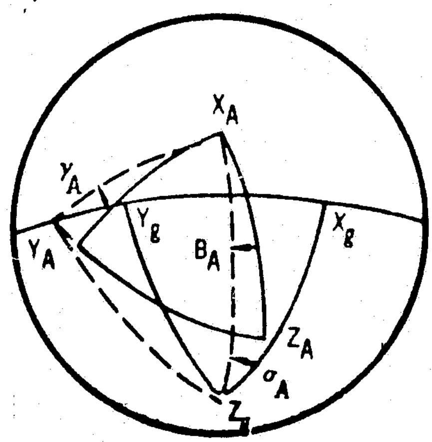

Figure 12.—
Relationship between Local-Geocentric Axes and Wind Axes

Appropriate transformations are

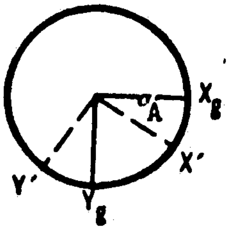

$$\begin{vmatrix} X' \\ Y' \\ Z_g \end{vmatrix} = \begin{vmatrix} \cos\sigma_A & \sin\sigma_A & 0 \\ -\sin\sigma_A & \cos\sigma_A & 0 \\ 0 & 0 & 1 \end{vmatrix} \begin{vmatrix} X_g \\ Y_g \\ Z_g \end{vmatrix} \qquad (87)$$

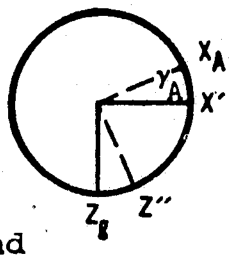

$$\begin{vmatrix} X_A \\ Y' \\ Z'' \end{vmatrix} = \begin{vmatrix} \cos\gamma_A & 0 & -\sin\gamma_A \\ 0 & 1 & 0 \\ \sin\gamma_A & 0 & \cos\gamma_A \end{vmatrix} \begin{vmatrix} X' \\ Y' \\ Z_g \end{vmatrix} \qquad (88)$$

and

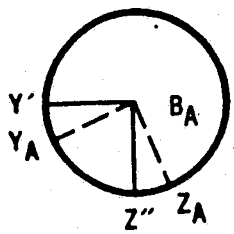

$$\begin{vmatrix} X_A \\ Y_A \\ Z_A \end{vmatrix} = \begin{vmatrix} 1 & 0 & 0 \\ 0 & \cos B_A & \sin B_A \\ 0 & -\sin B_A & \cos B_A \end{vmatrix} \begin{vmatrix} X_A \\ Y' \\ Z'' \end{vmatrix} \qquad (89)$$

The complete transformation from local geocentric horizon coordinates to wind axes then is

$$\begin{vmatrix} X_A \\ Y_A \\ Z_A \end{vmatrix} = \begin{vmatrix} \cos\gamma_A\cos\sigma_A & \cos\gamma_A\sin\sigma_A & -\sin\gamma_A \\ -\sin\sigma_A\cos B_A + \sin\gamma_A\cos\sigma_A\sin B_A & \cos\sigma_A\cos B_A + \sin\gamma_A\sin\sigma_A\sin B_A & \cos\gamma_A\sin B_A \\ \sin\sigma_A\sin B_A + \sin\gamma_A\cos\sigma_A\cos B_A & -\cos\sigma_A\sin B_A + \sin\gamma_A\sin\sigma_A\cos B_A & \cos\gamma_A\cos B_A \end{vmatrix} \begin{vmatrix} X_g \\ Y_g \\ Z_g \end{vmatrix}$$

which defines a direction cosine set

$$\begin{vmatrix} X_A \\ Y_A \\ Z_A \end{vmatrix} = \begin{vmatrix} r_1 & s_1 & t_1 \\ r_2 & s_2 & t_2 \\ r_3 & s_3 & t_3 \end{vmatrix} \begin{vmatrix} X_g \\ Y_g \\ Z_g \end{vmatrix} \qquad (90)$$

The resolution of forces from wind axes to local geocentric then becomes

$$\begin{vmatrix} F_{X_g} \\ F_{Y_g} \\ F_{Z_g} \end{vmatrix} = \begin{vmatrix} r_1 & r_2 & r_3 \\ s_1 & s_2 & s_3 \\ t_1 & t_2 & t_3 \end{vmatrix} \begin{vmatrix} F_{X_A} \\ F_{Y_A} \\ F_{Z_A} \end{vmatrix} \tag{91}$$

For the rotating-planet, the local geocentric components must be resolved into the X_e-Y_e-Z_e system. The required direction cosines are given by Equation

$$\begin{vmatrix} F_{X_e} \\ F_{Y_e} \\ F_{Z_e} \end{vmatrix} = \begin{vmatrix} i_1 & i_2 & i_3 \\ j_1 & j_2 & j_3 \\ k_1 & k_2 & k_3 \end{vmatrix} \begin{vmatrix} F_{X_g} \\ F_{Y_g} \\ F_{Z_g} \end{vmatrix} \tag{92}$$

The combined transformation from wind axes to local geocentric can be defined as a single matrix transformation

$$\begin{vmatrix} F_{X_e} \\ F_{Y_e} \\ F_{Z_e} \end{vmatrix} = \begin{vmatrix} o_1 & o_2 & o_3 \\ p_1 & p_2 & p_3 \\ q_1 & q_2 & q_3 \end{vmatrix} \begin{vmatrix} F_{X_A} \\ F_{Y_A} \\ F_{Z_A} \end{vmatrix} + \begin{vmatrix} mg_{X_e} \\ mg_{Y_e} \\ mg_{Z_e} \end{vmatrix} \tag{93}$$

Body-axis coordinates.-- Origin of this system is the vehicle center of gravity with x-axis along the geometric longitudinal axis of the body. Positive direction of the x-axis is from center of gravity to the front of the body. The y-axis is positive to starboard extending from the center of gravity in a water-line plane. The z-axis forms a right-handed orthogonal system. To permit the use of body (x, y, z) axes aerodynamic data, and to convert the body axes components of thrust to the wind axes system, a coordinate transformation must be made. The coordinate transformation shown in Figure 13 involves rotation first through angle of attack, α, then through an auxiliary angle, β'. Noting that

$$\tan \beta' = \frac{v}{u} \cos \alpha = \tan \beta \cos \alpha \tag{94}$$

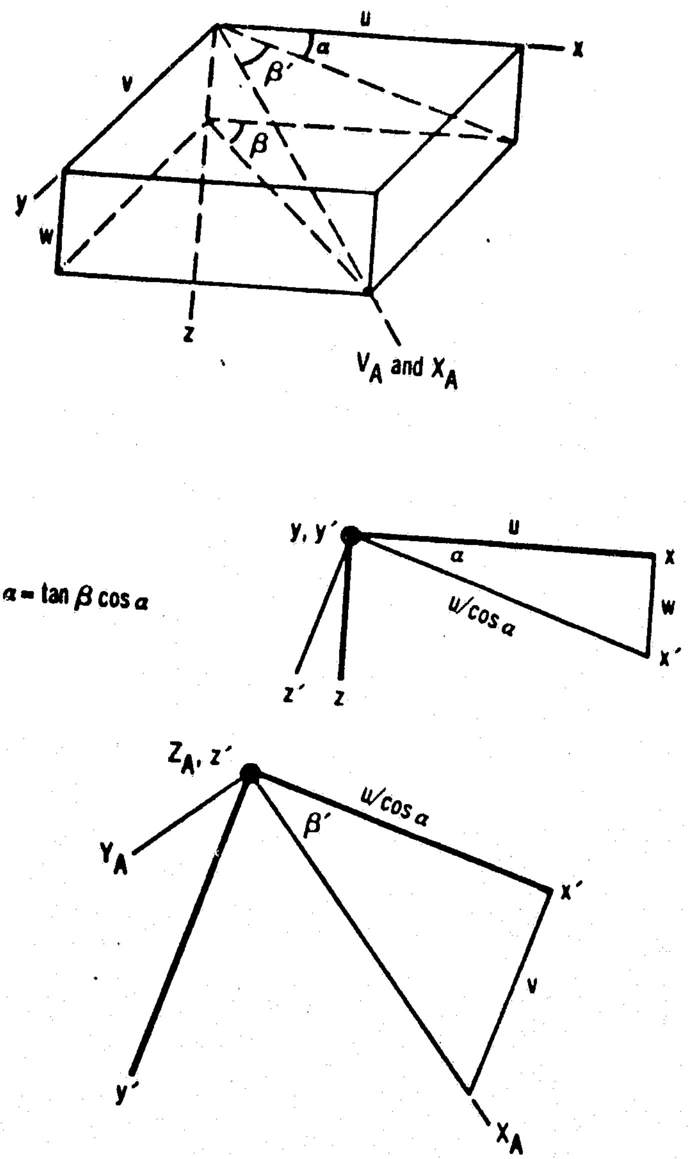

$$\tan \beta' = \frac{v}{u} \cos \alpha = \tan \beta \cos \alpha$$

Figure 13.— Relationship Between Body Axes and Wind Axes

the transformation is

$$\begin{vmatrix} x' \\ y' \\ z' \end{vmatrix} = \begin{vmatrix} \cos\alpha & 0 & \sin\alpha \\ 0 & 1 & 0 \\ -\sin\alpha & 0 & \cos\alpha \end{vmatrix} \begin{vmatrix} x \\ y \\ z \end{vmatrix}$$

$$\begin{vmatrix} X_A \\ Y_A \\ Z_A \end{vmatrix} = \begin{vmatrix} \cos\beta' & \sin\beta' & 0 \\ -\sin\beta' & \cos\beta' & 0 \\ 0 & 0 & 1 \end{vmatrix} \begin{vmatrix} x' \\ y' \\ z' \end{vmatrix}$$

$$= \begin{vmatrix} \cos\beta' \cos\alpha & \sin\beta' & \cos\beta' \sin\alpha \\ -\sin\beta' \cos\alpha & \cos\beta' & -\sin\beta' \sin\alpha \\ -\sin\alpha & 0 & \cos\alpha \end{vmatrix} \begin{vmatrix} x \\ y \\ z \end{vmatrix} \tag{95}$$

which defines the (u, v, w) direction cosines

$$\begin{vmatrix} X_A \\ Y_A \\ Z_A \end{vmatrix} = \begin{vmatrix} u_1 & u_2 & u_3 \\ v_1 & v_2 & v_3 \\ w_1 & w_2 & w_3 \end{vmatrix} \begin{vmatrix} x \\ y \\ z \end{vmatrix} \tag{96}$$

which define the force coefficient transformation

$$\begin{vmatrix} -C_D \\ C_{Y_A} \\ -C_L \end{vmatrix} = \begin{vmatrix} u_1 & u_2 & u_3 \\ v_1 & u_2 & u_3 \\ w_1 & w_2 & w_3 \end{vmatrix} \begin{vmatrix} -C_A \\ C_y \\ -C_N \end{vmatrix} \tag{97}$$

The relationship between body and wind-axes aerodynamic coefficients is now established. Note the negative directions of the coefficients relative to the axes.

Inertial coordinates.-- The selected inertial coordinates coincide with the earth references (X_e, Y_e, Z_e) system at time zero. At a later time they differ by the rotation of the earth,

$\omega_p t$. The transformation between inertial velocities and planet referenced velocities is derived as follows.

Let $\bar{R}$ be the displacement of the point-mass, (See Figure 9).

In inertial coordinates

$$R = X\bar{1}_X + Y\bar{1}_Y + Z\bar{1}_Z \tag{98}$$

and

$$\bar{V} = \dot{\bar{R}} = \dot{X}\bar{1}_X + \dot{Y}\bar{1}_Y + \dot{Z}\bar{1}_Z \tag{99}$$

In planet-referenced coordinates

$$\bar{R} = X_e\bar{1}_{X_e} + Y_e\bar{1}_{Y_e} + Z_e\bar{1}_{Z_e}$$

However, due to the rotation of the X_e, Y_e, Z_e coordinate system, the velocity is

$$V = \dot{\bar{R}} = \frac{\delta\bar{R}}{\delta t} + \bar{\omega}_p \times \bar{R} \tag{100}$$

where

$$\frac{\delta\bar{R}}{\delta t} = \dot{X}_e\bar{1}_{X_e} + \dot{Y}_e\bar{1}_{Y_e} + \dot{Z}_e\bar{1}_{Z_e} \tag{101}$$

The planet's rotation is about the Z-axis which is also the Z_e-axis. Therefore,

$$\bar{\omega}_p = -\omega_p\bar{1}_Z = -\omega_p\bar{1}_{Z_e}$$

and the required cross product is

$$\bar{\omega}_p \times \bar{R} = \begin{vmatrix} \bar{1}_{X_e} & \bar{1}_{Y_e} & \bar{1}_{Z_e} \\ 0 & 0 & -\omega_p \\ X_e & Y_e & Z_e \end{vmatrix} = (Y_e\omega_p)\bar{1}_{X_e} - (X_e\omega_p)\bar{1}_{Y_e} \tag{102}$$

If Equations (99), (101), and (102) are substituted into Equation (189), it follows that

$$\dot{X}\bar{1}_X + \dot{Y}\bar{1}_Y + \dot{Z}\bar{1}_Z = (\dot{X}_e + \omega_p Y_e)\bar{1}_{X_e} + (\dot{Y}_e - \omega_p X_e)\bar{1}_{Y_e} + (\dot{Z}_e)\bar{1}_{Z_e} \tag{103}$$

The relation between the unit vectors in the inertial system and unit vectors in the planet referenced system are obtained by a single rotation about the Z-axis.

The transformation matrix is

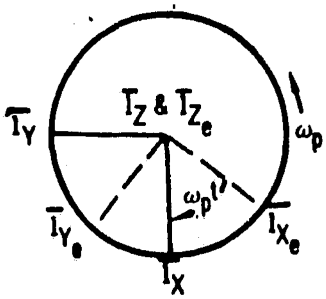

$$\begin{vmatrix} \bar{1}_{X_e} \\ \bar{1}_{Y_e} \\ \bar{1}_{Z_e} \end{vmatrix} = \begin{vmatrix} \text{Cos } \omega_p t & -\text{Sin } \omega_p t & 0 \\ \text{Sin } \omega_p t & \text{Cos } \omega_p t & 0 \\ 0 & 0 & 1 \end{vmatrix} \begin{vmatrix} \bar{1}_X \\ \bar{1}_Y \\ \bar{1}_Z \end{vmatrix} \tag{104}$$

The transformation from planet-referenced velocities to inertial velocities is made with the inverse of the matrix of Equation (104), and the component relations derived in Equation (103)

$$\begin{vmatrix} \dot{X} \\ \dot{Y} \\ \dot{Z} \end{vmatrix} = \begin{vmatrix} \text{Cos } \omega_p t & \text{Sin } \omega_p t & 0 \\ -\text{Sin } \omega_p t & \text{Cos } \omega_p t & 0 \\ 0 & 0 & 1 \end{vmatrix} \begin{vmatrix} \dot{X}_e + \omega_p Y_e \\ \dot{Y}_e - \omega_p X_e \\ \dot{Z}_e \end{vmatrix} \tag{105}$$

The components of inertial velocities are used to calculate the inertial speed of the body as

$$V_I = \sqrt{\dot{X}^2 + \dot{Y}^2 + \dot{Z}^2} \tag{106}$$

Equation (106), is valid regardless of the inertial coordinate system involved.

<u>Local-geocentric to geodetic coordinates</u>.-- Positions on the planet are specified in terms of geodetic latitude and altitude (for a given longitude) while the motion of the body is computed in a planetocentric system which is independent of the surface. In the computer program, flight-path angle λ and heading angle σ are calculated with respect to the local geocentric coordinates. By definition λ_D and σ_D are angles measured with respect to the local geodetic. Although the maximum difference that can exist between the two coordinate systems is 11 minutes of arc, it may be desirable to know λ_D and σ_D more accurately than is obtained when measured from the local geocentric.

It will be necessary to resolve the geocentric latitude to geodetic latitude for an accurate determination of position. Figure 14 presents the geometry required for describing the position of a point in a meridian plane of a planet shaped in the form of an oblate spheroid.

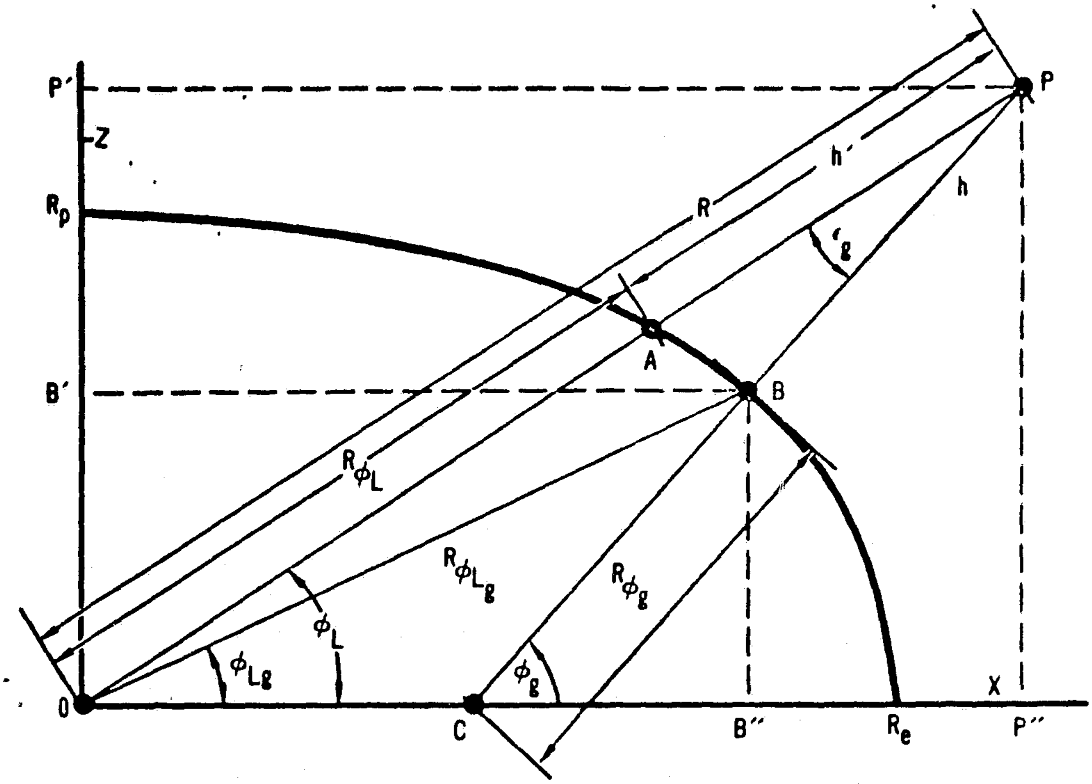

Figure 14.— Planet-Oblateness Effect on Latitude and Altitude

It is apparent from this figure that the most significant difference between the geocentric referenced position and the geodetic position is the distance $\overline{AB}$ on the surface of the reference spheroid. The distance can be defined by a knowledge of the angle ϕ_L; the geocentric latitude; ϕ_g, the geodetic latitude; the corresponding radii; and the distance $\overline{OC}$.

The relationship between the geocentric and geodetic latitude of a point on the surface of a planet which is an oblate spheroid is obtained as follows. The equation for the surface in a meridian plane is

$$\frac{X^2}{R_e^2} + \frac{Z^2}{R_p^2} = 1 \tag{107}$$

The tangent of the geodetic latitude can be found by determining the negative reciprocal of the slope of a tangent to this ellipse. The expression for this tangent is

$$\text{Tan } \phi_g = - \left. \frac{1}{\frac{d(-Z)}{dX}} \right|_B = - \frac{R_e^2 \, Z_B}{R_p^2 \, X_B} \tag{108}$$

Note that Z_B is a negative number in the northern hemisphere.

The tangent of the geocentric latitude of point B is

$$\text{Tan } \phi_{L_g} = -\frac{Z_B}{X_B} \tag{109}$$

Substituting Equation (109) into Equation (108), gives the required relation

$$\text{Tan } \phi_g = \frac{R_e^2}{R_p^2} \text{ Tan } \phi_{L_g} \tag{110}$$

The expression for the radius of the planet at point B in terms of the geocentric latitude of the point and the equatorial and polar radii is obtained by the rectangular to polar coordinate transformation

$$-Z_B = R_{\phi_{L_g}} \text{ Sin } \phi_{L_g} \tag{111}$$

$$X_B = R_{\phi_{L_g}} \text{ Cos } \phi_{L_g} \tag{112}$$

and, solving for $R_{\phi_{L_g}}$ by substituting Equations (111) and (112) into Equation (107) gives

$$R_{\phi_{L_g}} = \frac{R_e R_p}{\sqrt{R_p^2 \text{ Sin}^2 \phi_{L_g} + R_e^2 \text{ Cos}^2 \phi_{L_g}}} \tag{113}$$

$$= \frac{\cos \phi_L}{\cos \phi_{L_g}} R_e \Big/ \sqrt{[(R_e/R_p)(\tan \phi_{L_g}/\tan \phi_L)]^2 \sin^2 \phi_L + \cos^2 \phi_L}$$

It may be seen from Figure 14 that

$$\overline{B'P'} = \overline{OP'} - \overline{OB'} \tag{114}$$

or

$$h \sin \phi_g = \overline{OP} \sin \phi_L - R_{\phi_{L_g}} \sin \phi_{L_g} \tag{115}$$

Likewise

$$\overline{B''P''} = \overline{OP''} - \overline{OG''} \tag{116}$$

or

$$h \cos \phi_g = \overline{OP} \cos \phi_L - R_{\phi_{L_g}} \cos \phi_{L_g} \tag{117}$$

If Equation (115) is divided by Equation (117) and then the quotient is divided by $\tan \phi_{L_g}$, there results

$$\left(\frac{\tan\ \phi_g}{\tan\ \phi_{L_g}}\right) = \left[\overline{OP}\ \left(\frac{\sin\ \phi_L}{\sin\ \phi_{L_g}}\right) - R\phi_{L_g}\right] / \left[\overline{OP}\ \left(\frac{\cos\ \phi_L}{\cos\ \phi_{L_g}}\right) - R\phi_{L_g}\right] \tag{118}$$

or

$$(R_e/R_p)^2\ \left(\frac{\cos\ \phi_L}{\cos\ \phi_{L_g}}\right) = \left(\frac{\cos\ \phi_L}{\sin\ \phi_{L_g}}\right) + \left[(R_e{}^2 - R_p{}^2)/R_p{}^2\right]\left[R\phi_{L_g}/\overline{OP}\right] \tag{119}$$

Finally, if Equation (119) is multiplied by $(R_p \sin \phi_{L_g})/(R_e \sin \phi_L)$, it follows that

$$\left(\frac{R_e}{R_p}\right)(\tan\ \phi_{L_g}/\tan\ \phi_L) = \left(\frac{R_p}{R_e}\right) + \left[1 - (R_p/R_e)^2\right]\left(\frac{R_e\ \sin\ \phi_{Lg}}{R_p\ \sin\ \phi_L}\right)(R\phi_{L_g}/\overline{OP}) \tag{120}$$

Let

$$U = (R_e\ \tan\ \phi_{L_g}/R_p\ \tan\ \phi_L)$$

$$= (R_p\ \tan\ \phi_g/R_e\ \tan\ \phi_L) \tag{121}$$

Then it follows from Equations (113) and (120) that

$$U = \left(\frac{R_p}{R_e}\right) + [R_e/\overline{OP}]\ [U/\sqrt{U^2\ \sin^2\ \phi_L + \cos^2\ \phi_L}]\ [1 - (R_p/R_e)^2] \tag{122}$$

Equation (122) is solved by an iterative scheme.

Then

$$\phi_g = \tan^{-1}\left[\left(\frac{R_e\ U}{R_p}\right)\tan\ \phi_L\right] \tag{123}$$

The flight-path and heading angles corrected to the local geodetic latitude are computed by

$$\gamma_D = \mathrm{Sin}^{-1}\left(\frac{-\dot{Z}_{g_1}}{V_{g_1}}\right) = \mathrm{Sin}^{-1}\left(\frac{-\ \dot{Z}_g - \{\dot{X}_g(\phi_g - \phi_L)\}}{V_g}\right) \tag{124}$$

Since the magnitude of vector V_g is equal to the magnitude of vector V_{g_1}

and

$$\sigma_D = \mathrm{Sin}^{-1}\left(\frac{\dot{Y}_g}{\sqrt{\dot{X}_{g_1}{}^2 + \dot{Y}_{g_1}{}^2}}\right) = \mathrm{Sin}^{-1}\left(\frac{\dot{Y}_g}{\sqrt{\{\dot{X}_g + \dot{Z}_g(\phi_g - \phi_L)\}^2 + \dot{Y}_g{}^2}}\right) \tag{125}$$

Auxiliary Computations

In addition to the computations which can be made from the problem formulation as presented in preceding sections, several other quantities are available as optional calculations.

a. Planet-surface referenced range, R_D

b. Great-circle range, R_g

c. Down- and cross-range, X_D and Y_D

d. Theoretical burnout velocity, V_{theo}

e. Velocity losses, V_P, V_{grav}, V_D, and V_{ML}

f. Orbital variables and satellite target

Planet-surfaced referenced range.-- The total distance traveled over the surface of the planet is computed as the integrated surface range. If the distance traveled by the vehicle over a given portion of the trajectory is

$$R_D' = \int_{t_1}^{t_2} V_g \, dt \tag{126}$$

then the curvilinear planet surface referenced range is

$$R_D = \int_{t_1}^{t_2} \frac{R_{\phi_L}}{R} V_g \cos \gamma \, dt \tag{127}$$

The flight-path angle, λ, is referenced to local geocentric coordinates for this computation.

Great-circle range.-- Great-circle distance from the launch point to the instantaneous vehicle position, R_g, may also be required. Expressions for this distance are derived as follows.

By spherical trigonometry, (see Figure 15)

$$\cos \frac{R_g}{R'} = \cos(90-\phi_L)\cos(90-\phi_{L_o}) + \sin(90-\phi_L)\sin(90-\phi_{L_o}) \cos(\theta_L-\theta_{L_o}) \tag{128}$$

or simplifying

$$\cos \frac{R_g}{R'} = \sin \phi_L \sin \phi_{L_o} + \cos \phi_L \cos \phi_{L_o} \cos(\theta_L-\theta_{L_o}) \tag{129}$$

Therefore,

$$R_g = R' \cos^{-1} \left[\sin \phi_L \sin \phi_{L_o} + \cos \phi_L \cos \phi_{L_o} \cos(\theta_L-\theta_{L_o})\right] \tag{130}$$

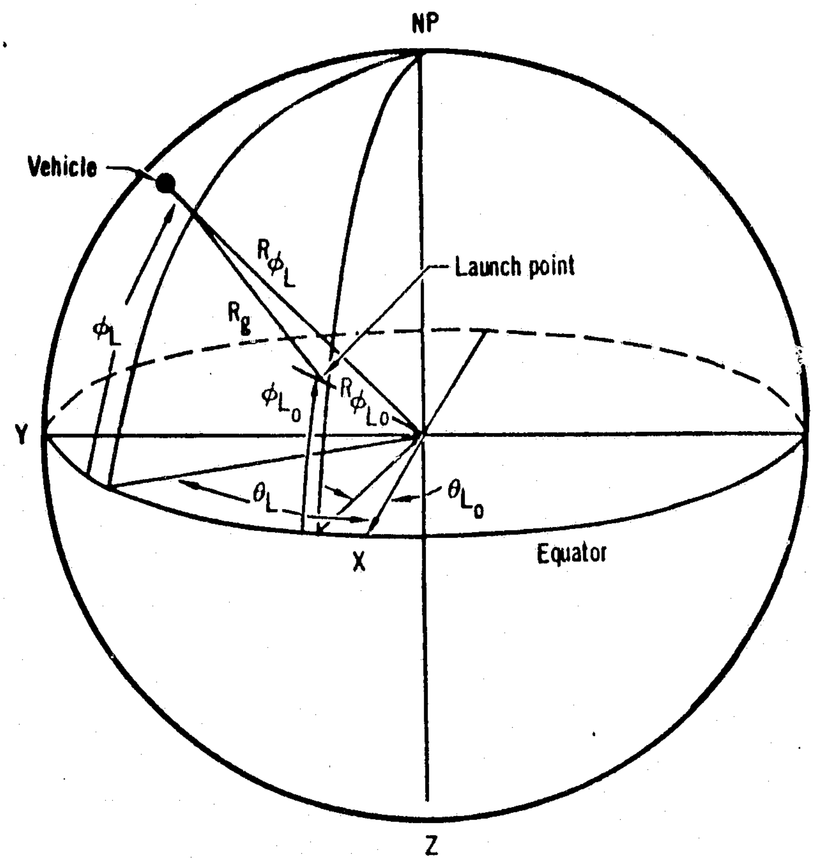

Figure 15.—Great-Circle Range

However, since the planets are generally oblate spheroids, R' is not a constant radius. An approximation may be obtained by averaging the planet's radius at the launch point and at the vehicle's position. Therefore, define the average radius, R', as

$$R' = \frac{R_{\phi_L} + R_{\phi_{L_o}}}{2} \tag{131}$$

and the surface-referenced great-circle range from the launch point to the vehicle is

$$R_g = \left[\frac{R_{\phi_L} + R_{\phi_{L_o}}}{2}\right] \text{Cos}^{-1}\left[\text{Sin}\,\phi_L \ \text{Sin}\ \phi_{L_o} + \text{Cos}\ \phi_L\ \text{Cos}\ \phi_{L_o}\ \text{Cos}(\theta_L - \theta_{L_o})\right] \tag{132}$$

<u>Down- and cross-range</u>.-- Down- and cross-range from the initial great circle can be determined. The initial great circle is determined from the input quantities σ_o, ϕ_{L_o}, and

θ_{L_o} (see Figure 16) Then the cross range of a particular trajectory point is defined as the perpendicular distance from the point to the initial great circle. The downrange is then the distance along the initial great circle from the initial point to the point P at which the cross range is measured. From the spherical triangle, Figure 16, the great circle range LF to the point F is computed by Equation (132).

The right spherical triangle LPF is solved for the downrange, X_D, and the cross range, Y_D.

$$X_D = R' \cos^{-1}\left(\frac{\text{Cos LF}}{\text{Cos}\,(\sin^{-1}(\sin LF \sin \xi))}\right) \tag{133}$$

$$Y_D = R' \sin^{-1}(\sin LF \sin \xi) \tag{134}$$

where

$$\xi = \zeta - \sigma_o \tag{135}$$

R' is defined by Equation (131)

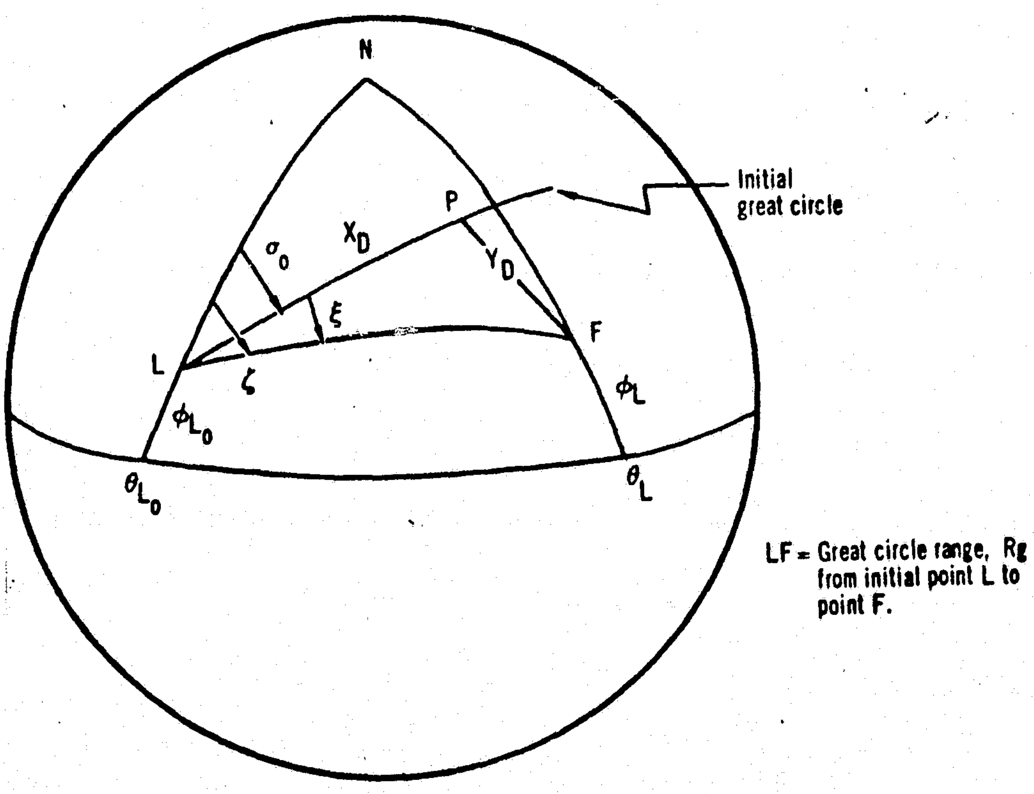

Figure 16.—Downrange and Crossrange Geometry

Theoretical burnout velocity and losses.-- For trajectory and performance optimization studies, it is convenient to know the theoretical burnout velocity possible and the velocity losses due to gravity, aerodynamic drag, and atmospheric back pressure upon the engine nozzle. These quantities may be computed as follows:

Theoretical Velocity

$$V_{theo} = \int_{t_1}^{t_2} \frac{T_{VAC}}{m} dt \tag{136}$$

Speed Loss Due to Gravity

$$V_{grav} = \int_{t_1}^{t_2} -g_{Z_g} \operatorname{Sin} \gamma \, dt \tag{137}$$

Speed Loss Due to Aerodynamic Drag

$$V_D = \int_{t_1}^{t_2} \frac{D}{m} dt \tag{138}$$

Speed Loss Due to Atmosphere Back Pressure Upon the Engine Nozzle

$$V_P = \int_{t_1}^{t_2} - \frac{PA_e}{m} dt \tag{139}$$

Maneuvering Losses

$$V_{ML} = \int_{t_1}^{t_2} \left(\frac{T_{VAC} - PA_e}{m}\right) \left(\cos \alpha - 1\right) dt. \tag{140}$$

The resultant velocity $V_g'(t_2)$ is obtained by adding the components computed to the initial value $V_g'(t_1)$

$$V_g'(t_2) = V_g'(t_1) + V_{theo} + V_{grav} + V_D + V_P \tag{141}$$

The maneuvering losses are valid only if λ_T is zero for the engine.

Orbital variables and satellite target.-- Certain functions of use in orbital trajectory calculations have been added to the point mass equations of motion used in the Steepest Descent Optimization Program. These functions permit the specification of terminal conditions in inertial space when this is convenient. A further set of functions will permit rendezvous calculations with a satellite in a circular orbit about a central planet.

Orbital variable calculations commence immediately after the calculation of vehicle inertial velocity. Flight path angles in inertial space are computed from the expressions

$$\sigma_I = \tan^{-1}\left(\frac{\dot{Y}_g + \omega_p |R| \cos\phi_L}{\dot{X}_g}\right) \tag{142}$$

$$\gamma_I = \sin^{-1}\left(\frac{\dot{Z}_g}{|V_I|}\right) \tag{143}$$

The inclination angle, i, is the angle between the plane containing the velocity vector and the center of the earth, and the equatorial plane.

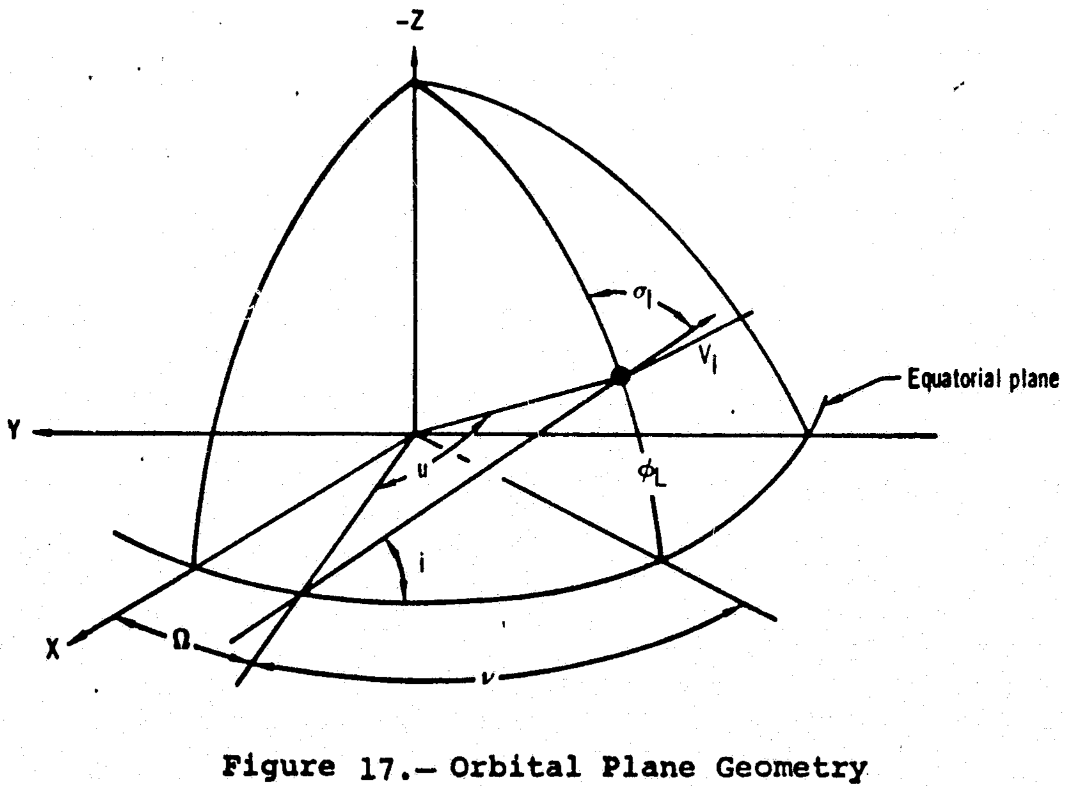

Figure 17.– Orbital Plane Geometry

Applying spherical trigonometry to Figure 17, we obtain the relationship

$$\cos i = \cos \phi_L \sin \sigma_I \tag{144}$$

The difference in longitude between the vehicle and the ascending node, ν, is given by

$$\tan \nu = \sin \phi_L \tan \sigma_I \tag{145}$$

The inertial longitude is given by

$$\theta_I = \theta_L - \omega_p t \tag{146}$$

and the inertial longitude of the ascending node by

$$\Omega = \theta_I - \nu \tag{147}$$

It is convenient to know the central angle, u, in the orbital plane. Measuring from the ascending node, we obtain

$$\tan u = \frac{\tan \phi_L}{\cos \sigma_I} \tag{148}$$

The orbital variable calculation introduces positional and velocity information from a second body. This body is a satellite considered in a circular orbit about the earth. Its orbital height, h_s, is specified and remains constant. Position in the orbit is computed from an initial central angle, ϕ_{s_o}, by the expression

$$\phi_s = \phi_{s_o} + \omega_s t \tag{149}$$

The satellite angular velocity is obtained from the satellite inertial velocity, V_{c_s}, where

$$V_{c_s} = \sqrt{\frac{\mu_g}{(R_e+h_s)}} \tag{150}$$

where μ_g is the gravitational potential constant and R_e the earth radius. It should be noted that Equation (150) assumes a spherical earth; for the earth radius is taken as constant, and none of the higher order gravitational harmonics are included. Knowing V_{c_s}, it follows that

$$\omega_s = \frac{V_{c_s}}{R_e+h_s} \tag{151}$$

The variables of this section provide sufficient information to either rendezvous with or terminate the trajectory in a specified position relative to the satellite.

VEHICLE CHARACTERISTICS

Methods by which the aerodynamic, propulsive, and physical characteristics of a vehicle are introduced into the computer program are presented in this section. Form and preparation of the input data are discussed, together with methods by which stages and staging may be used to increase the effective data storage area allotted to a description of the vehicle's properties.

Aerodynamic Coefficients

The primary objective of the aerodynamic data input subprogram is to provide for a complete accounting of the various contributions to the aerodynamic forces and moments regardless of the flight conditions of the vehicle being considered. Two techniques are available for use in the digital computer program: (a) an n-dimensional table look-up and interpolation and (b) an m-order polynomial function of n variables prepared by "curve fit" techniques. In the first method, the proper value for each term is obtained by an interpolation in "n" dimensions where the number of dimensions is taken to be the number of parameters to be varied independently plus the dependent variable. This method has the advantage of accurately describing most non-linear variations with reasonable preparation effort. The amount of storage space which must be allocated to such a method, however, can achieve unreasonable proportions and may require substantial computing time for the interpolation as the number of dimensions are increased. The second method has essentially the opposite characteristics; that is, a large amount of data may be represented with a small amount of storage space, and computation time is held to reasonable limits, but the data variations which may be represented must be regular. A substantial amount of effort can be required for the preparation of data by a curve-fit technique. Both these methods are very convenient when the amount of data to be handled is moderate, but tend to become unmanageable when large amounts of data are required. This usually occurs when the program, having several degrees of freedom, is committed to one or the other of these two techniques. Therefore, the computer program incorporates both of the techniques discussed as a compromise to take advantage of the more desirable features of both. To do this, a general set of data equations have been programmed which define each of the aerodynamic forces. In general, the coefficients for these equations will be obtained from a curve-read interpolation. Several simplifications may be made to the equations depending on the flight condition and vehicle to be considered.

Often the particular application will not require some of the terms listed in order to describe the flight path and vehicle under consideration. The subprogram is arranged so that the computer will assign a constant value to any curve for which the data has not been supplied. For most curves, the constant value will be zero. This technique may be used to reduce the time required for the preparation of data. Values intermediate to those introduced in a tabular listing will be obtained by linear interpolation.

Aerodynamic Forces

Aerodynamic forces are customarily defined by three mutually perpendicular forces. These are lift (L), drag (D), and side force (Y). Lift force is perpendicular to the velocity vector in a vertical plane; drag force is measured along the velocity vector but in opposite direction; side force is measured in the horizontal plane, positive toward the right, provided the bank angle is zero. If the bank angle is not zero, L and Y will be rotated by $-B_A$ about the velocity vector. Coordinates are shown in Figure 18.

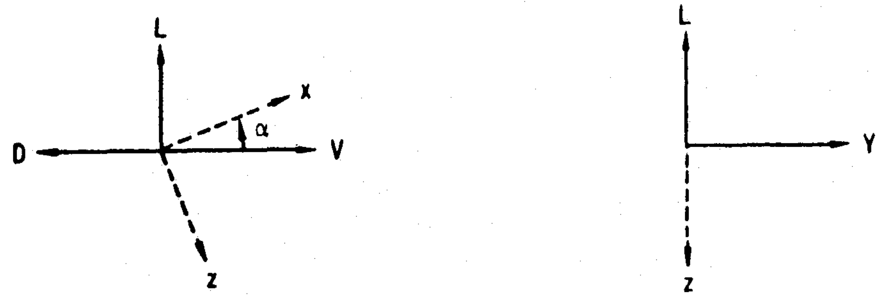

Figure 18.— Aerodynamic Forces - Wind Axes

These forces may be expressed in the form

$$L = q(V,h)\ SC_L(V,h,\alpha,\beta) \tag{152}$$

$$D = q(V,h)\ SC_D(V,h,\alpha,\beta) \tag{153}$$

$$Y = q(V,h)\ SC_Y(V,h,\alpha,\beta) \tag{154}$$

where q is the dynamic pressure and S a convenient reference area. The aerodynamic coefficients C_L, C_D, and C_Y may be expressed in terms of the aerodynamic derivatives.

$$C_L = C_{L_o} + C_{L_\alpha}\alpha + C_{L_\alpha 2}\alpha|\alpha| + C_{L_\beta}|\beta|$$

$$+ C_{L_\beta 2}\beta^2 + C_{L_{\alpha\beta}}\alpha|\beta| \tag{155}$$

$$C_D = C_{D_o} + C_{D_\alpha}|\alpha| + C_{D_\alpha 2}\alpha^2 + C_{D_\beta}|\beta|$$

$$+ C_{D_\beta 2}\beta^2 + C_{D_{\alpha\beta}}|\alpha||\beta| \tag{156}$$

$$C_Y = C_{Y_o} + C_{Y_\alpha}|\alpha| + C_{Y_\alpha 2}\alpha^2 + C_{Y_\beta}\beta$$

$$+ C_{Y_\beta 2}\beta|\beta| + C_{Y_{\alpha\beta}}|\alpha|\beta \tag{157}$$

Alternatively, the aerodynamic derivatives may be expressed as tabular functions of Mach number (M_N), α, and β, that is, functions of the state variables and the control variables.

On occasion, it may be convenient to measure the aerodynamic forces in the body axis coordinate system introduced in a preceding section, pages 28 to 30. In this case, normal force, (n_f), is measured along the -z axis, side force (y) along the y axis, and axial force (a) along the -x axis, as in Figure 19.

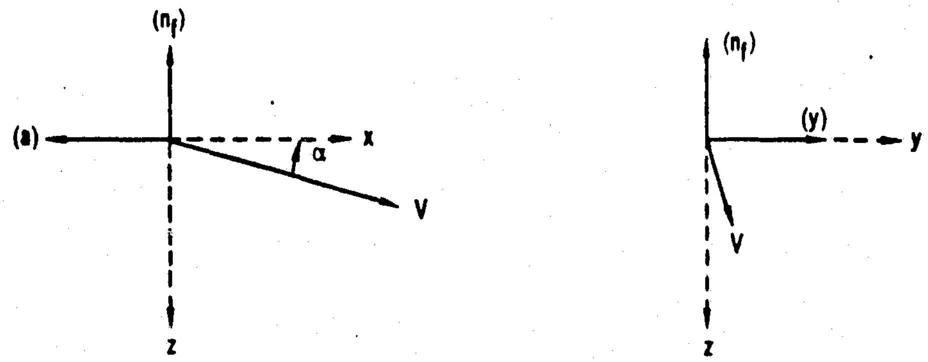

Figure 19.— Aerodynamic Force in Body Axes

The specification of forces in the body axis system is similar to that in the wind axis system

$$n_f = qSC_N \tag{158}$$

$$a = qSC_A \tag{159}$$

$$y = qSC_y \tag{160}$$

where the body axis aerodynamic coefficients are

$$C_N = C_{N_o} + C_{N_\alpha} + C_{N_\alpha 2} \alpha |\alpha| + C_{N_\beta}|\beta| + C_{N_\beta 2} \beta^2 + C_{N_{\alpha\beta}} \alpha |\beta| \tag{161}$$

$$C_A = C_{A_o} + C_{A_\alpha}|\alpha| + C_{A_\alpha 2} \alpha^2 + C_{A_\beta}|\beta| + C_{A_\beta 2} \beta^2 + C_{A_{\alpha\beta}} |\alpha\beta| \tag{162}$$

$$C_y = C_{y_o} + C_{y_\alpha}|\alpha| + C_{y_\alpha 2}\alpha^2 + C_{y_\beta}\beta + C_{y_\beta 2} \beta|\beta| + C_{y_{\alpha\beta}} |\alpha|\beta \tag{163}$$

Thrust and Fuel Flow Data

The techniques employed to introduce thrust and fuel-flow data into the equations of motion are developed in an approach similar to that employed for aerodynamic data. An n-dimensional tabular listing and interpolation technique is used with the independent variables being defined by the type of propulsion unit being considered. For the present formulation, the propulsion units are grouped into the following options: (1) rocket, (2) air breathing engine.

Propulsion option (1) rocket.-- The thrust of a rocket motor is assumed variable with stage time, altitude,and,if the rocket is controllable, it will also vary with throttle setting. The altitude effect is determined by the exit area of the nozzle, A_e, and the ambient pressure, P. If the thrust is specified for some constant ambient air pressure, the altitude correction can be calculated within the subprogram. If the rocket motor is uncontrolled, the vacuum thrust, in pounds, will be introduced by a tabular listing as a function of time, in seconds, and corrected as follows:

$$T = \text{Max} \ [T_{vac} - PA_e, 0] \tag{164}$$

The propellant consumption rate is specified by a tabular listing in slugs per second as a function of time,in seconds, for the single engine options, or computed from the thrust and the engine specific impulse, I_{SP}, for the multiple engine options.

If the rocket is controlled, the propellant mass flow rate $\dot{m}_f$ is introduced by a tabular listing as a function of throttle setting. The thrust is then specified by a tabular listing as a function of mass flow rate.

Propulsion option (2) air breathing engines.—An air-breathing engine is strongly affected by the environmental conditions under which it is operating. Engines which would be grouped in this classification are turbojets, ramjets, pulsejets, turboprops, and reciprocating machines. The parameters considered significant in the program are

(a) Altitude (h-ft)

(b) Mach number (M_N)

(c) Angle of attack (α-degrees), and

(d) Throttle setting (N-units defined by problem)

Both the thrust and fuel flow are functions of these variables. In order to accommodate these variables, a five-dimensional tabular listing and interpolation are used to obtain both thrust and fuel flow. The thrust has no further correction as the effects of all parameters are assumed included in the interpolated value.

Engine perturbation factors.—The engine options include provision for two data scaling factors for use in parametric studies. These are in the form

$$T = \varepsilon_{13} T_{VAC} + \varepsilon_{14} \tag{165}$$

Components of the thrust vector.—The equations used to reduce the thrust vector to its components along the body axes are

$$T_x = T \cos\lambda_T \tag{166}$$

$$T_y = -T \sin\lambda_T \cos\phi_T \tag{167}$$

and

$$T_z = -T \sin\lambda_T \sin\phi_T \tag{168}$$

ϕ_T and λ_T are defined and explained in the control variable section.

Reference weight and propellant consumed.—Rate of change of vehicle mass, $\dot{m}$, is set equal to the negative of the total mass flow rate, $-\dot{m}_t$. $\dot{m}$ is integrated to give variation of vehicle mass, m. The instantaneous mass is used in the computation of the body motion. The reference weight is obtained by an auxiliary calculation

$$W_T = m(32.174) \tag{169}$$

The propellant consumed is computed as

$$m_f = m_o - m \tag{170}$$

where m_o is a reference mass input equal to the initial vehicle mass

Stages and Staging

A problem common in missile performance analyses and encountered frequently in airplane performance work is that of staging or the release of discrete masses from the continuing airframe. The effect of dropping a booster rocket or fuel tanks is often great enough to require that the complete set of aerodynamic data be changed. Configuration changes at constant weight, such as extending drag brakes or turning on afterburners, may also require revising the aerodynamic or physical characteristics of the vehicle. Another use of the staging technique is possible with the present computer program which does not involve physical changes to the configuration; this technique may be used to revise the aerodynamic descriptors as a function of aerodynamic attitude or Mach number. With this use of the stage concept, accurate descriptions of the forces acting upon the vehicle may be maintained over wide attitude ranges, if required.

VEHICLE ENVIRONMENT

The models for simulating the environment in which a vehicle will operate are presented in this section. This environment includes the atmosphere properties, wind velocity, and the field associated with the planet over which the vehicle is moving. The shape of the planet and the conversion from geodetic to geocentric latitudes are also considered. In the discussions which follow, the descriptions of vehicle environment pertain to the planet Earth. The environmental simulation may be extended to any planet by replacing appropriate constants in the describing equations.

Atmosphere

The concept of a model atmosphere was introduced many years ago, and over the years several models have been developed. Reference 15 outlines the historical background of the gradual evolution of the ARDC model. The original (1956) ARDC model (Reference 15) was revised to reflect the density variation with altitude that was obtained from an analysis of artificial satellite orbit data. This revision is the widely used 1959 ARDC Model Atmosphere and is the basic option in the present program.

The advantage of a model atmosphere is that it provides a common reference upon which performance calculations can be based. The model is not intended to be the "final word" on the properties of the atmosphere for a particular time and location. The atmosphere properties are quite variable and are affected by many parameters other than altitude. At the present time, the "state-of-the-art" is not advanced to the point where these parameters can be accounted for; it may be several years before the effects of some parameters can be evaluated.

1959 ARDC Model Atmosphere.-- The 1959 ARDC Model Atmosphere is specified in layers assuming either isothermal or linear temperature lapse-rate sections. This construction makes it very convenient to incorporate other atmospheres, either from specifications for design purposes or for other planets. The relations which mathematically specify the 1959 ARDC Model Atmosphere are as follows (Reference 16) **the 1959 ARDC Model Atmosphere is divided into 11 layers as noted in the table below.**

Layer	H_b-Lower Altitude (Geopotential) Meters	Upper Altitude (Geopotential) Meters
1	0	11,000
2	11,000	25,000
3	25,000	47,000
4	47,000	53,000
5	53,000	79,000
6	79,000	90,000
7	90,000	105,000
8	105,000	160,000
9	160,000	170,000
10	170,000	200,000
11	200,000	700,000

For layers 1, 3, 5, 7, 8, 9, 10, and 11, a linear molecular-scale temperature lapse-rate is assumed and the following equations are used:

$$H_{gp} = \frac{.3048h}{1 + .3048h/6356766} \quad \text{Meters} \qquad (171)$$

$$T_M = (T_M)_b \left[1 + K_1(H_{gp} - H_b)\right] \quad {}^{\circ}R \qquad (172)$$

$$T = T_M\left[A - B \tan^{-1}\left(\frac{H_{gp} - C}{D}\right)\right] \quad {}^{\circ}R \qquad (173)$$

$$P = P_b\left[1 + K_1(H_{gp} - H_b)\right]^{-K_2} \quad \text{Lb./Ft.}^2 \qquad (174)$$

$$\rho = \rho_b\left[1 + K_1(H_{gp} - H_b)\right]^{-(1+K_2)} \quad \text{Slugs/Ft.}^3 \qquad (175)$$

$$V_s = 49.021175(T_M)^{1/2} \quad \text{Ft./Sec.} \qquad (176)$$

$$\nu = 2.269681 \times 10^{-8}\left[\frac{T^{3/2}}{(T+198.72)\rho}\right] \quad \text{Ft.}^2\text{/Sec.} \qquad (177)$$

For the isothermal layers 2, 4, and 6, the following changes are made

$$P = P_b e^{-K_3(Hgp-H_b)} \qquad (178)$$

$$\rho = \rho_b e^{-K_3(Hgp-H_b)} \qquad (179)$$

Values of the temperature, pressure, density, and altitude at the base of each altitude layer are listed below along with the appropriate values K_1, K_2, and K_3.

Quantity	Layer 1	2	3	4	5	6
K_1	$-.22556913 \times 10^{-4}$	0	$.13846580 \times 10^{-4}$	0	$-.15920187 \times 10^{-4}$	0
K_2	-5.2561222	0	11.388265	0	-7.5921765	0
K_3	0	$.15768852 \times 10^{-3}$	0	$.12086887 \times 10^{-3}$	0	$.20623442 \times 10^{-3}$
T_b	518.688	389.988	389.988	508.788	508.788	298.188
P_b	2116.2170	472.67599	51.975418	2.5154578	1.2180383	2.1082485×10^{-2}
ρ_b	2.37692×10^{-3}	7.0611078×10^{-4}	7.7643892×10^{-5}	2.8803201×10^{-6}	1.3947125 x 10[illegible]	4.1190042 x 10[illegible]
H_b	0	11000.	25000.	47000.	53000.	79000.

Quantity	Layer 7	8	9	10	11
K_1	$.24145841 \times 10^{-4}$	$.88628910 \times 10^{-4}$	$.75434123 \times 10^{-5}$	$.35071476 \times 10^{-5}$	$.22212914 \times 10^{-5}$
K_2	8.5411986	1.7082397	3.4164794	6.8329589	9.7613698
K_3	0	0	0	0	0
T_b	298.188	406.188	2386.188	2566.188	2836.188
P_b	2.1811754×10^{-3}	1.5564912×10^{-4}	7.5604667×10^{-6}	5.8971644×10^{-6}	2.9769746×10^{-6}
ρ_b	4.2614856×10^{-9}	$2.2324424 \times 10^{-10}$	$1.8458849 \times 10^{-12}$	$1.3387990 \times 10^{-12}$	$6.1150607 \times 10^{-13}$
H_b	90000.	105000.	160000.	170000.	200000.

Values of the appropriate constants to be applied in the temperature equation, Equation (173), are listed below.

H_{gp}(Km)	A	B	C	D
0-90	1.	0.	-	-
90-180	.75951115	.17416404	220,000.	25,000.
180-1200	.93578678	.27396592	180,000.	140,000.

U. S. Standard Atmosphere, 1962.--The part of the U.S. Standard Atmosphere, 1962, below 90 kilometers geometric altitude (295,276 ft. altitude) is defined in the same way as the 1959 model--by the hydrostatic equation and a piecewise linear variation of temperature with geopotential altitude. Equations (171) to (179) are, therefore, applicable with a different set of constants. These constants, based on the published tabulation of atmosphere properties (Reference 17) at the base altitudes, are presented below. The 1962 model uses a different set of relationships above 90 kilometers. These have not been included. The tables define 1962 model properties between sea level and 295,800 ft. geometric altitude.

Values of the temperature, pressure, density, and altitude at the base of each altitude layer are listed below along with the appropriate values of K_1, K_2, and K_3.

Quantity	Layer 1	Layer 2	Layer 3	Layer 4
K_1	$-.2255877 \times 10^{-4}$	0	$.48012406 \times 10^{-5}$	$.12199559 \times 10^{-4}$
K_2	$-.5255871 \times 10^{1}$	0	$.32844801 \times 10^{2}$	$.12202470 \times 10^{2}$
K_3	0	$.1576958 \times 10^{-3}$	0	0
T_b	518.67	389.97	389.97	413.104
P_b	2116.217	472.6812	114.3431	17.22518
ρ_b	$.2377002 \times 10^{-2}$	$.7061512 \times 10^{-3}$	$.1708202 \times 10^{-3}$	$.2429209 \times 10^{-4}$
H_b	0	10999.474	19999.191	32354.854

Quantity	Layer 5	Layer 6	Layer 7	Layer 8
K_1	0	$-.7383899 \times 10^{-5}$	$-.1572230 \times 10^{-4}$	0
K_2	0	$-.1709562 \times 10^{+2}$	$-.8602817 \times 10$	0
K_3	$.1262323 \times 10^{-3}$	0	0	$.1891214 \times 10^{-3}$
T_b	487.17	487.17	454.668	325.170
P_b	2.302550	1.226346	.3766873	.2106440
ρ_b	$.2753526 \times 10^{-5}$	$.1466537 \times 10^{-5}$	$.4826665 \times 10^{-6}$	$.3773977 \times 10^{-7}$
H_b	47051.501	52042.023	61077.348	79192.936

Within the altitude range considered, T and T_M (Equation (173)) are equal.

Atmosphere limitations.-- The validity of the 1959 ARDC model is limited to altitudes below 700 km; although the program is arranged to extrapolate the relationships to greater altitudes, if desired. Extrapolation to greater altitudes is accomplished by altering the cutoff altitude.

At an altitude greater than 2.6×10^6 feet, no calculations are made, and the program sets kinematic viscosity, speed of sound, pressure, temperature, and density to zero. At and below

sea level the parameters, pressure, temperature, and density are set to the values below. Other terms are computed as normal.

$$\text{Pressure} = 2116.2170 \ \text{Lb/Ft}^2 \tag{180}$$

$$\text{Temperature} = 518.688 \ ^{\circ}\text{R} \tag{181}$$

$$\text{Density} = 2.37692 \times 10^{-3} \ \text{Slugs/Ft}^3 \tag{182}$$

At altitudes between 90 kilometers and 2.6×10^6 feet, the speed of sound is set to 846.50255, and kinematic viscosity is set to 2.3519252×10^{-7} over density. Other terms are computed as normal.

The 1962 model is limited to altitudes below 295,8000 feet (90 kilometers). It is suggested that zero values be returned above that altitude. At and below sea level, the sea level values should be employed. When the atmosphere constants are determined from the published tabulations at the base altitude, the calculated values at intermediate altitudes may not agree with the tabulated values to the number of significant figures in the tables. This has been allowed for in the 1959 model by developing coefficients with the necessary extra precision to give agreement between the calculated values and published tables at all altitudes. The values calculated by the 1962 model are good to about four significant figures, which should be adequate for most purposes.

Kinematic viscosity and speed of sound lose their physical significance at very high altitudes, and are not normally defined by model atmospheres above 90 kilometers. The constant values by the 1959 model option were added to provide data required by the aerodynamic heating routine. The aerodynamic heating calculation should not be used with the 1962 model option above 90 kilometers. The constant values of ν and V_s in the 1959 model will give reasonable values of Mach number and Reynolds number for use in the aerodynamics calculations to altitudes somewhat above 90 kilometers, say 350,000 feet, above which constant aerodynamic coefficients should be used.

Winds Aloft

The winds-aloft subprogram provides for three separate methods of introducing the wind vector: as a function of altitude, a function of range, and a function of time. This facilitates the investigation of wind effects for the conventional performance studies. The wind vector is approximated by a series of straight line segments for each of the methods mentioned above.

Four options are used to define the wind vector in the computer program. The three components of the wind vector in a geodetic horizon coordinate system can be specified as tabular listings with linear interpolations (curve reads) in the following options.

Wind options (0).-- In this option the wind vector is zero throughout the problem. This allows the analyst the option of evaluating performance without the effects of wind. This option causes the winds-aloft computations to be bypassed.

Wind option (1).-- In this option the components of the wind vector are specified as a function of time. Wind speeds are specified in feet per second and time in seconds.

Wind option (2).-- The three components of the wind vector are introduced as a function of altitude in this option. Wind speed is specified in feet per second and altitude in feet.

Wind option (3).-- In this option the components of the wind vector are introduced as a function of range. Wind speed is specified in feet per second and range in nautical miles. The range utilized in this computation is the great-circle range.

By staging of the wind option, it is possible to switch from one method of reading wind data to another during the computer run. Care must be exercised in this operation, however, as the switching will introduce sharp-edged gusts if there are sizeable differences in the wind vector from one option to another at the time of switching. This effect should be avoided except in cases where gust effects are being studied.

Gravity

This section presents the equations necessary for the introduction of the gravity components into the equations of motion. These components were determined by taking partial derivatives of the gravity potential equation. The potential equation adopted has been recommended for use in the Six-Degree-of-Freedom Flight-Path Study computer program by AFCRC. Constants for the potential equation were determined from References 18, 19 and 20.

Spherical harmonics are normally used to define the gravity potential field of the Earth, References 18 through 20. Each harmonic term in the potential is due to a deviation of the potential from that of a uniform sphere. In the present analysis the second-, third-, and fourth-order terms are considered. The first-order term, which would account for the error introduced by assuming that the mass center of the Earth

is at the origin of the geocentric coordinate system is assumed to be zero. With this assumption

$$U = \frac{\mu_g}{R}\left[1 + \frac{J}{3}\left(\frac{R_e}{R}\right)^2 P_2 + \frac{H}{5}\left(\frac{R_e}{R}\right)^3 P_3 + \frac{K}{30}\left(\frac{R_e}{R}\right)^4 P_4 + \cdots\right] \quad (183)$$

where P_2, P_3, and P_4 are Legendre functions of geocentric latitude ϕ_L expressed as

$$\begin{aligned} P_2 &= 1 - 3\sin^2\phi_L \\ P_3 &= 3\sin\phi_L - 5\sin^3\phi_L \\ P_4 &= 3 - 30\sin^2\phi_L + 35\sin^4\phi_L \end{aligned} \quad (184)$$

The gravitational acceleration along any line is the partial derivative of U along that line. At this point, it should be noted that the three mutually perpendicular directions in the spherical coordinate system are identical (other than sign) to those in the local-geocentric-horizon coordinate system which is defined previously. Therefore, the acceleration in the ϕ_L direction is identical to g_{X_g}, and the acceleration in the R direction is identical to $-g_{Z_g}$. Or in the equation form:

$$g_{Z_g} = -\frac{\partial U}{\partial R} = -\frac{\mu_g}{R}\left[-\frac{2J}{3}\left(\frac{R_e^2}{R^3}\right) P_2 - \frac{3H}{5}\left(\frac{R_e^3}{R^4}\right) P_3 - \frac{4K}{30}\left(\frac{R_e^4}{R^5}\right) P_4\right]$$
$$+ \frac{\mu_g}{R^2}\left[1 + \frac{J}{3}\left(\frac{R_e}{R}\right)^2 P_2 + \frac{H}{5}\left(\frac{R_e}{R}\right)^3 P_3 + \frac{K}{30}\left(\frac{R_e}{R}\right)^4 P_4\right] \quad (185)$$

$$g_{X_g} = \frac{1}{R}\frac{\partial U}{\partial \phi_L} = \frac{\mu_g}{R^2}\left[\frac{J}{3}\left(\frac{R_e}{R}\right)^2 (-6\sin\phi_L\cos\phi_L)\right. \quad (186)$$
$$+ \frac{H}{5}\left(\frac{R_e}{R}\right)^3 (3\cos\phi_L - 15\sin^2\phi_L\cos\phi_L)$$
$$\left. + \frac{K}{30}\left(\frac{R_e}{R}\right)^4 (-60\sin\phi_L\cos\phi_L + 140\sin^3\phi_L\cos\phi_L)\right]$$

Collecting terms:

$$g_{Z_g} = \frac{\mu_g}{R^2}\left[1 + J\left(\frac{R_e}{R}\right)^2 P_2 + \frac{4H}{5}\left(\frac{R_e}{R}\right)^3 P_3 + \frac{K}{6}\left(\frac{R_e}{R}\right)^4 P_4\right] \quad (187)$$

$$g_{X_g} = \frac{\mu_g}{R^2}\left[-2J\left(\frac{R_e}{R}\right)^2 P_5 + \frac{3H}{5}\left(\frac{R_e}{R}\right)^3 P_6 + \frac{2K}{3}\left(\frac{R_e}{R}\right)^4 P_7\right] \quad (188)$$

where

$$P_5 = \sin \phi_L \cos \phi_L$$

$$P_6 = \cos \phi_L (1 - 5 \sin^2 \phi_L)$$

$$P_7 = \sin \phi_L \cos \phi_L (-3 + 7 \sin^2 \phi_L) \qquad (189)$$

Equations (187) and (188) are used in the gravity subroutine with the following values recommended for the constants:

$$\mu_g = 1.407698 \times 10^{16} \text{ ft.}^3/\text{sec.}^2$$

$$R_e = 20{,}925{,}631. \text{ ft.}$$

$$J = 1623.41 \times 10^{-6}$$

$$K = 6.37 \times 10^{-6} \qquad (190)$$

It should be noted that these constants and equations pertain to the planet Earth; however, it is possible to use these same equations for any other planet. For this reason, the values of these constants is an input to the program so that the applicable constants may be inserted for the planet under consideration. Due to limited knowledge of the gravitational fields of other planets, it is probable that zero values would be assigned to some of the harmonic coefficients when the program is used for entry studies on other planets.

The above equations are applicable to a non-rotating planet as the centrifugal relieving effects caused by the planet's rotation are included in the equations of motion. In addition, the effects of local anomalies must be added if it is desired to make a weight-to-mass conversion based on a measured weight. The program has the options of retaining the first, third, and fourth order terms.

AIRCRAFT CHARACTERISTICS

Weights

During the 1962 F4H-1 time-to-climb record flights, Reference 21, a considerable effort was made to reduce the vehicle flight weight. Production F4H-1 and record flight vehicle empty weights were:

Vehicle	Empty Weight	ΔW
Production F4H-1	29365	-
Record Flight Vehicle (3KM-15KM)	25903	3462
Record Flight Vehicle (20KM-30KM)	25520	3845

In addition to weight saving measures the record breaking vehicles employed non-standard General Electric J79-GE-8 engines and the record attempts were deliberately made during cold weather conditions to improve propulsion system performance characteristics for weight comparison purposes.

In standard F4H-1 aircraft empty weight quoted in the 1960 weight statement, Reference 22, and the currently quoted empty weight of in-service F4-C aircraft, Reference 23, at Edwards AFB are:

Vehicle	Empty Weight
F4H-1 (F4B)(1960 weight statement)	27345
F4-C (Edwards AFB 1975)	32500-33500 (Net)

For the present report it will be assumed that an average Edwards AFB F4-C might be made available to NASA and an empty weight (net) of 33000 lbs. will be utilized. In addition, Edwards AFB pilots have indicated that safety considerations dictate 2000 lbs. fuel on-board at approach and a requirement for 600 lbs. of fuel for a descent from 40000 feet. Early calculations indicate that zoom climbs to high altitude will consume approximately 1600 lbs. of fuel. Based on these figures it is assumed that vehicle weight at zoom commencement should be approximately 37500 lbs. (1166 slugs).

Propulsion

The F4-C Phantom is powered by two J79-GE-12 engines having a nominal rating of 17000 lbs. static thrust at sea level per engine. Thrust produced by these engines and their fuel flow varies strongly with Mach number, altitude, and throttle setting. That is, the thrust and fuel flow are of the form

$$T = T\ (M,\ h,\ N) \tag{191}$$

$$\dot{W} = \dot{W}\ (M,\ h,\ N) \tag{192}$$

where

T = Thrust, lbs.

$\dot{W}$ = Fuel flow, lbs./hour

M = Mach number

h - Altitude, feet

N = Throttle parameter

The F4-C engines have a wide range of throttle setting capability both with and without afterburners ignited. This capability is illustrated by Table I which presents thrust and specific fuel consumption for the related J79-GE-17 engine which powers the Phantom F4-E vehicle.

Actual thrust and fuel flow capability of the J79-GE-12 engine which powers the F4-C is presented in tabular fashion in Table II. These tables are in a form acceptable to the ATOP program of References 1 and 2 which is used to perform the trajectory optimization studies of this report. Format of Tables II(a) and (b) is as follows:

Thrust

$$\begin{aligned} \text{TTABoO} = {} & H_1,\ H_2,\ ---\ H_H, \\ & M_1,\ M_2,\ ---\ M_M, \\ & N_1,\ N_2, \\ & T_{H_1M_1N_1},\ T_{H_2M_1N_1},\ ---, \\ & ---\ T_{H_HM_1N_1},\ T_{H_1M_2N_1},\ --- \\ & ---\ T_{H_HM_MN_2} \end{aligned}$$

Fuel Flow

$$\begin{aligned} \text{TTAB11} = {} & H_1,\ H_2,\ ---\ H_H \\ & M_1,\ M_2,\ ---\ M_M \\ & N_1,\ N_2, \\ & W_{H_1M_1N_1}\ ---\ W_{H_HM_MN_2} \end{aligned}$$

The data of Tables II(a) and II(b) was made available through the studies of Reference 3.

TABLE I. TYPICAL EFFECT OF THROTTLE SETTING ON THRUST AND SPECIFIC FUEL CONSUMPTION OF THE PHANTOM F4-E (J79-GE-17) ENGINES.

(lbs. fuel/hour/lb. thrust)

Power	Thrust (lbs.)	R.P.M.	Specific Fuel Consumption
Max. Afterburner	17900.	7460	1.965
Military	11870.	7460	.84
Normal	11100.	7435	.81
90% Normal	10000.	7140	.79
75% Normal	8330.	6900	.76
Idle	350.	5000	1130 lbs./hour

TABLE II(a). THRUST OF THE J79-GE-12 ENGINE WHICH POWERS THE F4-C PHANTOM.

```
INDTFF     4
BURNRS     2.0
IT10W      19
IT10X      25
IT10Y      2
TTAB10     0,5000.,10000.,15000.                      1     ALT
TTAB10     20000.,25000.,30000.,35000.                5
TTAB10     36089.,40000.,45000.,50000.                9
TTAB10     55000.,60000.,65000.,70000.                13
TTAB10     75000.,75010.,120000.                      17
TTAB10     0,.050,.100,.250                           20    MACH
TTAB10     .400,.550,.700,.800                        24
TTAB10     .900,1.050,1.077,1.150                     28
TTAB10     1.247,1.272,1.360,1.470                    32
TTAB10     1.550,1.650,1.750,1.840                    36
TTAB10     1.950,2.100,2.200,2.300,2.400              40
TTAB10     1.,2.                                      45    MAX,IDLE
TTAB10     13360.,11360.,9590.,0                      47    MAX,M=0
TTAB10     0,0,0,0                                    51
TTAB10     0,0,0,0                                    55
TTAB10     0,0,0,0                                    59
TTAB10     0,0,0                                      63
TTAB10     14520.,12280.,10390.,0                     66    M=.050
TTAB10     0,0,0,0                                    70
TTAB10     0,0,0,0                                    74
TTAB10     0,0,0,0                                    78
TTAB10     0,0,0                                      82
TTAB10     14880.,12670.,10690.,0                     85    M=.100
TTAB10     0,0,0,0                                    89
TTAB10     0,0,0,0                                    93
TTAB10     0,0,0,0                                    97
TTAB10     0,0,0                                      101
TTAB10     15210.,13020.,11000.,9220.                 104   M=.250
TTAB10     7710.,0,0,0                                108
TTAB10     0,0,0,0                                    112
TTAB10     0,0,0,0                                    116
TTAB10     0,0,0                                      120
TTAB10     15520.,13390.,11330.,9520.                 123   M=.400
TTAB10     7940.,6560.,5370.,4360.                    127
TTAB10     4160.,0,0,0                                131
TTAB10     0,0,0,0                                    135
TTAB10     0,0,0                                      139
TTAB10     16080.,14030.,11980.,10080.                142   M=.550
TTAB10     8420.,6970.,5690.,4620.                    146
TTAB10     4440.,3610.,2750.,0                        150
TTAB10     0,0,0,0                                    154
TTAB10     0,0,0                                      158
TTAB10     16970.,14900.,12990.,11050.                161   M=.700
TTAB10     9220.,7610.,6220.,5110.                    165
TTAB10     4870.,3970.,3040.,2300.                    169
TTAB10     1770.,0,0,0                                173
TTAB10     0,0,0                                      177
TTAB10     17840.,15690.,13790.,11840.                180   M=.800
TTAB10     9950.,8260.,6790.,5520.                    184
TTAB10     5270.,4310.,3300.,2510.                    188
TTAB10     1910.,1460.,1110.,840.                     192
TTAB10     0,0,0                                      196
TTAB10     19000.,16740.,14630.,12710.                199   M=.900
TTAB10     10810.,9030.,7420.,6080.                   203
TTAB10     5790.,4730.,3630.,2760.                    207
TTAB10     2100.,1600.,1210.,920.                     211
TTAB10     0,0,0                                      215
TTAB10     19940.,18610.,16240.,14340.                218   M=1.050
```

ORIGINAL PAGE IS OF POOR QUALITY

TABLE II(a). THRUST OF THE J79-GE-12 ENGINE WHICH POWERS THE F4-C PHANTOM (cont'd).

```
TTAB10    12400.,10500.,8730.,7180.          222
TTAB10    6850.,5610.,4310.,3310.            226
TTAB10    2500.,1890.,1440.,1100.            230
TTAB10    810.,0,0                           234
TTAB10    19800.,18970.,16600.,14690.        237   M=1.077
TTAB10    12690.,10770.,9000.,7400.          241
TTAB10    7070.,5810.,4460.,3420.            245
TTAB10    2590.,1950.,1500.,1130.            249
TTAB10    840.,0,0                           253
TTAB10    19380.,19380.,17680.,15680.        256   M=1.150
TTAB10    13530.,11630.,9820.,8080.          260
TTAB10    7730.,6340.,4890.,3760.            264
TTAB10    2850.,2140.,1630.,1240.            268
TTAB10    920.,0,0                           272
TTAB10    0,19900.,19310.,17030.             275   M=1.247
TTAB10    14790.,12900.,10990.,9060.         279
TTAB10    8680.,7120.,5520.,4240.            283
TTAB10    3220.,2420.,1850.,1400.            287
TTAB10    1050.,0,0                          291
TTAB10    0,20500.,19420.,17390.             294   M=1.272
TTAB10    15180.,13240.,11300.,9310.         298
TTAB10    8960.,7350.,5700.,4380.            302
TTAB10    3340.,2510.,1900.,1450.            306
TTAB10    1100.,0,0                          310
TTAB10    0,0,19950.,18440.                  313   M=1.360
TTAB10    16490.,14330.,12350.,10220.        317
TTAB10    9840.,8080.,6290.,4850.            321
TTAB10    3710.,2800.,2100.,1610.            325
TTAB10    1230.,0,0                          329
TTAB10    0,0,20300.,19630.                  332   M=1.470
TTAB10    17870.,15630.,13640.,11400.        336
TTAB10    10960.,9030.,7030.,5450.           340
TTAB10    4190.,3180.,2390.,1820.            344
TTAB10    1390.,0,0                          348
TTAB10    0,0,0,19800.                       351   M=1.550
TTAB10    18520.,16490.,14540.,12280.        355
TTAB10    11800.,9720.,7580.,5890.           359
TTAB10    4540.,3450.,2600.,1980.            363
TTAB10    1510.,0,0                          367
TTAB10    0,0,0,0                            370   M=1.650
TTAB10    19010.,17380.,15550.,13380.        374
TTAB10    12850.,10590.,8290.,6440.          378
TTAB10    4980.,3790.,2870.,2170.            382
TTAB10    1650.,0,0                          386
TTAB10    0,0,0,0                            389   M=1.750
TTAB10    19200.,17790.,16300.,14340.        393
TTAB10    13820.,11410.,8940.,6960.          397
TTAB10    5400.,4130.,3120.,2350.            401
TTAB10    1790.,0,0                          405
TTAB10    0,0,0,0                            408   M=1.840
TTAB10    0,17900.,16600.,14910.             412
TTAB10    14550.,12010.,9380.,7360.          416
TTAB10    5690.,4390.,3330.,2500.            420
TTAB10    1890.,0,0                          424
```

TABLE II(a). THRUST OF THE J79-GE-12 ENGINE WHICH POWERS THE F4-C PHANTOM (cont'd).

```
TTAB10     0,0,0,0                                   427   M=1.950
TTAB10     0,0,16710.,15250.                         431
TTAB10     14980.,12390.,9700.,7610.                 435
TTAB10     5900.,4560.,3490.,2620.                   439
TTAB10     1960.,0,0                                 443
TTAB10     0,0,0,0                                   446   M=2.100
TTAB10     0,0,16710.,15370.                         450
TTAB10     15070.,12500.,9820.,7690.                 454
TTAB10     6000.,4630.,3570.,2680.                   458
TTAB10     2010.,0,0                                 462
TTAB10     0,0,0,0                                   465   M=2.200
TTAB10     0,0,16650.,15230.                         469
TTAB10     14890.,12390.,9740.,7630.                 473
TTAB10     5960.,4620.,3560.,2680.                   477
TTAB10     2020.,0,0                                 481
TTAB10     0,0,0,0                                   484   M=2.300
TTAB10     0,0,0,14920.                              488
TTAB10     14510.,12060.,9510.,7420.                 492
TTAB10     5810.,4530.,3470.,2640.                   496
TTAB10     2000.,0,0                                 500
TTAB10     0,0,0,0                                   503   M=2.400
TTAB10     0,0,0,0                                   507
TTAB10     13780.,11470.,9060.,7100.                 511
TTAB10     5560.,4320.,3330.,2520.                   515
TTAB10     1930.,0,0                                 519
TTAB10     320.,280.,250.,0                          522   IDLE,M=0
TTAB10     0,0,0,0                                   526
TTAB10     0,0,0,0                                   530
TTAB10     0,0,0,0                                   534
TTAB10     0,0,0                                     538
TTAB10     260.,220.,200.,0                          541   M=.050
TTAB10     0,0,0,0                                   545
TTAB10     0,0,0,0                                   549
TTAB10     0,0,0,0                                   553
TTAB10     0,0,0                                     557
TTAB10     200.,180.,160.,0                          560   M=.100
TTAB10     0,0,0,0                                   564
TTAB10     0,0,0,0                                   568
TTAB10     0,0,0,0                                   572
TTAB10     0,0,0                                     576
TTAB10     -40.,-30.,-10.,0                          579   M=.250
TTAB10     10.,30.,110.,200.                         583
TTAB10     230.,300.,350.,350.                       587
TTAB10     0,0,0,0                                   591
TTAB10     0,0,0                                     595
TTAB10     -310.,-260.,-210.,-165.                   598   M=.400
TTAB10     -130.,-75.,10.,105.                       602
TTAB10     120.,190.,255.,290.                       606
TTAB10     0,0,0,0                                   610
TTAB10     0,0,0                                     614
TTAB10     -610.,-510.,-440.,-355.                   617   M=.550
TTAB10     -295.,-220.,-125.,-10.                    621
TTAB10     10.,70.,155.,220.                         625
                                                     629
```

TABLE II(a). THRUST OF THE J79-GE-12 ENGINE WHICH POWERS THE F4-C PHANTOM (cont'd).

```
TTAB10    0,0,0                                633
TTAB10    -1005.,-860.,-730.,-620.             636    M=.700
TTAB10    -510.,-390.,-260.,-140.              640
TTAB10    -100.,-40.,60.,150.                  644
TTAB10    0,0,0,0                              648
TTAB10    0,0,0                                652
TTAB10    -1380.,-1150.,-1000.,-860.           655    M=.800
TTAB10    -690.,-525.,-370.,-220.              659
TTAB10    -190.,-100.,0,100.                   663
TTAB10    0,0,0,0                              667
TTAB10    0,0,0                                671
TTAB10    -1910.,-1550.,-1300.,-1060.          674    M=.900
TTAB10    -855.,-655.,-500.,-320.              678
TTAB10    -280.,-190.,-60.,50.                 682
TTAB10    0,0,0,0                              686
TTAB10    0,0,0                                690
TTAB10    -2450.,-2010.,-1640.,-1350.          693    M=1.050
TTAB10    -1095.,-880.,-695.,-480.             697
TTAB10    -445.,-310.,-160.,-30.               701
TTAB10    0,0,0,0                              705
TTAB10    0,0,0                                709
TTAB10    -2390.,-2110.,-1705.,-1410.          712    M=1.077
TTAB10    -1140.,-910.,-725.,-505.             716
TTAB10    -475.,-340.,-180.,-50.               720
TTAB10    0,0,0,0                              724
TTAB10    0,0,0                                728
TTAB10    -940.,-2350.,-1910.,-1560.           731    M=1.150
TTAB10    -1250.,-1010.,-810.,-600.            735
TTAB10    -550.,-405.,-230.,-90.               739
TTAB10    0,0,0,0                              743
TTAB10    0,0,0                                747
TTAB10    0,-790.,-2180.,-1755.                750    M=1.247
TTAB10    -1420.,-1140.,-910.,-700.            754
TTAB10    -655.,-495.,-300.,-145.              758
TTAB10    0,0,0,0                              762
TTAB10    0,0,0                                766
TTAB10    0,-140.,-2050.,-1810.                769    M=1.272
TTAB10    -1460.,-1160.,-940.,-725.            773
TTAB10    -690.,-520.,-310.,-155.              777
TTAB10    0,0,0,0                              781
TTAB10    0,0,0                                785
TTAB10    0,0,0,-1960.                         788    M=1.360
TTAB10    -1590.,-1260.,-1015.,-795.           792
TTAB10    -755.,-600.,-375.,-210.              796
TTAB10    0,0,0,0                              800
TTAB10    0,0,0                                804
TTAB10    0,0,3000.,600.                       807    M=1.470
TTAB10    -1550.,-1390.,-1090.,-855.           811
TTAB10    -810.,-670.,-450.,-275.              815
TTAB10    0,0,0,0                              819
TTAB10    0,0,0                                823
TTAB10    0,0,0,2650.                          826    M=1.550
TTAB10    350.,-1200.,-1125.,-895.             830
TTAB10    -845.,-705[illegible]                834
```

TABLE II(a). THRUST OF THE J79-GE-12 ENGINE WHICH POWERS THE F4-C PHANTOM (cont'd).

```
TTAB10     0,0,0,0                          838
TTAB10     0,0,0                            842
TTAB10     0,0,0,0                          845   M=1.650
TTAB10     2400.,525.,-1175.,-925.          849
TTAB10     -870.,-740.,-595.,-395.          853
TTAB10     0,0,0,0                          857
TTAB10     0,0,0                            861
TTAB10     0,0,0,0                          864   M=1.750
TTAB10     1280.,2450.,660.,-955.           868
TTAB10     -900.,-780.,-650.,-470.          872
TTAB10     0,0,0,0                          876
TTAB10     0,0,0                            880
TTAB10     0,0,0,0                          883   M=1.840
TTAB10     0,1380.,2350.,510.               887
TTAB10     80.,130.,75.,60.                 891
TTAB10     0,0,0,0                          895
TTAB10     0,0,0                            899
TTAB10     0,0,0,0                          902   M=1.950
TTAB10     0,0,1340.,2400.                  906
TTAB10     2300.,1950.,1500.,1200.          910
TTAB10     0,0,0,0                          914
TTAB10     0,0,0                            918
TTAB10     0,0,0,0                          921   M=2.100
TTAB10     0,0,210.,1170.                   925
TTAB10     1275.,1030.,810.,645.            929
TTAB10     0,0,0,0                          933
TTAB10     0,0,0                            937
TTAB10     0,0,0,0                          940   M=2.200
TTAB10     0,0,-700.,390.                   944
TTAB10     575.,470.,370.,280.              948
TTAB10     0,0,0,0                          952
TTAB10     0,0,0                            956
TTAB10     0,0,0,0                          959   M=2.300
TTAB10     0,0,0,-460.                      963
TTAB10     -230.,-180.,-140.,-125.          967
TTAB10     0,0,0,0                          971
TTAB10     0,0,0                            975
TTAB10     0,0,0,0                          978   M=2.400
TTAB10     0,0,0,0                          982
TTAB10     -1240.,-1000.,-800.,-640.        986
TTAB10     0,0,0,0                          990
TTAB10     0,0,0                            994
```

TABLE II(b). FUEL FLOW OF THE J79-GE-12 ENGINE WHICH POWERS THE F4-C PHANTOM.

```
IT11W    19
IT11X    25
IT11Y    2
TTAB11   0,5000.,10000.,15000.                      1     ALT
TTAB11   20000.,25000.,30000.,35000.                5
TTAB11   36089.,40000.,45000.,50000.                9
TTAB11   55000.,60000.,65000.,70000.                13
TTAB11   75000.,75010.,120000.                      17
TTAB11   0,.050,.100,.250                           20    MACH
TTAB11   .400,.550,.700,.800                        24
TTAB11   .900,1.050,1.077,1.150                     28
TTAB11   1.247,1.272,1.360,1.470                    32
TTAB11   1.550,1.650,1.750,1.840                    36
TTAB11   1.950,2.100,2.200,2.300,2.400              40
TTAB11   1.,2.                                      45    MAX,IDLE
TTAB11   28800.,24600.,20700.,0                     47    MAX,M=0
TTAB11   0,0,0,0                                    51
TTAB11   0,0,0,0                                    55
TTAB11   0,0,0,0                                    59
TTAB11   0,0,0                                      63
TTAB11   30750.,26300.,22000.,0                     66    M=.050
TTAB11   0,0,0,0                                    70
TTAB11   0,0,0,0                                    74
TTAB11   0,0,0,0                                    78
TTAB11   0,0,0                                      82
TTAB11   31650.,27050.,22650.,0                     85    M=.100
TTAB11   0,0,0,0                                    89
TTAB11   0,0,0,0                                    93
TTAB11   0,0,0,0                                    97
TTAB11   0,0,0                                      101
TTAB11   33480.,28600.,24120.,20050.                104   M=.250
TTAB11   16750.,0,0,0                               108
TTAB11   0,0,0,0                                    112
TTAB11   0,0,0,0                                    116
TTAB11   0,0,0                                      120
TTAB11   35300.,30380.,25730.,21500.                123   M=.400
TTAB11   17850.,14700.,12180.,9950.                 127
TTAB11   9580.,0,0,0                                131
TTAB11   0,0,0,0                                    135
TTAB11   0,0,0                                      139
TTAB11   37580.,32600.,27850.,23450.                142   M=.550
TTAB11   19400.,15950.,13080.,10780.                146
TTAB11   10310.,8750.,6940.,0                       150
TTAB11   0,0,0,0                                    154
TTAB11   0,0,0                                      158
TTAB11   40570.,35320.,30550.,25960.                161   M=.700
TTAB11   21600.,17730.,14550.,11870.                165
TTAB11   11390.,9630.,7740.,6030.                   169
TTAB11   4680.,0,0,0                                173
TTAB11   0,0,0                                      177
TTAB11   43280.,37450.,32550.,27820.                180   M=.800
TTAB11   23420.,19350.,15820.,12860.                184
TTAB11   12310.,10390.,8390.,6570.                  188
TTAB11   5080.,3970.,3060.,2360.                    192
TTAB11   0,0,0                                      196
TTAB11   46550.,40260.,34750.,29820.                199   M=.900
TTAB11   25380.,21130.,17350.,14050.                203
TTAB11   13380.,11280.,9110.,7180.                  207
TTAB11   5570.,4310.,3350.,2590.                    211
TTAB11   0,0,0                                      215
TTAB11   47650.,45450.,38800.,33420.                218   M=1.050
TTAB11   28550.,24100.,20020.,16250.                222
TTAB11   15550.,13040.,10490.,8340.                 226
TTAB11   6490.,5010.,3900.,3000.                    230
TTAB11   2300.,0,0                                  234
```

TABLE II (b). FUEL FLOW OF THE J79-GE-12 ENGINE WHICH POWERS THE F4-C PHANTOM (cont'd).

```
TTAB11      29100.,24650.,20550.,16670.          241
TTAB11      16010.,13420.,10780.,8600.           245
TTAB11      6690.,5170.,4000.,3090.              249
TTAB11      2380.,0,0                            253
TTAB11      47170.,46650.,42220.,36380.          256    M=1.150
TTAB11      30750.,26240.,22000.,17950.          260
TTAB11      17270.,14450.,11570.,9270.           264
TTAB11      7230.,5600.,4330.,3340.              268
TTAB11      2570.,0,0                            272
TTAB11      0,47200.,45850.,39530.               275    M=1.247
TTAB11      33350.,28450.,24000.,19770.          279
TTAB11      19020.,15900.,12710.,10210.          283
TTAB11      8010.,6230.,4820.,3720.              287
TTAB11      2880.,0,0                            291
TTAB11      0,47330.,45980.,40320.               294    M=1.272
TTAB11      34100.,29120.,24570.,20300.          298
TTAB11      19520.,16310.,13020.,10480.          302
TTAB11      8270.,6420.,4970.,3840.              306
TTAB11      2970.,0,0                            310
TTAB11      0,0,46370.,42680.                    313    M=1.360
TTAB11      37130.,31480.,26550.,22030.          317
TTAB11      21180.,17690.,14100.,11320.          321
TTAB11      9020.,7060.,5470.,4230.              325
TTAB11      3290.,0,0                            329
TTAB11      0,0,46670.,45000.                    332    M=1.470
TTAB11      40250.,34750.,29200.,24350.          336
TTAB11      23350.,19530.,15520.,12430.          340
TTAB11      10000.,7900.,6120.,4770.             344
TTAB11      3700.,0,0                            348
TTAB11      0,0,0,45420.                         351    M=1.550
TTAB11      41900.,36650.,31330.,26150.          355
TTAB11      25070.,20940.,16630.,13310.          359
TTAB11      10680.,8570.,6630.,5180.             363
TTAB11      4000.,0,0                            367
TTAB11      0,0,0,0                              370    M=1.650
TTAB11      43400.,38500.,33970.,28450.          374
TTAB11      27340.,22730.,18090.,14420.          378
TTAB11      11550.,9330.,7330.,5700.             382
TTAB11      4420.,0,0                            386
TTAB11      0,0,0,0                              389    M=1.750
TTAB11      44330.,39850.,35770.,30700.          393
TTAB11      29650.,24600.,19560.,15580.          397
TTAB11      12450.,10030.,8030.,6270.            401
TTAB11      4870.,0,0                            405
TTAB11      0,0,0,0                              408    M=1.840
TTAB11      0,40670.,36670.,32300.               412
TTAB11      31310.,26050.,20670.,16440.          416
TTAB11      13100.,10520.,8510.,6710.            420
TTAB11      5210.,0,0                            424
TTAB11      0,0,0,0                              427    M=1.950
TTAB11      0,0,37400.,33470.                    431
TTAB11      32620.,27190.,21540.,17120.          435
TTAB11      13640.,10930.,8840.,7100.            439
TTAB11      5540.,0,0                            443
```

TABLE II(b). FUEL FLOW OF THE J79-GE-12 ENGINE WHICH POWERS THE F4-C PHANTOM (cont'd).

```
TTAB11      0,0,0,0                                   446   M=2.100
TTAB11      0,0,38330.,34450.                         450
TTAB11      33680.,28080.,22220.,17670.               454
TTAB11      14100.,11280.,9110.,7370.                 458
TTAB11      5820.,0,0                                 462
TTAB11      0,0,0,0                                   465   M=2.200
TTAB11      0,0,38940.,34800.                         469
TTAB11      33930.,28300.,22440.,17810.               473
TTAB11      14200.,11380.,9190.,7440.                 477
TTAB11      5940.,0,0                                 481
TTAB11      0,0,0,0                                   484   M=2.300
TTAB11      0,0,0,34950.                              488
TTAB11      33820.,28190.,22380.,17780.               492
TTAB11      14170.,11370.,9160.,7430.                 496
TTAB11      5990.,0,0                                 500
TTAB11      0,0,0,0                                   503   M=2.400
TTAB11      0,0,0,0                                   507
TTAB11      33140.,27640.,21970.,17450.               511
TTAB11      13930.,11160.,9020.,7320.                 515
TTAB11      5960.,0,0                                 519
TTAB11      1275.,1085.,915.,0                        522   IDLE,M=0
TTAB11      0,0,0,0                                   526
TTAB11      0,0,0,0                                   530
TTAB11      0,0,0,0                                   534
TTAB11      0,0,0                                     538
TTAB11      1195.,1005.,860.,0                        541   M=.050
TTAB11      0,0,0,0                                   545
TTAB11      0,0,0,0                                   549
TTAB11      0,0,0,0                                   553
TTAB11      0,0,0                                     557
TTAB11      1140.,970.,835.,0                         560   M=.100
TTAB11      0,0,0,0                                   564
TTAB11      0,0,0,0                                   568
TTAB11      0,0,0,0                                   572
TTAB11      0,0,0                                     576
TTAB11      1045.,900.,765.,655.                      579   M=.250
TTAB11      550.,500.,500.,500.                       583
TTAB11      500.,500.,500.,500.                       587
TTAB11      0,0,0,0                                   591
TTAB11      0,0,0                                     595
TTAB11      955.,810.,700.,600.                       598   M=.400
TTAB11      500.,500.,500.,500.                       602
TTAB11      500.,500.,500.,500.                       606
TTAB11      0,0,0,0                                   610
TTAB11      0,0,0                                     614
TTAB11      805.,685.,585.,500.                       617   M=.550
TTAB11      500.,500.,500.,500.                       621
TTAB11      500.,500.,500.,500.                       625
TTAB11      0,0,0,0                                   629
TTAB11      0,0,0                                     633
TTAB11      575.,500.,500.,500.                       636   M=.700
TTAB11      500.,500.,500.,500.                       640
TTAB11      500.,500.,500.,500.                       644
TTAB11      0,0,0,0                                   648
```

TABLE II(b). FUEL FLOW OF THE J79-GE-12 ENGINE WHICH POWERS THE F4-C PHANTOM (cont'd).

```
TTAB11    0,0,0                                652
TTAB11    590.,515.,500.,500.                  655   M=.800
TTAB11    500.,500.,500.,500.                  659
TTAB11    500.,500.,500.,500.                  663
TTAB11    0,0,0,0                              667
TTAB11    0,0,0                                671
TTAB11    1305.,1090.,905.,675.                674   M=.900
TTAB11    565.,500.,500.,500.                  678
TTAB11    500.,500.,500.,500.                  682
TTAB11    0,0,0,0                              686
TTAB11    0,0,0                                690
TTAB11    1655.,1390.,1155.,950.               693   M=1.050
TTAB11    770.,630.,500.,500.                  697
TTAB11    500.,500.,500.,500.                  701
TTAB11    0,0,0,0                              705
TTAB11    0,0,0                                709
TTAB11    2000.,1425.,1195.,985.               712   M=1.077
TTAB11    800.,650.,500.,500.                  716
TTAB11    500.,500.,500.,500.                  720
TTAB11    0,0,0,0                              724
TTAB11    0,0,0                                728
TTAB11    4375.,1555.,1295.,1070.              731   M=1.150
TTAB11    870.,715.,550.,500.                  735
TTAB11    500.,500.,500.,500.                  739
TTAB11    0,0,0,0                              743
TTAB11    0,0,0                                747
TTAB11    0,4030.,1445.,1200.                  750   M=1.247
TTAB11    990.,805.,640.,500.                  754
TTAB11    500.,500.,500.,500.                  758
TTAB11    0,0,0,0                              762
TTAB11    0,0,0                                766
TTAB11    0,4900.,1720.,1235.                  769   M=1.272
TTAB11    1015.,835.,655.,520.                 773
TTAB11    500.,500.,500.,500.                  777
TTAB11    0,0,0,0                              781
TTAB11    0,0,0                                785
TTAB11    0,8500.,4450.,1400.                  788   M=1.360
TTAB11    1145.,920.,735.,585.                 792
TTAB11    545.,500.,500.,500.                  796
TTAB11    0,0,0,0                              800
TTAB11    0,0,0                                804
TTAB11    0,0,8500.,4600.                      807   M=1.470
TTAB11    1400.,1055.,845.,675.                811
TTAB11    630.,505.,500.,500.                  815
TTAB11    0,0,0,0                              819
TTAB11    0,0,0                                823
TTAB11    0,0,0,7400.                          826   M=1.550
TTAB11    3860.,1390.,945.,755.                830
TTAB11    700.,575.,500.,500.                  834
TTAB11    0,0,0,0                              838
TTAB11    0,0,0                                842
TTAB11    0,0,0,0                              845   M=1.650
TTAB11    6750.,3740.,1105.,855.               849
TTAB11    815.,665.,[illegible]                853
```

ORIGINAL PAGE IS OF POOR QUALITY

TABLE II(b). FUEL FLOW OF THE J79-GE-12 ENGINE WHICH POWERS THE F4-C PHANTOM (cont'd).

```
TTAB11      0,0,0                                   861
TTAB11      0,0,0,0                                 864   M=1.750
TTAB11      5905.,6250.,3395.,980.                  868
TTAB11      0,0,0,0                                 857
TTAB11      950.,760.,620.,510.                     872
TTAB11      0,0,0,0                                 876
TTAB11      0,0,0                                   880
TTAB11      0,0,0,0                                 883   M=1.840
TTAB11      0,5445.,5750.,2890.                     887
TTAB11      2340.,1860.,1490.,1170.                 891
TTAB11      0,0,0,0                                 895
TTAB11      0,0,0                                   899
TTAB11      0,0,0,0                                 902   M=1.950
TTAB11      0,0,4895.,5250.                         906
TTAB11      4900.,4150.,3250.,2580.                 910
TTAB11      0,0,0,0                                 914
TTAB11      0,0,0                                   918
TTAB11      0,0,0,0                                 921   M=2.100
TTAB11      0,0,4155.,4235.                         925
TTAB11      4235.,3510.,2750.,2160.                 929
TTAB11      0,0,0,0                                 933
TTAB11      0,0,0                                   937
TTAB11      0,0,0,0                                 940   M=2.200
TTAB11      0,0,3480.,3715.                         944
TTAB11      3780.,3140.,2450.,1925.                 948
TTAB11      0,0,0,0                                 952
TTAB11      0,0,0                                   956
TTAB11      0,0,0,0                                 959   M=2.300
TTAB11      0,0,0,3100.                             963
TTAB11      3190.,2630.,2065.,1620.                 967
TTAB11      0,0,0,0                                 971
TTAB11      0,0,0                                   975
TTAB11      0,0,0,0                                 978   M=2.400
TTAB11      0,0,0,0                                 982
TTAB11      2335.,1935.,1525.,1175.                 986
TTAB11      0,0,0,0                                 990
TTAB11      0,0,0                                   994
```

Aerodynamics

Aerodynamics for the F4-C are functions of Mach number, altitude, and angle-of-attack. For three-degree-of-freedom trajectory calculations lift and drag coefficient variations are required. Lift coefficient is a direct table lookup of the form

$$C_L = C_L\ (\alpha,\ M,\ h)$$

Drag coefficient has two components

$$C_D = C_{D_1}\ (\alpha,\ M,\ h) + \Delta C_L\ (M)$$

Actual values of lift coefficient and drag coefficients employed for the F4-C trajectory calculations are given in Tables III(a) to III(c). Tabular format of these tables is similar to that employed in the propulsion section. Source of the F4-C data is the Air Force Flight Dynamics Laboratory through the study of Reference 9.

TABLE III(a). LIFT COEFFICIENT vs. α and M , F4-C AIRCRAFT

```
AREFF      530.
INDAER     1
INDBAD     1
INDA90     1
IA90X      15
IA90Y      12
IA90Z      0
ATAB90     -4.0,-2.0,0.0,2.0,4.0                     1     ALPHD
ATAB90     6.0,8.0,10.0,12.0,14.0                    6
ATAB90     16.0,18.0,20.0,22.0,24.0                  11
ATAB90     0.0,0.5,0.7,0.8,0.9,0.95                  16    AMACH
ATAB90     1.1,1.3,1.5,1.7,2.0,2.4                   22
ATAB90     -.210,-.102,.009,.120,.237                28    M=0.0
ATAB90     .347,.460,.565,.658,.740                  33
ATAB90     .810,.849,.832,.853,.895                  38
ATAB90     -.210,-.102,.009,.120,.237                43    M=0.5
ATAB90     .347,.460,.565,.658,.740                  48
ATAB90     .810,.849,.832,.853,.895                  53
ATAB90     -.217,-.106,.009,.122,.238                58    M=0.7
ATAB90     .353,.469,.570,.662,.742                  63
ATAB90     .807,.815,.810,.852,.890                  68
ATAB90     -.221,-.109,.009,.126,.241                73    M=0.8
ATAB90     .363,.486,.587,.675,.749                  78
ATAB90     .809,.820,.819,0.,0.                      83
ATAB90     -.253,-.121,.011,.142,.277                88    M=0.9
ATAB90     .391,.494,.590,.677,.748                  93
ATAB90     .804,.831,.859,0.,0.                      98
ATAB90     -.260,-.119,.019,.151,.277                103   M=0.95
ATAB90     .395,.504,.598,.680,.752                  108
ATAB90     .813,.865,.906,.949,.988                  113
ATAB90     -.250,-.123,.005,.131,.255                118   M=1.1
ATAB90     .383,.520,.620,.708,.789                  123

ATAB90     .860,.927,.983,1.029,1.062                128
ATAB90     -.222,-.119,-.012,.095,.201               133   M=1.3
ATAB90     .308,.412,.516,.617,.703                  138
ATAB90     .785,.860,.928,.981,1.023                 143
ATAB90     -.207,-.113,-.019,.076,.170               148   M=1.5
ATAB90     .261,.351,.437,.516,.592                  153
ATAB90     .661,.727,.783,0.,0.                      158
ATAB90     -.180,-.101,-.020,.061,.141               163   M=1.7
ATAB90     .223,.303,.380,.452,.519                  168
ATAB90     .582,.642,.699,0.,0.                      173
ATAB90     -.152,-.083,-.015,.054,.121               178   M=2.0
ATAB90     .189,.255,.320,.384,.447                  183
ATAB90     .506,.561,.613,0.,0.                      188
ATAB90     -.120,-.061,-.004,.052,.113               193   M=2.4
ATAB90     .170,.226,.282,.339,.388                  198
ATAB90     .435,0.,0.,0.,0.                          203
```

ORIGINAL PAGE IS OF POOR QUALITY

TABLE III(b). DRAG COEFFICIENT vs. C_L and MACH., F4-C AIRCRAFT

```
INDA91    1
IA91X     17
IA91Y     33
ATAB91    0.,.05,.1,.15                        1
ATAB91    .2,.25,.3,.35                        5
ATAB91    .4,.45,.5,.55                        9
ATAB91    .6,.65,.7,.75                        13
ATAB91    .8                                   17
ATAB91    0.,.400,.450,.500                    18
ATAB91    .550,.600,.650,.700                  22
ATAB91    .750,.800,.825,.850                  26
ATAB91    .875,.900,.925,.950                  30
ATAB91    .975,1.00,1.05,1.10                  34
ATAB91    1.20,1.30,1.40,1.50                  38
ATAB91    1.60,1.70,1.80,1.90                  42
ATAB91    2.00,2.10,2.20,2.30                  46
ATAB91    2.40                                 50
ATAB91    .0180,.0183,.0191,.0204              51     M=0.
ATAB91    .0225,.0252,.0285,.0332              55
ATAB91    .0395,.0475,.0575,.0700              59
ATAB91    .0862,.1055,.1275,.1505              63
ATAB91    .1780                                67
ATAB91    .0180,.0183,.0191,.0204              68     M=.4
ATAB91    .0225,.0252,.0285,.0332              72
ATAB91    .0395,.0475,.0575,.0700              76
ATAB91    .0862,.1055,.1275,.1505              80
ATAB91    .1780                                84
ATAB91    .0180,.0183,.0191,.0204              85     M=.45
ATAB91    .0225,.0252,.0285,.0332              89
ATAB91    .0395,.0475,.0575,.0702              93
ATAB91    .0865,.1064,.1285,.1520              97
ATAB91    .1795                                101
ATAB91    .0180,.0183,.0191,.0204              102    M=.5
ATAB91    .0225,.0252,.0285,.0332              106
ATAB91    .0395,.0475,.0579,.0715              110
ATAB91    .0880,.1080,.1303,.1535              114
ATAB91    .1809                                118
ATAB91    .0180,.0183,.0191,.0204              119    M=.55
```

TABLE III(b). DRAG COEFFICIENT vs. C_L and MACH, F4-C AIRCRAFT
(Cont'd.)

```
ATAB91     ,0225,.0252,.0285,.0332          123
ATAB91     ,0396,.0477,.0585,.0725          127
ATAB91     ,0900,.1100,.1323,.1555          131
ATAB91     ,1825                            135
ATAB91     ,0180,.0183,.0191,.0204          136    M=.6
ATAB91     ,0225,.0252,.0287,.0336          140
ATAB91     ,0399,.0488,.0600,.0743          144
ATAB91     ,0919,.1120,.1345,.1575          148
ATAB91     ,1844                            152
ATAB91     ,0180,.0183,.0191,.0204          153    M=.65
ATAB91     ,0225,.0252,.0289,.0341          157
ATAB91     ,0410,.0502,.0615,.0760          161
ATAB91     ,0940,.1143,.1365,.1600          165
ATAB91     ,1869                            169
ATAB91     ,0180,.0183,.0191,.0205          170    M=.7
ATAB91     ,0226,.0256,.0294,.0347          174
ATAB91     ,0424,.0515,.0635,.0779          178
ATAB91     ,0962,.1165,.1389,.1625          182
ATAB91     ,1902                            186
ATAB91     ,0184,.0186,.0194,.0208          187    M=.75
ATAB91     ,0228,.0258,.0301,.0361          191
ATAB91     ,0439,.0532,.0660,.0802          195
ATAB91     ,0984,.1190,.1416,.1658          199
ATAB91     ,1943                            203
ATAB91     ,0188,.0193,.0202,.0214          204    M=.8
ATAB91     ,0235,.0267,.0312,.0374          208
ATAB91     ,0455,.0555,.0677,.0825          212
ATAB91     ,1010,.1220,.1450,.1700          216
ATAB91     ,1990                            220
ATAB91     ,0194,.0198,.0204,.0219          221    M=.825
ATAB91     ,0241,.0273,.0319,.0382          225
ATAB91     ,0463,.0566,.0692,.0839          229
ATAB91     ,1027,.1240,.1470,.1723          233
ATAB91     ,2017                            237
ATAB91     ,0200,.0202,.0212,.0224          238    M=.85
ATAB91     ,0246,.0279,.0327,.0391          242
ATAB91     ,0474,.0578,.0704,.0850          246
ATAB91     ,1039,.1250,.1490,.1748          250
ATAB91     ,2045                            254
ATAB91     ,0206,.0211,.0219,.0235          255    M=.875
ATAB91     ,0257,.0293,.0341,.0406          259
ATAB91     ,0491,.0598,.0722,.0867          263
ATAB91     ,1060,.1276,.1512,.1771          267
ATAB91     ,2075                            271
ATAB91     ,0214,.0218,.0229,.0246          272    M=.9
ATAB91     ,0269,.0306,.0357,.0426          276
ATAB91     ,0515,.0620,.0742,.0885          280
ATAB91     ,1075,.1300,.1535,.1800          284
ATAB91     ,2103                            288
ATAB91     ,0230,.0236,.0245,.0263          289    M=.925
ATAB91     ,0289,.0330,.0384,.0456          293
ATAB91     ,0538,.0643,.0768,.0913          297
ATAB91     ,1096,.1321,.1508,.1827          301
ATAB91     ,2133                            305
```

TABLE III(b). DRAG COEFFICIENT vs. C_L and MACH , F4-C AIRCRAFT (Cont'd.)

```
ATAB91   ,.0255,.0258,.0269,.0287                306   M=.95
ATAB91   ,.0320,.0367,.0423,.0496                310
ATAB91   ,.0578,.0678,.0800,.0942                314
ATAB91   ,.1114,.1340,.1583,.1858                318
ATAB91   ,.2168                                  322
ATAB91   ,.0320,.0325,.0338,.0357                323   M=.975
ATAB91   ,.0385,.0423,.0476,.0542                327
ATAB91   ,.0622,.0719,.0837,.0970                331
ATAB91   ,.1138,.1359,.1605,.1885                335
ATAB91   ,.2200                                  339
ATAB91   ,.0360,.0365,.0378,.0400                340   M=1.0
ATAB91   ,.0428,.0468,.0520,.0582                344
ATAB91   ,.0659,.0754,.0863,.0998                348
ATAB91   ,.1164,.1384,.1633,.1918                352
ATAB91   ,.2233                                  356
ATAB91   ,.0387,.0394,.0407,.0429                357   M=1.05
ATAB91   ,.0461,.0504,.0559,.0624                361
ATAB91   ,.0702,.0798,.0911,.1045                365
ATAB91   ,.1214,.1433,.1689,.1984                369
ATAB91   ,.2299                                  373
ATAB91   ,.0404,.0411,.0428,.0452                374   M=1.1
ATAB91   ,.0487,.0532,.0588,.0657                378
ATAB91   ,.0737,.0835,.0955,.1091                382
ATAB91   ,.1262,.1482,.1745,.2047                386
ATAB91   ,.2367                                  390
ATAB91   ,.0340,.0345,.0364,.0395                391   M=1.2
ATAB91   ,.0434,.0484,.0545,.0619                395
ATAB91   ,.0716,.0831,.0965,.1113                399
ATAB91   ,.1293,.1520,.1790,.2105                403
ATAB91   ,.2440                                  407
ATAB91   ,.0350,.0358,.0377,.0408                408   M=1.3
ATAB91   ,.0452,.0508,.0578,.0666                412
ATAB91   ,.0779,.0912,.1060,.1232                416
ATAB91   ,.1428,.1684,.1975,.2300                420
ATAB91   ,.2650                                  424
ATAB91   ,.0357,.0364,.0384,.0418                425   M=1.4
ATAB91   ,.0468,.0530,.0610,.0710                429
ATAB91   ,.0837,.0987,.1158,.1357                433
ATAB91   ,.1573,.1855,.2175,.2530                437
ATAB91   ,.2895                                  441
ATAB91   ,.0362,.0369,.0390,.0426                442   M=1.5
ATAB91   ,.0482,.0551,.0640,.0753                446
ATAB91   ,.0894,.1063,.1253,.1480                450
ATAB91   ,.1725,.2042,.2385,.2760                454
ATAB91   ,.3170                                  458
ATAB91   ,.0365,.0373,.0395,.0434                459   M=1.6
ATAB91   ,.0492,.0569,.0669,.0795                463
ATAB91   ,.0948,.1135,.1348,.1615                467
ATAB91   ,.1925,.2270,.2655,.3060                471
ATAB91   ,.3480                                  475
ATAB91   ,.0368,.0377,.0402,.0441                476   M=1.7
ATAB91   ,.0502,.0586,.0697,.0833                480
ATAB91   ,.1000,.1205,.1444,.1740                484
ATAB91   ,.2090,.2470,.2880,.3310                488
```

TABLE III(b). DRAG COEFFICIENT vs. C_L and MACH, F4-C AIRCRAFT
(Cont'd.)

```
ATAB91    .3780                              492
ATAB91    .0370,.0380,.0404,.0446            493   M=1.8
ATAB91    .0509,.0602,.0723,.0871            497
ATAB91    1052,.1272,.1528,.1830             501
ATAB91    .2232,.2650,.3090,.3560            505
ATAB91    .4060                              509
ATAB91    .0370,.0382,.0407,.0450            510   M=1.9
ATAB91    .0518,.0617,.0747,.0907            514
ATAB91    .1103,.1339,.1604,.1948            518
ATAB91    .2350,.2785,.3250,.3740            522
ATAB91    .4230                              526
ATAB91    .0370,.0383,.0410,.0454            527   M=2.0
ATAB91    .0527,.0632,.0772,.0945            531
ATAB91    .1153,.1401,.1675,.2037            535
ATAB91    .2450,.2890,.3360,.3860            539
ATAB91    .4375                              543
ATAB91    .0370,.0384,.0411,.0461            544   M=2.1
ATAB91    .0535,.0645,.0797,.0982            548
ATAB91    1204,.1454,.1738,.2107             552
ATAB91    .2525,.2970,.3460,.3990            556
ATAB91    .4490                              560
ATAB91    .0370,.0384,.0412,.0463            561   M=2.2
ATAB91    .0540,.0659,.0820,.1015,           565
ATAB91    .1254,.1506,.1800,.2175            569
ATAB91    .2600,.3060,.3550,.4080            573
ATAB91    .4590                              577
ATAB91    .0370,.0385,.0413,.0466            578   M=2.3
ATAB91    .0544,.0673,.0844,.1051            582
ATAB91    .1297,.1553,.1854,.2235            586
ATAB91    .2655,.3125,.3630,.4165            590
ATAB91    .4670                              594
ATAB91    .0370,.0386,.0414,.0468            595   M=2.4
ATAB91    .0550,.0686,.0868,.1085            599
ATAB91    .1333,.1595,.1900,.2288            603
ATAB91    .2715,.3190,.3700,.4250            607
ATAB91    .4750                              611
```

ORIGINAL PAGE IS
OF POOR QUALITY

TABLE III(c). ADDITIONAL DRAG COEFFICIENT vs. MACH NUMBER

F4-C AIRCRAFT

```
INDA01      1
INDA01      0
ATAB01      26,0.,-.0065,.7,-.0065,.725,-.0066
ATAB01      .75,-.00689,.8,-.00751,.825,-.00778                    8
ATAB01      .85,-.008,.875,-.00817,.89,-.0082                     14
ATAB01      .9,-.00817,.925,-.00792,.95,-.00746                   20
ATAB01      .97,-.00675,.975,-.0069,1.,-.00686                    26
ATAB01      1.05,-.00688,1.1,-.0069,1.15,-.00282                  32
ATAB01      1.2,.00156,1.3,.00154,1.4,.0015,1.6,.00142            38
ATAB01      1.8,.00134,2.,.00128,2.2,.0012,10.0,.0012             46
```

DATA CALIBRATION BY
LEVEL ACCELERATIONS

Trajectory Calculations

A series of level acceleration trajectory computations were performed to delineate maximum Mach number capabilities using the aircraft propulsive and aerodynamic characteristics of the previous section. Trajectories were simulated by using the commanded flight path angle (γ) option of the Reference 1 and 2 program. That is, the vehicle flies an angle-of-attack schedule which attempts to maintain a specified flight path angle history, in this case

$$\gamma = \gamma(t) = 0 \tag{195}$$

Table IV(a) presents a typical acceleration starting at 40000 feet with an initial velocity of 1000 feet per second. Vehicle initial mass is 1250 slugs (40217 lbs. weight). Maximum Mach number achieved is M = 2.06 at a time T = 375 seconds and range R = 99.02 nautical miles. Theoretical maximum altitude capability at the end point based on energy conversion is E = 102000 feet. Table IV(b) presents the terminal states achieved in a series of level accelerations starting at initial altitudes varying from 20000 to 50000 feet.

Some points should be made regarding these trajectory calculations. First, the maximum Mach number achievable is a function of the vehicle weight. As the weight diminishes vehicle lift coefficient for level flight diminishes and hence a reduction occurs in drag-due-to-lift. As the drag diminishes the vehicle speed can increase until thrust again equals drag. Maximum speed therefore increases slightly with reduced vehicle weight. Second, the flight path control used attempts to steer a given flight path angle by an iterative numerical process. Over the period of time involved (approximately 400 seconds) slight errors in flight path angle cause a cumulative altitude error. Thus initial and final altitudes differ to some extent. The final flight path angles of these simulations have little effect on maximum Mach number. Third, maximum trajectory simulation time was 400 seconds. At the highest altitude this is insufficient time to develop maximum velocities. Thus the maximum attainable Mach number at altitudes in excess of 40000 feet, and the corresponding theoretical altitudes are undefined by the simulations. Subsequent simulations revealed a maximum Mach number capability of 2.0 at 50000 feet. This results in a theoretical altitude capability of 107000 feet.

Figure 20 illustrates the level acceleration trajectories in the Mach altitude plane. Time checks are displayed at 50 second intervals. At the lower altitudes the closeness of the time checks at trajectory termination is an indication that the limiting Mach number for given vehicle weight is being approached. At the higher altitudes (H > 40000 feet) very slow acceleration capability is encountered. However, as the vehicle Mach number increases the increased spacing of the 50 second time checks indicates that the vehicle is travelling below its limiting Mach number.

TABLE IV(a)

EXPLORATORY F4-C ACCELERATION

FROM V = 1000 FT/SEC @ 40000'

T	M	H (FT)	γ^{o}	W (LBS)	R (NM)	E (FT)
0	1.03	40000.	0	40217.	0	55353.
50	1.21	39889.	1.2	39825.	8.93	61127.
100	1.40	39908.	1.4	39355.	19.30	68307.
150	1.60	40121.	1.6	38797.	31.20	77165.
200	1.79	40348.	1.8	38148.	44.65	86892.
250	1.94	40946.	0.1	37430.	59.45	94965.
300	2.01	40583.	0.1	36687.	75.09	99418.
350	2.05	40628.	0.02	35938.	91.11	101421.
375	2.06	40637.	0.01	35569.	99.02	101951.

TABLE IV(b)

TERMINAL STATES F4-C ACCELERATIONS

RUN	H_O	T_F	M_F	H_F	γ_F	W_F	R_F	E_F
1	40000.	375.	2.06	40637.	.01	35569.	99.02	101951.
2	40000.	400.	2.06	41320.	.02	35366.	105.77	102703.
3	35000.	400.	2.06	39257.	.24	34163.	112.06	100935.
4	35000.	400.	2.06	39259.	.24	34163.	112.08	100936.
5	30000.	400.	2.03	38417.	.78	33462.	111.20	98196.
6	25000.	350.	1.80	26610.	.26	33057.	94.72	77742.
7	20000.	250.	1.47	14048	-1.13	34552.	61.54	52006.
8	45000.	400.	1.91	45778.	.20	36715	93.04	98881
9	50000.	400.	1.35	49280.	.12	38062.	73.30	75490.

FIGURE 20. EXPLORATORY F4-C ACCELERATIONS

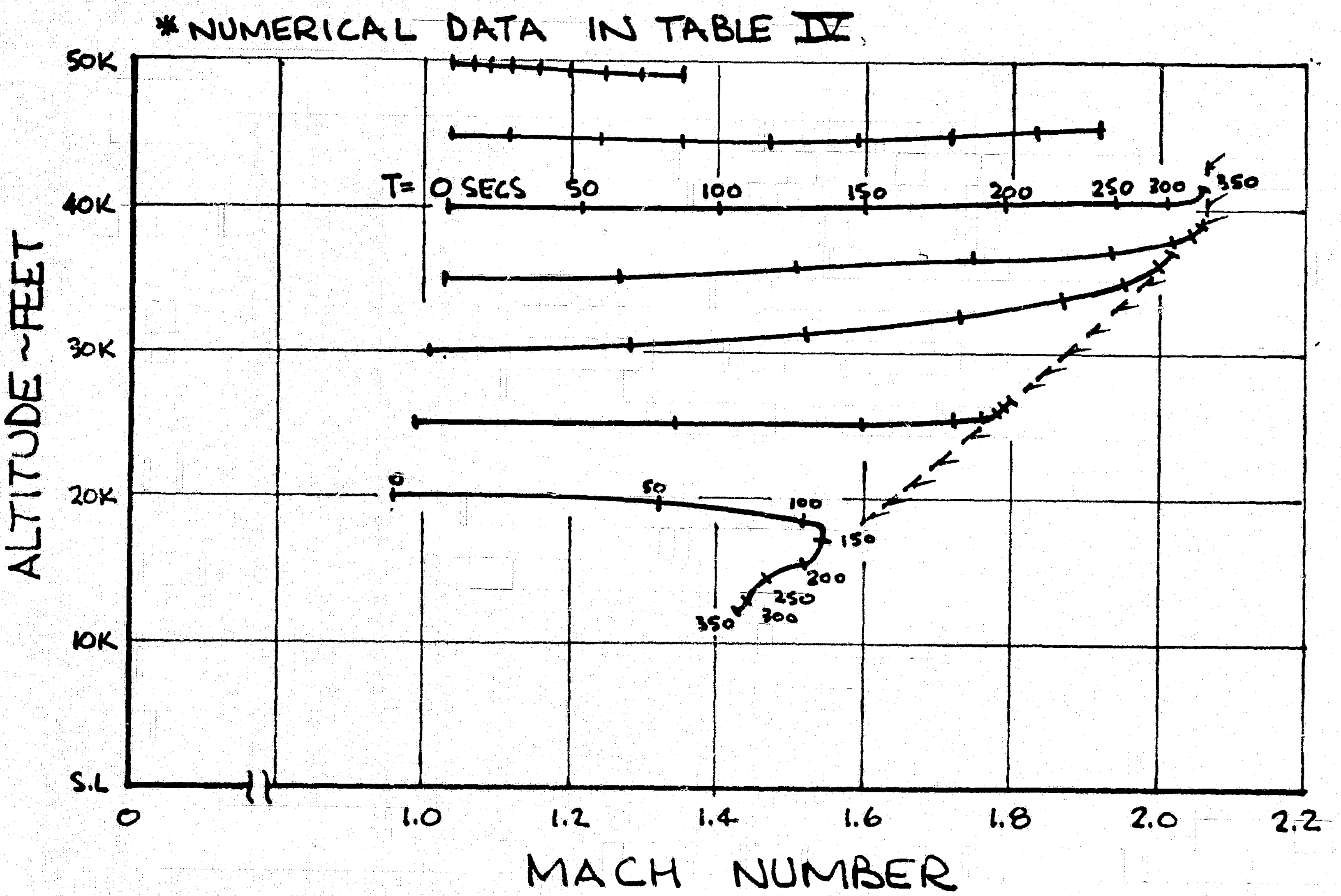

Maximum Mach Number Correlation

Level acceleration flight path calculations have been performed to establish F4-C maximum Mach number capability in the altitude range of prime interest for zoom commencement. Based on the results of Reference 25 this altitude is about 40000 feet. These calculations also serve to calibrate vehicle aerodynamic and propulsive characteristics employed. Thus in Reference 10 discussions with pilots who fly F4-C aircraft have indicated a maximum Mach number capability of 2.10 on occasion. The present maximum Mach number of 2.06 is in close agreement with this figure. It appears therefore that the aerodynamic and propulsive data of the previous section provides a good but slightly conservative model of the F4-C aircraft.

It may also be noted that Reference 26 provides a predicted Mach-altitude steady state flight envelope for the F4-C aircraft. This flight envelope is reproduced in Figure 21 for reference purposes. Again it may be seen that a maximum Mach number capability of 2.10 is predicted in the vicinity of 40000 feet. However, the vehicle weight employed in these calculations is not noted in Reference 26. The zoom weight of Reference 26 is 33238 pounds, somewhat below the value of 37500 lbs. employed in the present calculations.

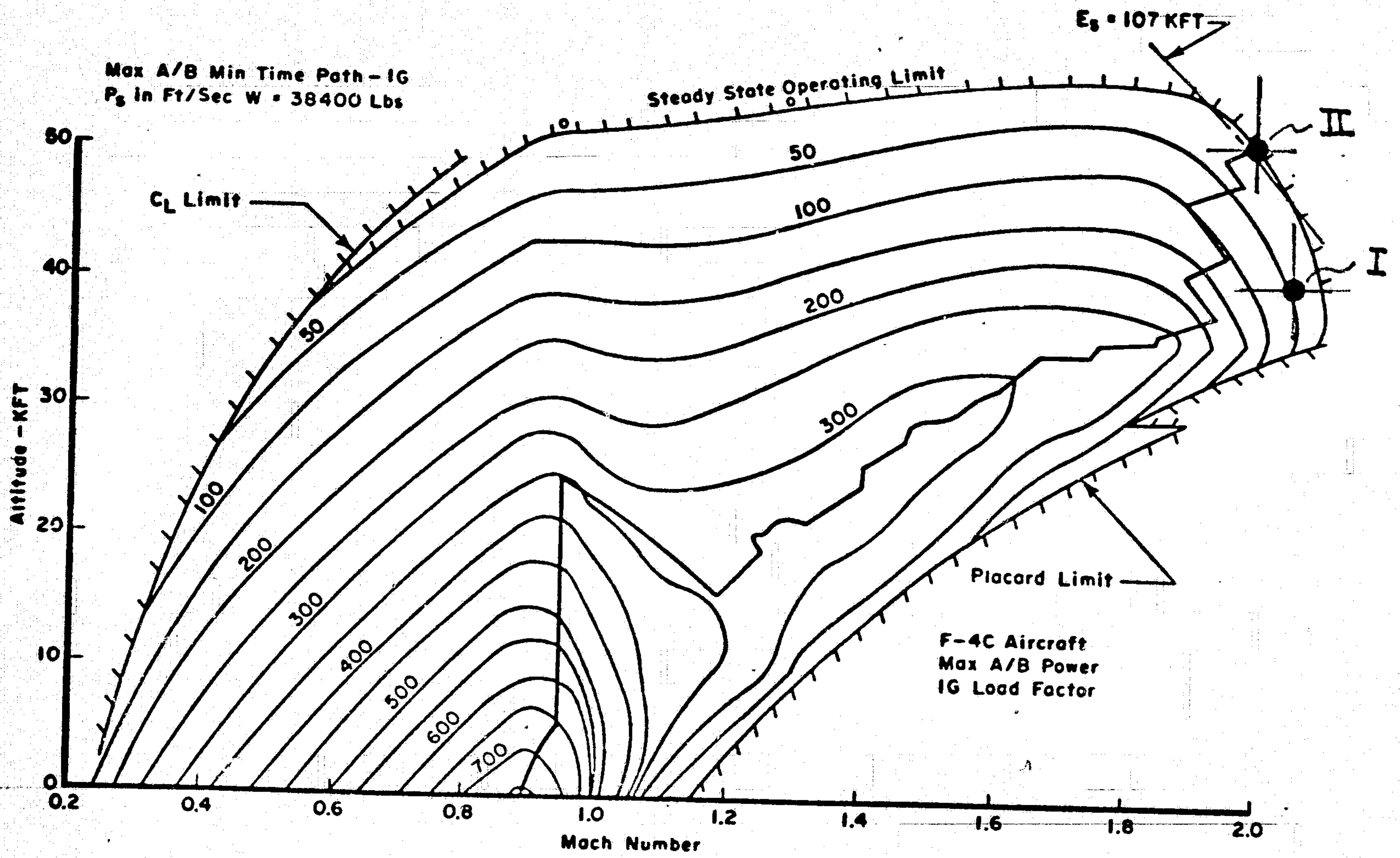

FIGURE 21. SPECIFIC EXCESS POWER (P_s) CONTOUR MAP

ENERGY MANEUVERABILITY METHOD

In the early fifties Rutowski, Reference 27 and Lush, Reference 28, independently proposed an energy maneuverability method for certain trajectory optimization problems. Their underlying assumption was that kinetic (velocity) and potential (altitude) energies are readily exchangeable and that the major factor in climbing to a flight condition (V, h) is the build-up of a specific energy corresponding to the flight point. Specific energy is defined as the vehicle energy content per unit weight of vehicle. That is

$$E = mg\ (h + V^2/2g) \tag{196}$$

and

$$E_s = h + V^2/2g \tag{197}$$

where

E = Vehicle energy

E_s = Specific energy

Further, accepting the hypothesis that energy build up is the dominant factor in achieving a given flight condition, local optimization at each point along a trajectory leads to the conclusion that the time derivative of specific energy, dE_s/dt, should be maximized at each energy level. This in turn implies that the vehicle should follow the loci of the tangency points between the contours

$$E_s = h + V^2/2g = \text{constant} \tag{198}$$

and

$$\dot{E}_S = dE_S/dt = V(T\cos\alpha - D)/mg = \text{constant} \tag{199}$$

Assuming the thrust is parallel to the velocity, the work done in time Δt is

$$\Delta E = (T - D)\ V\Delta t \tag{200}$$

or

$$\dot{E}_s = \frac{1}{W}\ \text{Limit}\ \left[\frac{\Delta E}{\Delta t}\right] = (T - D)\ \frac{V}{W} \tag{201}$$

This last expression may also be recognized as the first-order expression for steady-state rate-of-climb. Assuming equilibrium flight and small angles of attack

$$(T - D) = W \sin\gamma \tag{202}$$

so that rate of climb, R_c, is

$$R_c = V \sin\gamma = (T - D)\,\frac{V}{W} = \dot{E}_s \tag{203}$$

Time to fly between two specific energy levels E_{s_1} and E_{s_2} is simply

$$t = \int_{E_{s_1}}^{E_{s_2}} dt = \int_{E_{s_1}}^{E_{s_2}} \frac{dE}{(dE/dt)} \tag{204}$$

and it is assumed that an aircraft flown at constant energy requires negligible time for state changes.

The accuracy of the energy method has been examined in some detail in Reference 26. Both time-to-climb and the vehicle's ability to exchange kinetic and potential energies were considered. For maneuvers near the limit of a vehicle's zoom altitude capability time estimates by the energy method are inappropriate since a major part of the flight path involves a near constant-energy arc. Again the assumption of perfect ability to exchange kinetic for potential energy is seriously in error. To completely convert a vehicle's kinetic energy to potential energy requires vertical flight at the apogee. To achieve vertical flight from the higher energy states of a high performance aircraft involves a pullup from almost horizontal flight. This pullup creates large drag due to lift increments which dissipate energy. Maximum altitude capability is thus a sensitive trade between drag losses which dissipate energy, engine thrust, and energy producing capability near the aircraft operating limits, and the tendency to seek a high pullup angle to maximize energy exchange. In such a situation more exact methods of trajectory optimization based on the variational calculus must be employed. All optimum trajectories in this report are obtained through the ATOP program of References 1 and 2. Theoretical altitude capability based on energy content at zoom commencement will be employed only as a reference measure. This idealized altitude capability can be attained only if enough thrust is available to balance the drag forces during and after the high-g pullup.

PROGRAM VERIFICATION

In 1954, Rutowski published the energy-climb optimization procedure, Reference 27, which was based on a localized maximization of the aircraft energy buildup in the Mach-altitude plane. This was the first of several efforts which were developed in the 1960's and which used variational calculus methods for solving aircraft performance-optimization problems. The present program is based on the use of a variational steepest-descent algorithm and the formulation includes stage points and branched-trajectory options. The program is both versatile and computationally efficient, particularly when used with extremely complex high-ordered system equations.

The success of the variational steepest-descent method in the solution of aircraft performance optimization problems is evident from the strong support given to this technique by leading government research centers. The reason for this support is clear when the performance gains obtained by this method are examined. In Reference 25 are presented results related to several F-4B time-to-climb flights. Of particular interest are Figures 2 and 3 of this reference, which show paths in the Mach-altitude plane for a number of record flights. The actual flight paths flown are compared with the paths predicted by the programs of References 1 and 2, and it is found that a considerable increase in performance is obtained by attempting to follow the predicted optimum. In a typical case, a 23% improvement in performance over that of the flight handbook is obtained by both theory and actual flight, even when the path is not stringently followed. These results are included as Appendix A of the present report for reference purposes.

It is noted that this gain is obtained without vehicle modification, but simply by controlling the aircraft in a near optimal manner. It should also be observed that the performance sensitivity to departures from the optimal flight schedule is not very large, and that the derived optimal path is not difficult to implement.

Multiple Extremals

In certain applications, it may happen that multiple extremals exist between the initial and final conditions, such that small perturbations of each extremal produce a decrease in performance. During the present study two distincts sets of extremal trajectories were found from the initial conditions selected in Figure 21. Since the time-of-flight was free, and only the final altitude was to be maximized, it is apparent that this maximum altitude should be independent of the aircraft initial condition. Nevertheless, from both initial conditions, the F4-C immediately dives to lower altitudes, and this is followed by an abrupt pull-up to the near constant-energy zoom maneuver. The final altitude reached from the higher initial energy state (point II), however, was superior to that achieved on the path beginning at the lower energy state (point I). Since a trajectory could physically connect points I and II, and since the final altitude achieved from point II is greater than that achieved from point I, it is concluded that two extremal trajectories must emanate from point I. The optimization process has converged to the inferior extremal, (which in this case is a shorter flight) as illustrated in Figure 22. The multiple extremal problem is eliminated by beginning the computation at the highest energy level, for then the subarc I-II no longer exists.

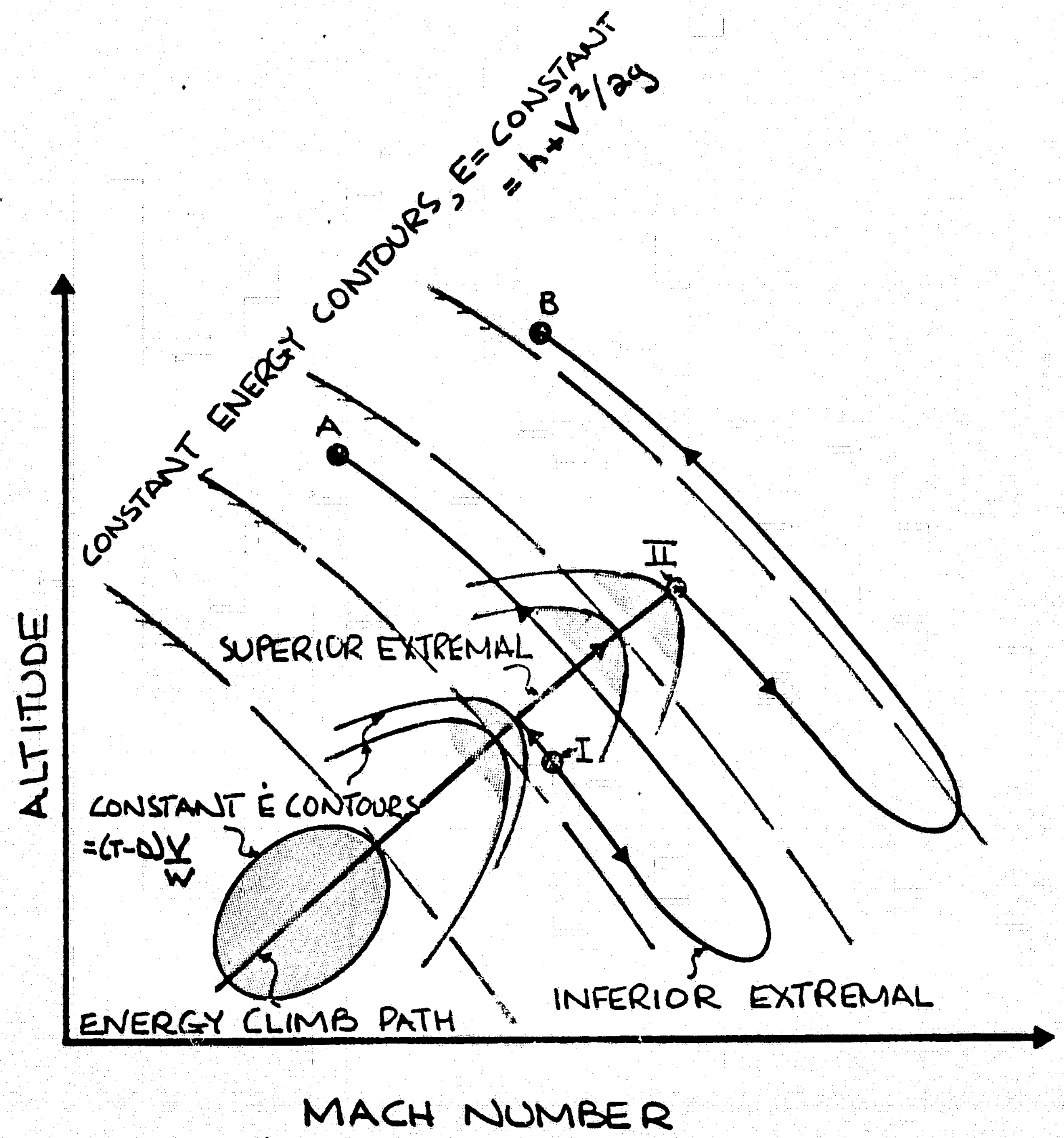

FIGURE 22. THE MULTIPLE EXTREMAL PROBLEM AND ITS SOLUTION

NUMERICAL RESULTS

The optimization program has been applied to the basic F4-C aircraft, as described by its inertial,thrust and aerodynamic characteristics. The parameter of principal interest was the terminal dynamic pressure, since the low density and low speeds at maximum altitude could make the aircraft difficult to control at this time. Additional results relate to the effects of increased thrust, horizontal winds, and decreased gross weight of the aircraft.

Terminal Dynamic Pressure Limits on Altitude Capability

The computations were performed with the F4-C initially at 50000 ft altitude, and at M = 2.06. The initial mass was 1166 slugs, and the terminal dynamic pressure was specified at 10, 20 or 40 psf. Results are shown in Figure 23, and it is seen that the maximum altitude varies from 88191 (q_f = 8.7 psf) to 82780 (q_f = 39.9 psf).

The question of specifying an adequate minimum dynamic pressure is one which must be answered by use of detailed simulations using both translational and rotational degrees of freedom. These simulations should include details as to the flight control system, and the aerodynamic stability deviations at large angles of attack and large sideslip angles. For reference purposes, it may be noted that recent F-15 high altitude time-to-climb record flight went safely over the top with a dynamic pressure less than 10 psf, Reference 29. It is doubtful that routine sampling of the upper atmosphere would be performed at such low dynamic pressures however.

Effect of Increased Thrust on Maximum Altitude

When the available thrust is increased by 10%, the maximum altitude increases, as shown in Figure 24. According to data provided by General Electric to McDonnell Aircraft, Reference 30, a 2% increase in engine rpm at M = 2.0 generates a thrust increase of the F4-C of 10%. This is increased to 12% at M = 2.2, and is decreased to 6% at M = 1.9. Since the Mach number on the nominal flight exceeds M = 2.0 for about 75% of the powered portion of the zoom climb maneuver, an average value of thrust increase equal to 10% has been assumed. As shown in Figure 24, an increment of 2000 to 4000 ft altitude is obtained from this thrust increase, depending on the final dynamic pressure specified.

Effect of Tail Winds on Maximum Altitude

The Mach number attainable by the F4-C at a particular altitude is independent of the winds, but the kinetic energy is not. That is, the inertial velocity of the aircraft is increased when a tail wind is acting on the aircraft, and this additional inertial velocity can be converted to an increment in final altitude. The wind profile given in Figure 25 was taken as representative, and it is noted that the initial extra velocity, at 50000 ft altitude is only 75 ft/sec.

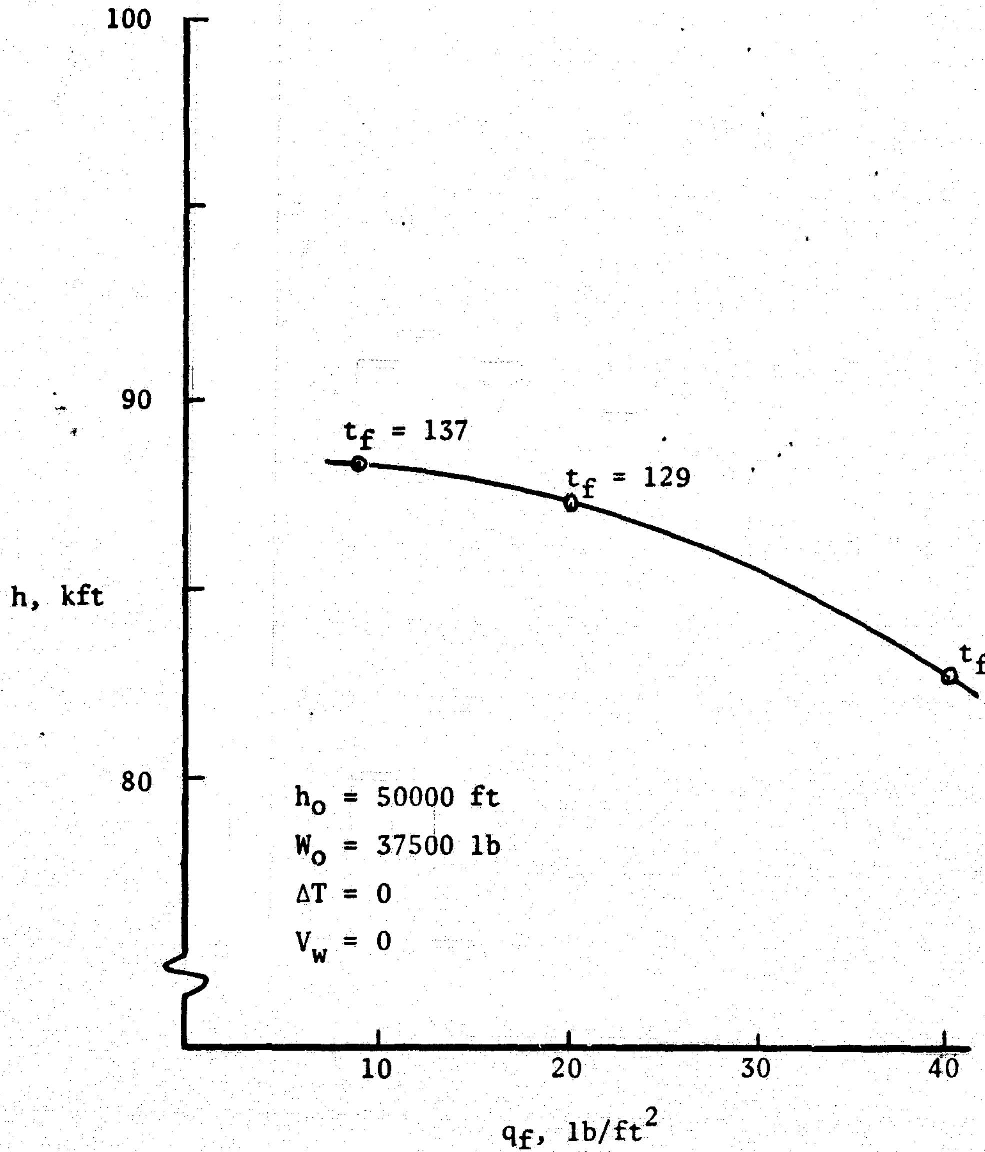

FIGURE 23. MAXIMUM ALTITUDE VARIATION WITH FINAL DYNAMIC PRESSURE

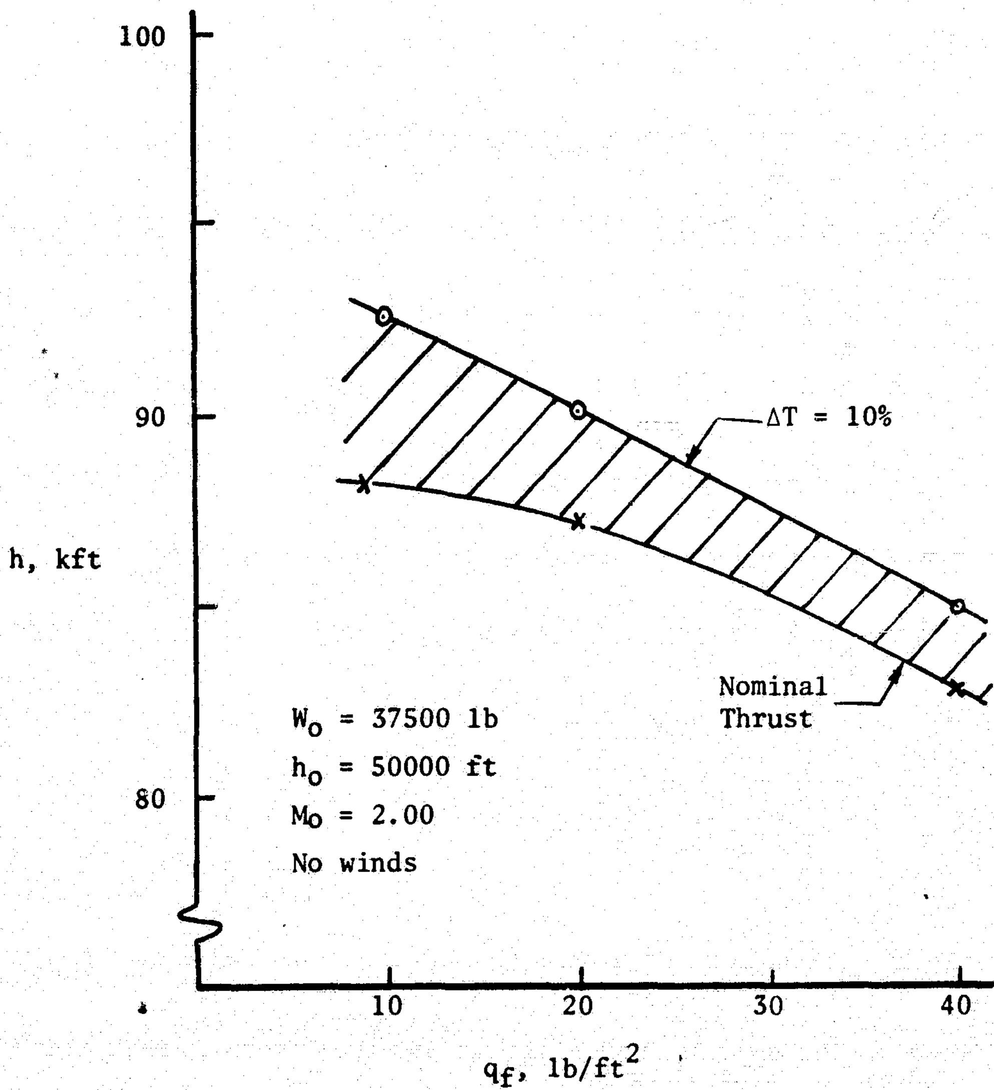

FIGURE 24. EFFECT OF EXTRA THRUST ON MAXIMUM ALTITUDE

The effects of this tail wind profile are shown in Figure 26, for terminal dynamic pressures of 10, 20 and 40 lb/ft^2. The 3 curves indicate that the wind and the extra thrust generate approximately equal altitude increments. It is a matter of interest that the minimum altitudes reached during the zoom-dive vary from about 33000 ft (q_f = 10 lb/ft^2) to 43000 ft (q_f = 40 lb/ft^2), and the peak wind velocities were assumed to occur between 30000 and 40000 ft.

Effect of Reduced Initial Mass on Maximum Altitude

When the aircraft mass is reduced due to the burning of fuel, greater accelerations result from a given thrust, and this has a modest effect on the altitude capabilities. The initial weight was reduced from 37500 lb to 32170 lb. The optimization procedure was then carried out at the initial Mach number of 2.10, because at this speed the drag is in equilibrium with the 10% additional thrust.

As shown in Figure 27 for a final dynamic pressure of 20 psf, the increase in maximum altitude due to this mass reduction is 1750 ft.

Transients in Selected Trajectory Variables

The transient variations of Mach number, angle of attack, altitude, etc., during a typical optimal flight are shown here in graphical form, to indicate the expected values attained by these variables. The flight chosen for this example is that for which the altitude reached is 92.6kft and the minimum dynamic pressure is 20 psf. This example includes the effects of winds and the additional thrust while the gross weight is at its nominal value. As shown in Figure 28, the dynamic pressure and the normal acceleration reach peak values during the zoom-maneuver, when the altitude is near its minimum. The angle of attack varies more smoothly, and has a peak value approximately mid-way between the minimum and maximum altitudes, when the flight path angle is also near its peak value of 45^o.

These results indicate that control variations during such a flight need not be abrupt or extreme, and that normal accelerations can be kept below 4 g's. In fact, the output data for the 12 cases given in Table V shows that the largest normal acceleration encountered is 3.96 g's, which could be significantly reduced by further trajectory shaping, or by introducing constraints for this quantity.

In Figure 29 is shown the trace of this representative trajectory in the Mach-altitude plane, at intervals of 8 seconds.

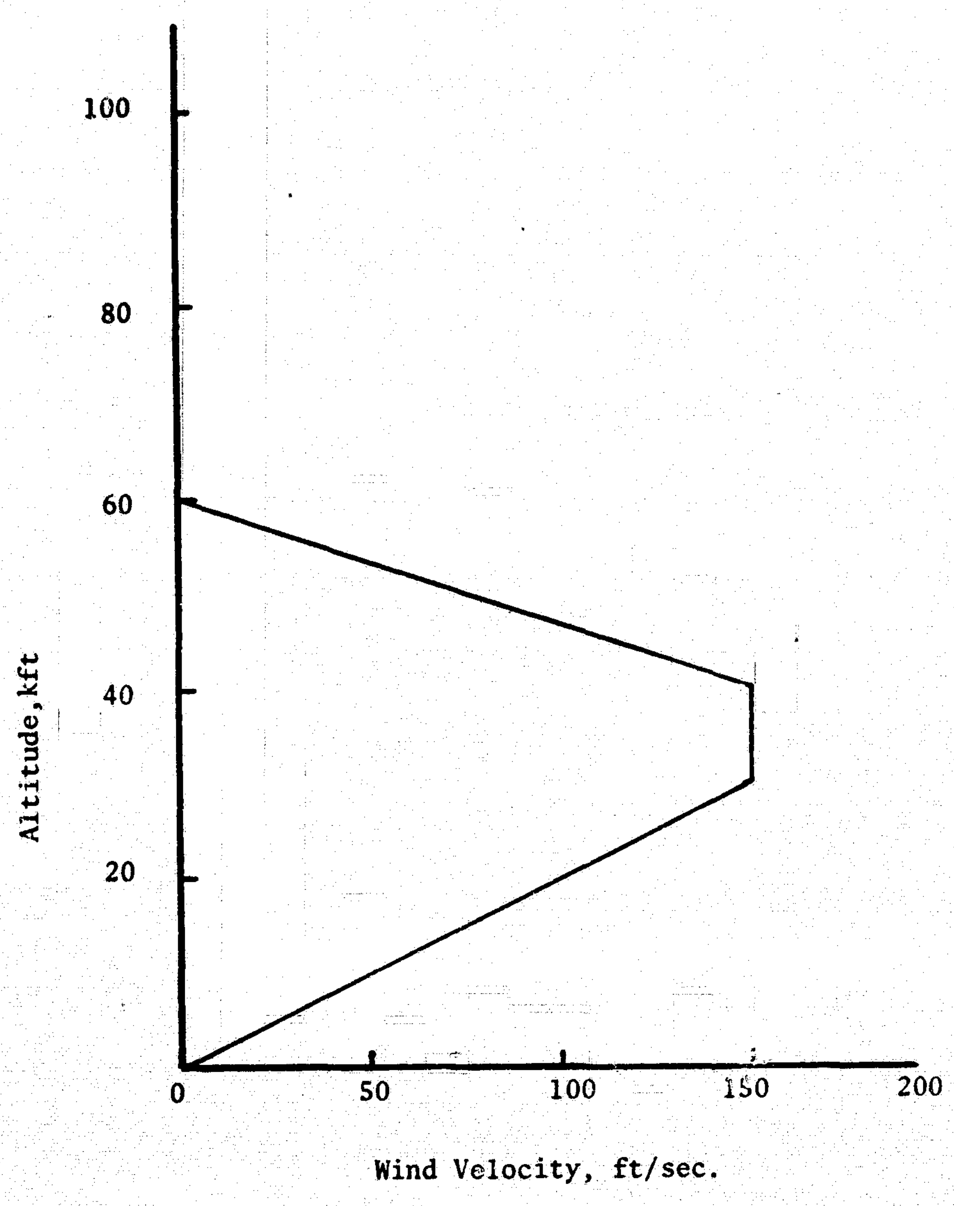

FIGURE 25. STRATOSPHERIC WIND PROFILE

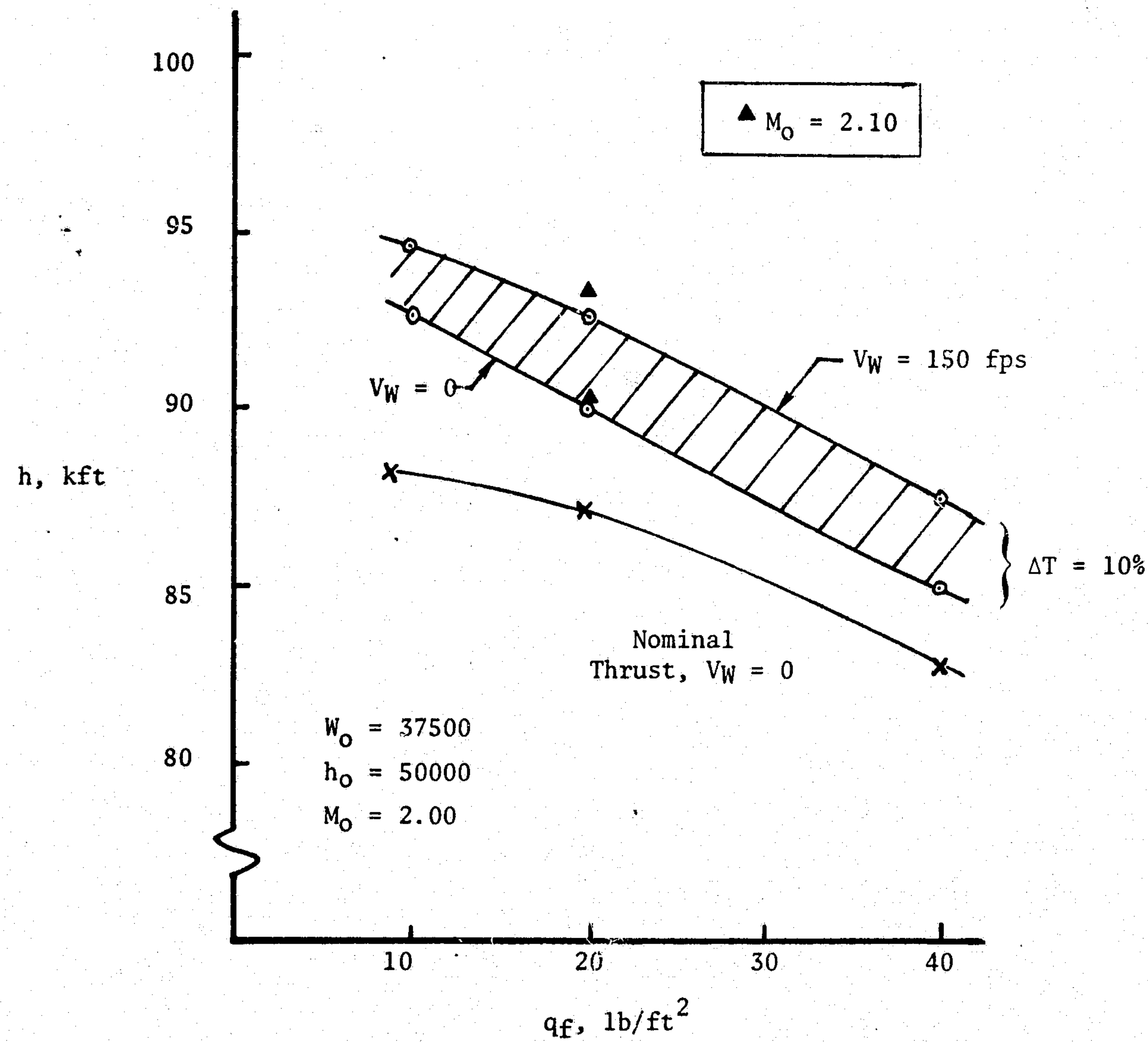

FIGURE 26. MAXIMUM ALTITUDE VARIATION WITH WINDS AND DYNAMIC PRESSURE

C-2

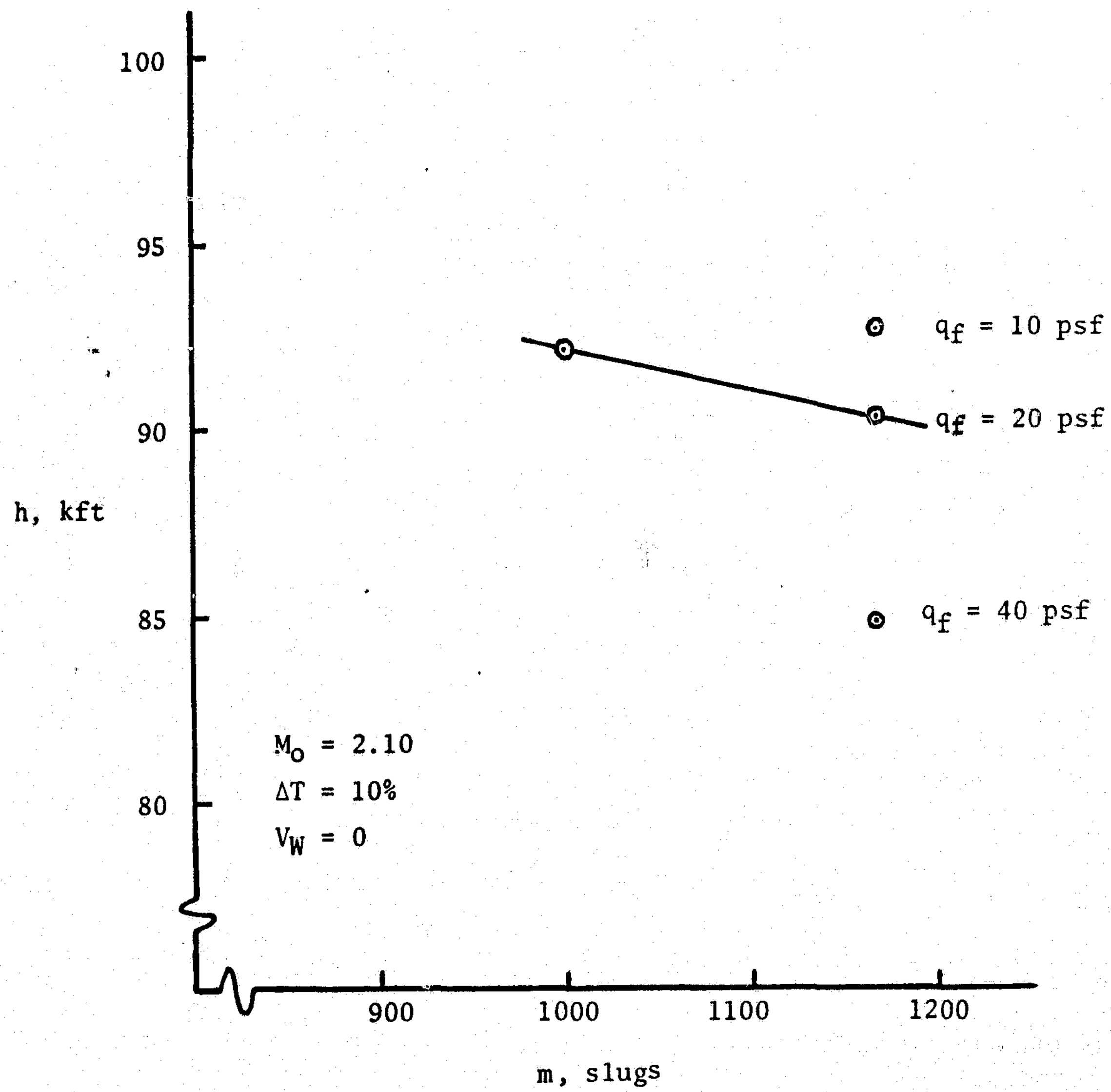

FIGURE 27. EFFECT OF WEIGHT REDUCTION ON FINAL ALTITUDE

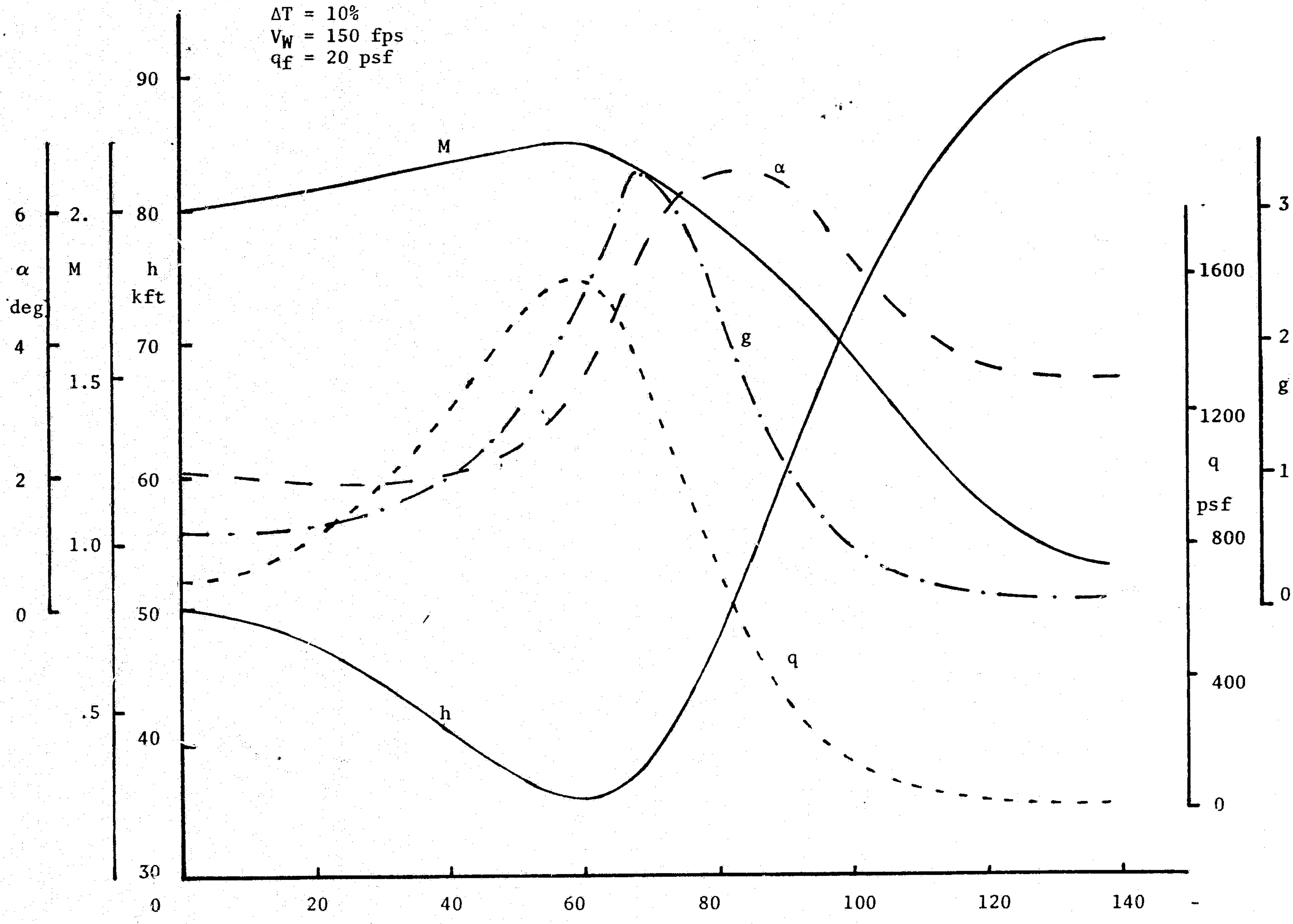

FIGURE 28. TIME HISTORIES OF SELECTED VARIABLES

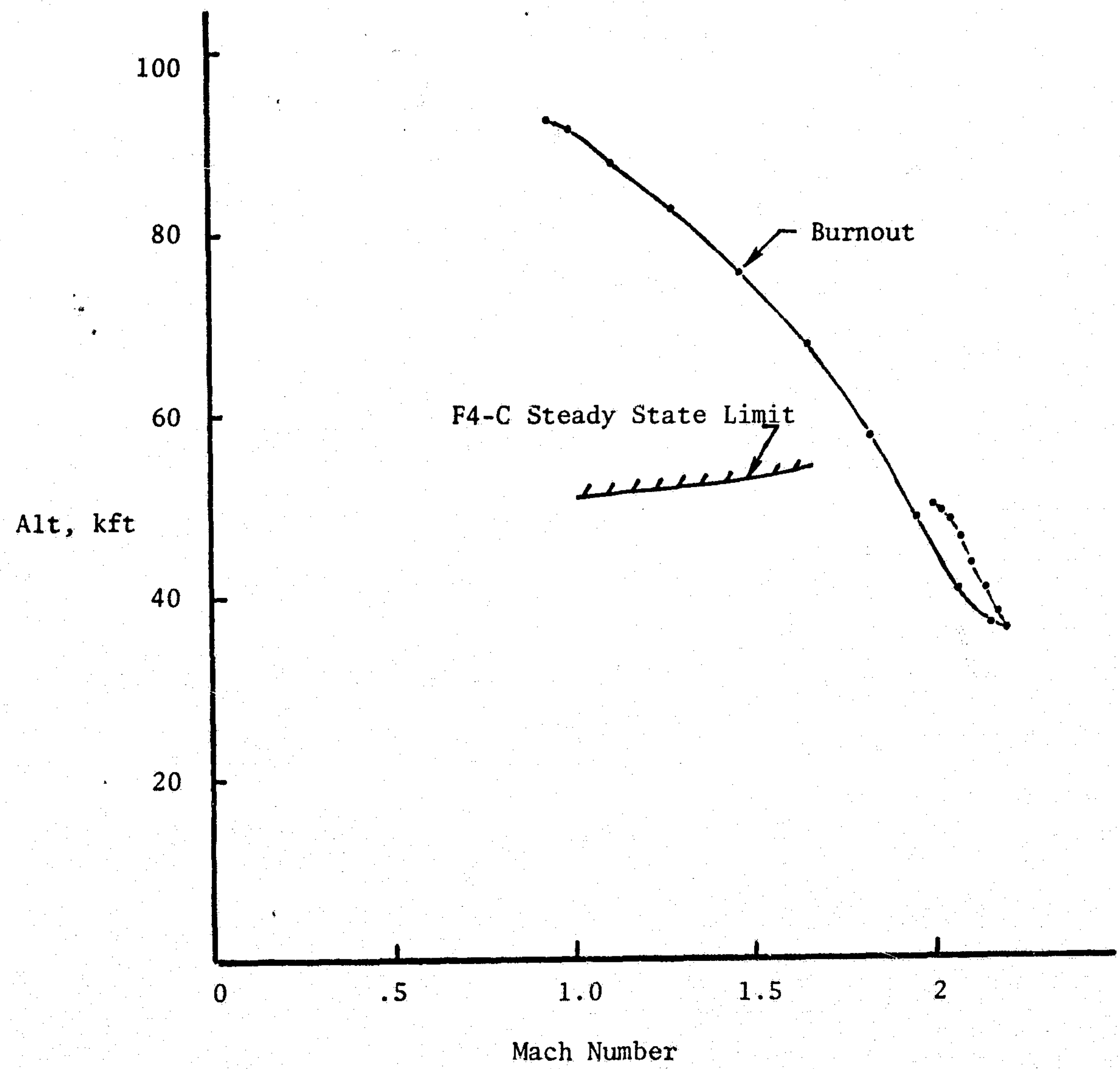

FIGURE 29. REPRESENTATIVE TRAJECTORY IN THE MACH-ALTITUDE PLANE

Energy Variations During Zoom-Climb Maneuver

Other interesting results can be prepared from the output data tabulated in Table V. These relate to the kinetic and potential energies and their rates of change, and a computation of these variables has been carried out by W. Page, the NASA technical monitor of the project. The results obtained show how the energy components vary during the maneuver, and help to explain how energy is lost during the transfer from low to high altitudes. If the thrust could be varied during the zoom-climb so as to cancel the drag, of course, the theoretical maximum final altitude could be reached by converting all of the initial kinetic energy to potential energy. However, the thrust capability varies with Mach number and altitude in a different way than does the drag, which also depends strongly on angle of attack. In addition, the final velocity must be high enough to permit aerodynamic control of the aircraft. Consequently, of the total initial energy available, a portion remains as kinetic energy as the aircraft passes over the top. The velocities at this time vary from 550 fps to 1150 fps, depending on the terminal dynamic pressure constraint imposed. The remaining energy loss is equivalent to only about 5000 feet altitude, and this is proportional to the time integral of the difference between thrust and drag during the maneuver.

The energy rate has been derived in equation (200) as

$$\frac{dE}{dt} = TV - DV \triangleq \frac{dE_T}{dt} + \frac{dE_D}{dt}$$

which is the sum of a "thrust energy" rate and a "drag energy" rate. In the energy state approximation, this is assumed to be equal to the sum of the potential energy rate and the kinetic energy rate

$$\frac{dE}{dt} = \frac{d}{dt}(mgh) + \frac{d}{dt}(\tfrac{1}{2}mV^2) \triangleq \frac{dE_p}{dt} + \frac{dE_k}{dt}$$

and these derivatives can be accurately approximated by finite differences read from the discrete printout in Table V. The result of the computation in a typical case is given in Figure 30, which shows in component form how the components of energy rate vary during the maneuver. Data for this example is given in Table V(e).

In this example, the final dynamic pressure is 20 psf, and the curves show that the energy remains nearly constant during the maneuver. That is, the thrust and drag energy rates are nearly equal and opposite, as are the potential and kinetic energy rates. Of the total energy loss of 17940 ft, about 35% is due to the imbalance of thrust and drag, while 65% remains in the form of kinetic energy as the aircraft passes over the top.

A second example of this type is shown in Figure 31, and in this example only the initial velocity differs from the values assumed in Figure 30. The Mach number is initially 2.1 in this case, for which numerical results are given in Table V(j). Here the total energy "loss" is 23430 ft, of which 52% is due to the imbalance of thrust and drag, and 48% remains in the form of final kinetic energy.

FIGURE 30. ZOOM-CLIMB TRAJECTORY ANALYSIS, h_o = 50000 ft, M_o = 2.0, q_{final} = 20, 110% thrust

Altitude reached 90034

Initial Theoretical Altitude 107965 (at starting condition)

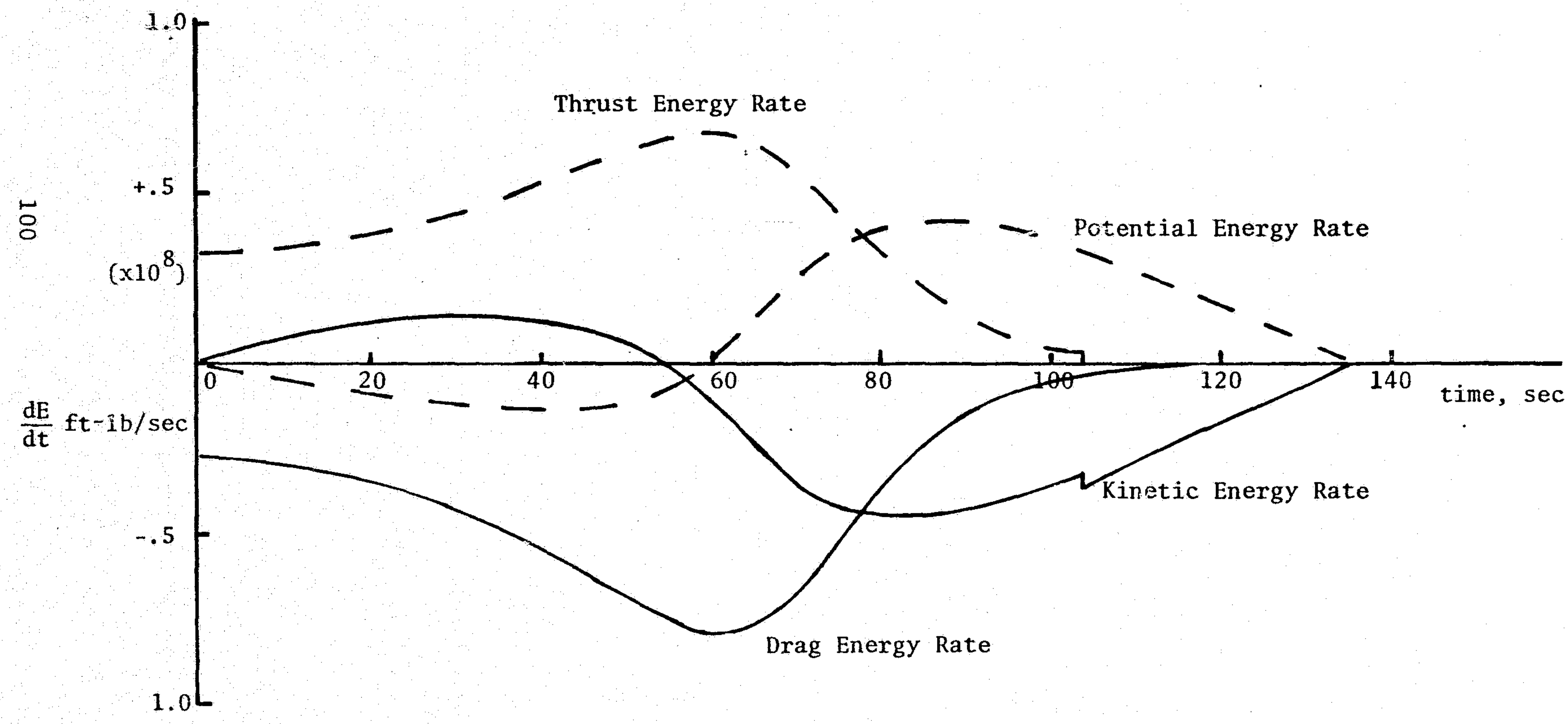

FIGURE 31. ZOOM-CLIMB TRAJECTORY ANALYSIS - ENERGY EXCHANGE TERMS

h_o = 50000 ft, M_O = 2.1, q_{final} = 20, 110% thrust

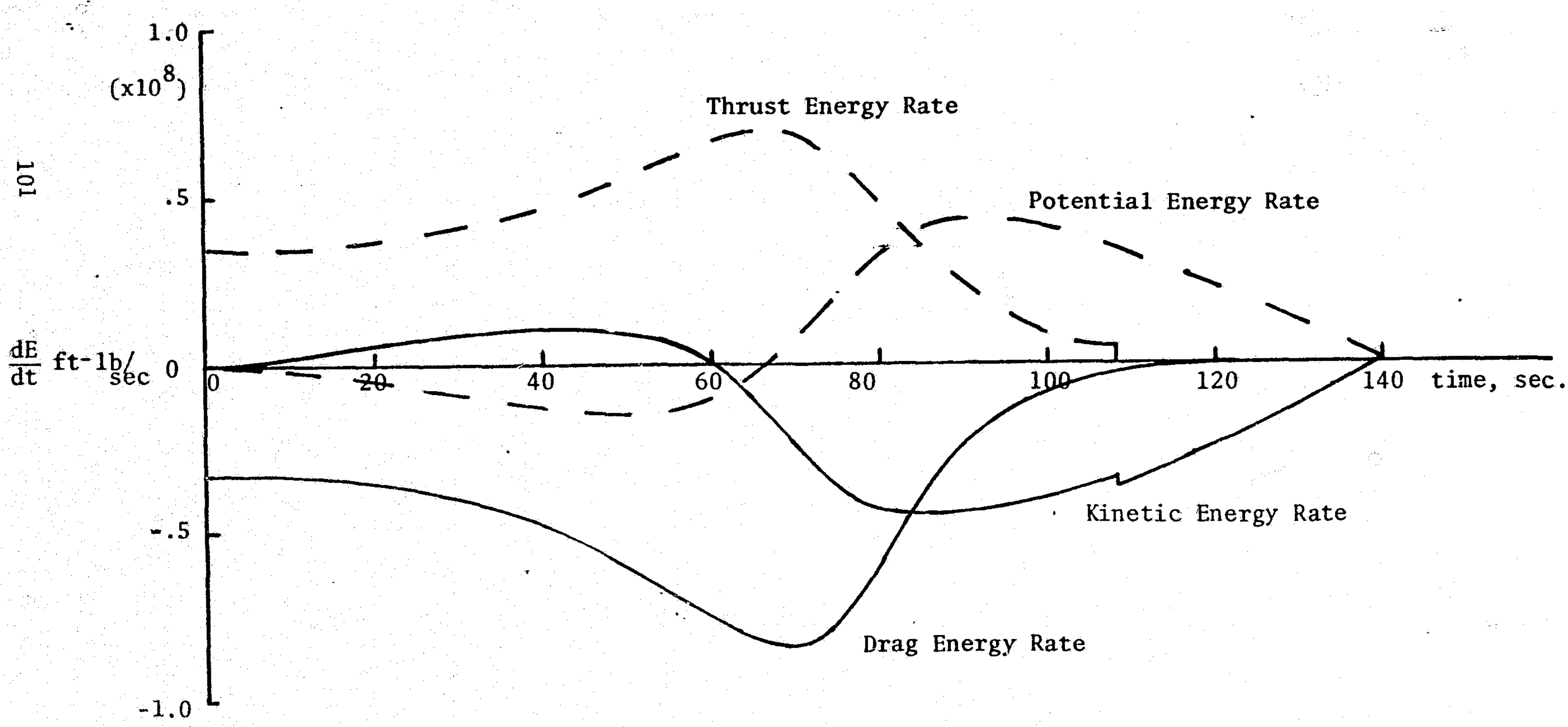

The time-variation of the specific energy is shown in Figure 32 for the two trajectories just discussed. It is seen that in both cases the energy increases slightly during the dive maneuver, when the thrust exceeds the drag, after which the energy reduces to its final value. These transients help to explain why the final altitude depends upon the initial Mach number, and why there is no unique answer to the question:

> What is the maximum altitude attainable for a given combination of aircraft, engine, wind and final dynamic pressure?

The dependence of the final altitude on the initial aircraft velocity (or total energy) in the altitude maximization problem finds an analogy in the problem of minimizing the arc length from the point P to the line-segment boundary in the sketch below.

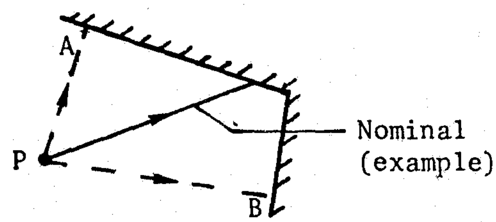

Here it is seen that a numerical perturbation method may converge to either of the local minima (A or B), depending principally on the nominal path assumed. Initial directions below the corner are likely to converge to B, and conversely for initial directions above the corner. By analogy, if the initial aircraft energy is less than the maximum attainable, the process does not first optimize the "initial condition", but rather begins the dynamic portion of the maneuver, and this may lead to an inferior optimum, as described in the discussion under "PROGRAM VERIFICATION".

When the initial velocity does not correspond to the maximum energy condition, as in the lower curve of Figure 32, the longitudinal acceleration due to the available thrust is extremely low. This means that a very long transient time (300 seconds or more) would be required to increase this initial velocity to the maximum energy value shown as the upper curve of Figure 32. The numerical process in this case instead begins with a zoom-dive maneuver, and maximum altitude is attained at about the same time as found for the upper curve, from the maximum energy initial condition. The final altitudes attained from these two initial velocities differ by less than 300 ft and this is a measure of the "error" introduced by the existence of multiple extremals.

FIGURE 32. EFFECT OF INITIAL SPEED ON SPECIFIC ENERGY

h_o = 50000 ft, q_{final} = 20, 110% thrust

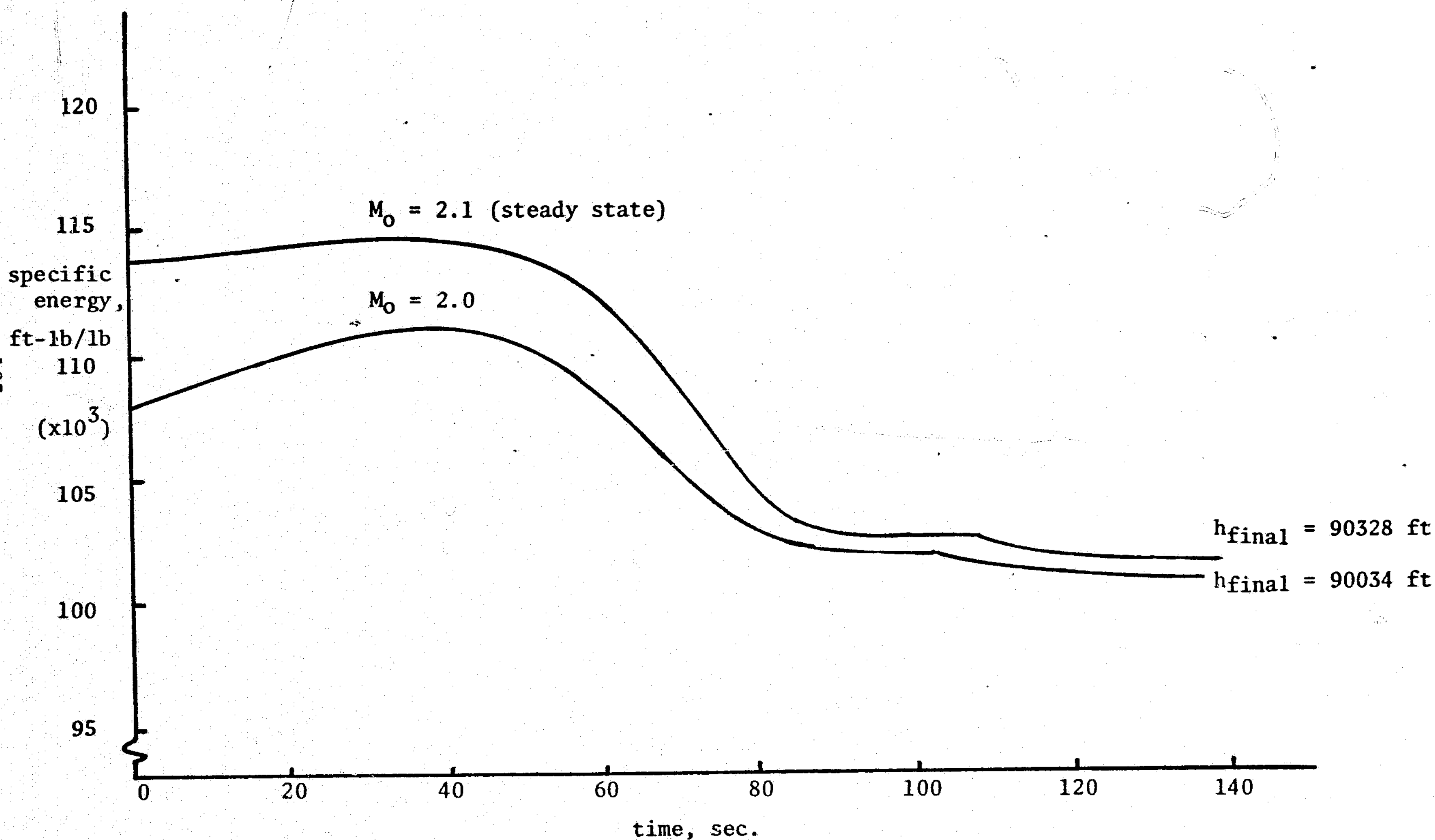

CONCLUSIONS

It has been shown that a standard F4-C aircraft, zooming at safe operational weights, is capable of monitoring upper atmosphere pollutant levels. Generally, altitudes attained varied through the interval from 85000 to 95000 ft, depending largely on terminal dynamic pressure, but the effect of improved thrust capability, of stratospheric winds and of reduced aircraft mass on altitude performance have also been investigated.

The peak normal accelerations on the optimal paths are high (up to 4 g's), but it is likely that further trajectory shaping could reduce these peak accelerations without significant effect on the maximum altitude. Other problems which will require additional study include:

i) Mechanization of the optimal paths for pilot guidance;

ii) Analysis of F4-C handling qualities at low dynamic pressure;

iii) Shaping of re-entry flight paths; and

iv) Effect of range safety and environmental acceptance of high-boom paths at prospective sampling sites.

TABLE V. COMPUTER OUTPUT DATA

	Run	ΔT	V_W	q_f	M_o	W_o	h_f
a.	1	0	0	8.7	2.00	37500	88191
b.	2	0	0	20			87167
c.	3	0	0	40			82780
d.	4	+10%	0	10			92645
e.	5	+10%	0	20			90033
f.	6	+10%	0	40			84928
g.	7	+10%	150	10			94625
h.	8	+10%	150	20			92612
i.	9	+10%	150	40	2.00		87403
j.	10	+10%	0	20	2.10		90371
k.	11	+10%	150	20	2.10	37500	93458
ℓ.	12	+10%	0	20	2.10	32170	92127

ZOOM TO GIVEN Q, CORRECTED DATA

	TIME	VG77F	HGC7F	GAM7D	VI77F	RG77N	AMACH	AMASPI
1	0,	1936,000	50000,00	0,	3465,625	0,	1,999844	17302,76
2	4,000000	1939,033	49926,72	-1,100506	3468,495	1,272169	2,002976	17379,70
3	8,000000	1944,714	49697,68	-2,291881	3473,633	2,546836	2,008845	17606,10
4	12,00000	1953,166	49300,85	-3,554145	3481,090	3,624970	2,017575	17994,01
5	16,00000	1964,417	48726,34	-4,859558	3490,857	5,107780	2,029198	18553,79
6	20,00000	1978,374	47968,02	-6,177627	3502,839	6,396475	2,043615	19292,50
7	24,00000	1994,808	47022,29	-7,490456	3516,821	7,691860	2,060591	20214,68
8	28,00000	2013,279	45888,01	-8,768910	3532,431	8,994623	2,079671	21322,88
9	32,00000	2033,242	44570,01	-9,953946	3549,309	10,30609	2,100292	22724,59
10	36,00000	2054,457	43082,48	-10,98218	3567,488	11,62630	2,122207	24516,19
11	40,00000	2075,941	41448,68	-11,78545	3586,333	12,95635	2,144399	26479,83
12	44,00000	2096,250	39705,81	-12,25879	3604,910	14,29680	2,165379	28646,55
13	48,00000	2114,343	37911,90	-12,23801	3622,868	15,64862	2,184067	31268,28
14	52,00000	2128,444	36153,83	-11,55103	3638,997	17,01277	2,198634	33833,27
15	56,00000	2134,508	34558,13	-9,773917	3650,056	18,38933	2,189058	35125,05
16	60,00000	2127,471	33350,92	-6,123442	3650,804	19,77645	2,170105	36035,17
17	64,00000	2104,786	32849,67	-,3300029	3633,146	21,16519	2,142199	36313,53
18	68,00000	2061,414	33371,50	8,061151	3581,143	22,53168	2,102916	35726,39
19	72,00000	1995,959	35228,82	18,68928	3478,563	23,82868	2,053163	33976,96
20	76,00000	1913,123	38438,04	29,88908	3326,963	24,99863	1,976213	29520,00
21	80,00000	1817,244	42709,14	39,72125	3148,825	26,00203	1,877171	23470,76
22	84,00000	1715,935	47578,94	47,14408	2975,545	26,84211	1,772552	17753,00
23	88,00000	1611,520	52665,21	52,25992	2820,516	27,54635	1,664066	13039,95
24	92,00000	1504,950	57706,61	55,45999	2686,578	28,14797	1,554579	9574,920
25	96,00000	1397,118	62540,44	57,10784	2572,351	28,67527	1,443191	6814,411
26	100,00000	1289,027	67066,22	57,50365	2474,971	29,15008	1,331535	4810,548
27	104,0000	1181,928	71222,47	56,83881	2391,920	29,58850	1,220904	3416,999
28	108,0000	1076,550	74972,26	55,24434	2320,353	30,00129	1,112051	2475,327
29	112,0000	970,0518	78285,26	52,60080	2256,531	30,39541	1,002041	0,
30	116,0000	869,2894	81134,82	48,77871	2203,954	30,77607	,8979560	0,
31	120,0000	776,4874	83512,49	43,49972	2162,414	31,14818	,8001401	0,
32	124,0000	693,9656	85408,14	36,53558	2130,245	31,51554	,7122974	0,
33	128,0000	625,7310	86816,29	27,69507	2106,524	31,87983	,6403996	0,
34	132,0000	576,9192	87733,91	16,92148	2091,071	32,24227	,5893337	0,
35	136,0000	552,7158	88159,23	4,639929	2083,792	32,60375	,5641187	0,
36	136,0000	552,7158	88159,23	4,639929	2083,792	32,60375	,5641187	0,
37	136,0000	552,7158	88159,23	4,639929	2083,792	32,60375	,5641187	0,
38	137,4508	550,7506	88191,66	3,3527612E-05	2083,161	32,73466	,5620757	0,
39	137,4508	550,7506	88191,66	3,3527612E-05	2083,161	32,73466	,5620757	0,
40	137,4508	550,7506	88191,66	3,3527612E-05	2083,161	32,73466	,5620757	0,
41	137,4508	550,7506	88191,66	4,0233135E-06	2083,161	32,73466	,5620757	0,
42	137,4508	550,7506	88191,66	4,0233135E-06	2083,161	32,73466	,5620757	0,
43	137,4508	550,7506	88191,66	4,0233135E-06	2083,161	32,73466	,5620757	0,
44	137,4508	550,7506	88191,66	4,0233135E-06	2083,161	32,73466	,5620757	0,
45	137,4508	550,7506	88191,66	0,	2083,161	32,73466	,5620757	0,

$\Delta T = 0$

$V_W = 0$

$q_f = 10$

TABLE V(a) Run 1

ZOOM TO GIVEN Q, COPRECTED DATA

	AMASS	ALPHO	TE77P	CL	CD	ANZ87G	ESPEF	DYNPP
1	1166,000	2,415621	15273,17	6,7928377E-02	4,0547911E-02	-,7005479	3473667	681,9943
2	1164,803	2,316952	15338,18	6,4595949E-02	4,0369967E-02	-,6728353	3477209	686,5349
3	1163,596	2,216843	15537,40	6,1205629E-02	4,0190411E-02	-,6506234	3480949	698,1714
4	1162,367	2,108858	15881,61	5,7544525E-02	3,9997949E-02	-,6313808	3484784	717,7491
5	1161,106	2,012802	16380,02	5,4280087E-02	3,9828643E-02	-,6216455	3488528	746,2735
6	1159,800	1,916326	17038,88	5,0954478E-02	3,9657711E-02	-,6163380	3491890	784,6801
7	1158,437	1,815812	17862,46	4,7523902E-02	3,9548975E-02	-,6143340	3494411	834,9104
8	1157,003	1,730575	18852,81	4,4655298E-02	3,9480324E-02	-,6233690	3495288	897,6772
9	1155,486	1,679629	20100,46	4,2967849E-02	3,9442983E-02	-,6533766	3493675	975,3934
10	1153,856	1,641965	21654,94	4,1747772E-02	3,9400055E-02	-,6975382	3489617	1069,341
11	1152,095	1,638257	23357,06	4,1646693E-02	3,9388348E-02	-,7684604	3481889	1180,641
12	1150,194	1,678808	25235,92	4,2955142E-02	3,9416593E-02	-,8768933	3468664	1306,618
13	1148,125	1,791882	27496,48	4,6522090E-02	3,9508992E-02	-1,048737	3449513	1450,721
14	1145,870	1,938201	29702,01	5,1074251E-02	3,9660675E-02	-1,264123	3423313	1599,283
15	1143,492	2,360803	30740,07	6,4630012E-02	4,0420456E-02	-1,694031	3365287	1710,372
16	1141,032	3,061547	31464,61	8,7356988E-02	4,1661614E-02	-2,301021	3331737	1778,942
17	1138,529	3,699358	31803,46	,1084052	4,3212929E-02	-2,913323	3267721	1774,465
18	1136,036	4,913781	31606,23	,1467171	4,7216305E-02	-3,747602	3194041	1666,806
19	1133,622	5,795302	30542,93	,1796646	5,1393455E-02	-3,957862	3120568	1457,566
20	1131,404	6,602035	26884,42	,2118972	5,6237504E-02	-3,713249	3061101	1158,162
21	1129,577	6,546236	21404,83	,2225119	5,7307076E-02	-2,870648	3018504	851,7445
22	1128,163	6,465794	16047,65	,2326206	5,7965117E-02	-2,120417	2994782	601,5721
23	1127,111	6,147212	11460,39	,2357324	5,7067046E-02	-1,485528	2982956	415,9890
24	1126,339	5,750116	7935,255	,2395672	5,5989752E-02	-1,033452	2977253	285,0863
25	1125,778	5,335246	5394,286	,2425932	5,4426507E-02	-,7147479	2974397	195,0195
26	1125,383	4,919548	3676,328	,2441480	5,2343584E-02	-,4924915	2972915	133,7305
27	1125,102	4,541620	2546,712	,2535816	5,0907954E-02	-,3518915	2972449	92,19858
28	1124,900	4,210738	1760,201	,2651002	4,8414329E-02	-,2545487	2972319	63,95641
29	1124,871	3,939712	0,	,2655900	4,1711330E-02	-,1738926	2968291	44,33002
30	1124,871	3,717363	0,	,2572439	2,3052903E-02	-,1175132	2965839	31,07899
31	1124,871	3,543982	0,	,2148230	1,6940523E-02	-6,9524635E-02	2964712	22,03467
32	1124,871	3,520683	0,	,2105980	1,6735879E-02	-4,9386807E-02	2964002	15,96581
33	1124,871	3,504246	0,	,2086744	1,6479217E-02	-3,7059912E-02	2963505	12,08011
34	1124,871	3,492665	0,	,2078809	1,6425560E-02	-2,9925749E-02	2963163	9,601229
35	1124,871	3,483935	0,	,2072135	1,6389530E-02	-2,6795760E-02	2962936	8,804347
36	1124,871	3,483935	0,	,2072135	1,6389530E-02	-2,6795760E-02	2962936	8,804347
37	1124,871	3,483935	0,	,2072135	1,6389530E-02	-2,6795760E-02	2962936	8,804347
38	1124,871	3,481319	0,	,2070480	1,6380594E-02	-2,6540717E-02	2962877	8,727513
39	1124,871	3,481319	0,	,2070480	1,6380594E-02	-2,6540717E-02	2962877	8,727513
40	1124,871	3,481319	0,	,2070480	1,6380594E-02	-2,6540717E-02	2962877	8,727513
41	1124,871	3,481319	0,	,2070480	1,6380594E-02	-2,6540717E-02	2962877	8,727513
42	1124,871	3,481319	0,	,2070480	1,6380594E-02	-2,6540717E-02	2962877	8,727513
43	1124,871	3,481319	0,	,2070480	1,6380594E-02	-2,6540717E-02	2962877	8,727513
44	1124,871	3,481319	0,	,2070480	1,6380594E-02	-2,6540717E-02	2962877	8,727513
45	1124,871	3,481319	0,	,2070480	1,6380594E-02	-2,6540717E-02	2962877	8,727513

CASE F4HA07 STAGE 1 CYCLE 14 PASS 2 PAGE 160

ZOOM TO GIVEN Q, CORRECTED DATA

	TIME	VG77F	HGC7F	GAM7D	VI77F	RG77N	AMACH	AMASP1
1	0,	1936,000	50000,00	0,	3465,625	0,	1,999844	17302,76
2	4,000000	1939,564	49914,59	-1,281504	3468,969	1,272330	2,003525	17392,55
3	8,000000	1946,208	49647,82	-2,669018	3474,878	2,547320	2,010388	17656,44
4	12,00000	1956,111	49184,52	-4,153207	3483,422	3,826341	2,020618	18109,60
5	16,00000	1969,211	48512,64	-5,654987	3494,536	5,110440	2,034150	18765,07
6	20,00000	1985,047	47635,22	-7,064324	3507,935	6,400828	2,050508	19620,19
7	24,00000	2002,973	46567,02	-8,285584	3523,285	7,698712	2,069026	20662,01
8	28,00000	2022,037	45337,05	-9,247488	3539,987	9,005061	2,088718	21862,80
9	32,00000	2041,363	43981,93	-9,884008	3557,549	10,32100	2,108681	23432,28
10	36,00000	2059,942	42554,77	-10,06864	3575,483	11,64775	2,127873	25147,14
11	40,00000	2076,197	41124,91	-9,757605	3592,414	12,98618	2,144664	26859,87
12	44,00000	2087,369	39789,25	-8,440956	3606,678	14,33671	2,156205	28506,33
13	48,00000	2089,755	38756,58	-5,468042	3614,540	15,69900	2,158669	29995,07
14	52,00000	2080,202	38270,69	-1,009132	3608,835	17,06702	2,148801	30669,96
15	56,00000	2056,307	38523,08	4,738978	3582,097	18,42577	2,124118	30250,54
16	60,00000	2017,283	39664,95	11,50582	3528,634	19,75090	2,083807	28462,10
17	64,00000	1967,420	41700,66	17,91137	3454,489	21,01614	2,032299	25717,37
18	68,00000	1906,722	44467,42	24,09443	3361,194	22,20511	1,969600	22233,60
19	72,00000	1835,692	47872,67	29,79156	3253,029	23,29936	1,896228	18626,63
20	76,00000	1758,517	51689,83	34,25568	3143,153	24,29962	1,816507	15105,23
21	80,00000	1674,583	55736,30	37,81137	3032,109	25,21040	1,729806	11917,83
22	84,00000	1586,089	59853,30	40,32748	2925,494	26,04064	1,638394	9306,554
23	88,00000	1493,847	63913,14	42,01758	2823,466	26,80099	1,543109	7004,778
24	92,00000	1400,328	67822,89	42,79707	2729,603	27,50120	1,446506	5232,258
25	96,00000	1308,483	71500,02	42,53263	2647,540	28,15369	1,351633	3912,912
26	100,00000	1219,916	74880,85	41,22327	2577,570	28,77007	1,260146	2947,717
27	104,0000	1130,355	77911,73	38,87118	2513,873	29,35920	1,167631	0,
28	108,0000	1047,255	80547,62	35,46242	2461,019	29,92696	1,081791	0,
29	112,0000	973,4391	82764,90	30,92202	2419,373	30,47997	1,004657	0,
30	116,0000	910,9807	84544,17	25,27086	2387,826	31,02355	,9367193	0,
31	120,0000	862,0247	85872,50	18,59309	2365,298	31,56125	,8839482	0,
32	124,0000	828,5241	86739,94	11,03420	2350,866	32,09555	,8480797	0,
33	128,0000	812,3333	87139,41	2,894597	2343,989	32,62793	,8308250	0,
34	128,0000	812,3333	87139,41	2,894597	2343,989	32,62793	,8308250	0,
35	128,0000	812,3333	87139,41	2,894597	2343,989	32,62793	,8308250	0,
36	129,3909	810,9802	87167,95	5,3644182E-06	2343,316	32,81286	,8293926	0,
37	129,3909	810,9802	87167,95	5,3644182E-06	2343,316	32,81286	,8293926	0,
38	129,3909	810,9802	87167,95	5,3644182E-06	2343,316	32,81286	,8293926	0,
39	129,3909	810,9802	87167,95	4,0233135E-06	2343,316	32,81286	,8293926	0,
40	129,3909	810,9802	87167,95	4,0233135E-06	2343,316	32,81286	,8293926	0,
41	129,3909	810,9802	87167,95	4,0233135E-06	2343,316	32,81286	,8293926	0,
42	129,3909	810,9802	87167,95	0,	2343,316	32,81286	,8293926	0,

TABLE V(b) Run 2

$\Delta T = 0$

$V_W = 0$

$q_f = 20$

ATOP III ATMOSPHERIC TRAJECTORY OPTIMIZATION PROGRAM VERSION 3,00 15 MAY 1972

CASE F4HA07 STAGE 1 CYCLE 14 PASS 2 PAGE 161

ZOOM TO GIVEN Q, CORRECTED DATA

	AMASS	ALPHD	TETZP	CL	CD	ANZB7G	ESPEF	DYNPP
1	1166.000	2,276066	15273,17	6,3252786E-02	4,0295458E-02	-,6545519	3473667	681,9943
2	1164,603	2,167067	15348,96	5,9574713E-02	4,0099149E-02	-,6237489	3477653	687,3096
3	1163,593	2,047888	15581,11	5,5548585E-02	3,9885656E-02	-,5958319	3482267	700,9140
4	1162,359	1,911212	15983,21	5,0863473E-02	3,9638998E-02	-,5667826	3486837	723,9332
5	1161,087	1,873392	16566,54	4,9531525E-02	3,9587990E-02	-,5766969	3491151	757,6266
6	1159,763	1,854038	17329,51	4,8845057E-02	3,9579110E-02	-,6057446	3494513	802,8659
7	1158,372	1,904252	18260,51	5,0458950E-02	3,9646199E-02	-,6694054	3496228	860,2976
8	1156,905	1,933952	19335,19	5,1372980E-02	3,9707371E-02	-,7360655	3495401	929,9034
9	1155,343	2,018446	20716,42	5,4059499E-02	3,9856445E-02	-,8405261	3491476	1011,267
10	1153,665	2,147041	22208,52	5,8145496E-02	4,0073248E-02	-,9627302	3484076	1102,560
11	1151,869	2,234801	23701,87	6,0887773E-02	4,0219800E-02	-1,117872	3472095	1199,379
12	1149,957	2,821146	25149,09	7,9765352E-02	4,1258306E-02	-1,562883	3452748	1292,360
13	1147,933	3,466264	26478,97	,1005816	4,2434046E-02	-2,064044	3424783	1360,996
14	1145,833	3,922803	27135,16	,1155240	4,3936835E-02	-2,401296	3369361	1380,327
15	1143,722	4,592610	26875,22	,1376550	4,6138136E-02	-2,758595	3347994	1332,595
16	1141,685	5,184656	25416,96	,1582370	4,8449537E-02	-2,888957	3304902	1214,255
17	1139,811	5,048671	23074,53	,1555431	4,7706051E-02	-2,456283	3270530	1047,714
18	1138,150	6,218240	20004,14	,1998020	5,3687216E-02	-2,591127	3241164	862,0035
19	1136,739	5,979602	16724,91	,2000179	5,3080720E-02	-2,045224	3216754	678,8398
20	1135,578	6,471271	13401,76	,2273655	5,7527806E-02	-1,776838	3199605	518,9929
21	1134,648	6,769154	10261,09	,2498532	6,0419527E-02	-1,457965	3184276	387,8382
22	1133,916	6,974698	7570,227	,2751942	6,4208996E-02	-1,181800	3170891	285,7766
23	1133,354	7,486064	5531.110	,3180805	7,0981777E-02	-,9964315	3157812	208,8061
24	1132,935	7,344081	4031,799	,3365711	7,1633021E-02	-,7673170	3146591	152,2273
25	1132,623	7,065473	2963,283	,3493453	7,0267871E-02	-,5823266	3138638	111.5127
26	1132,387	6,604997	2169,263	,3563944	6,7638406E-02	-,4385486	3134041	82,48417
27	1132,353	6,063386	0,	,3616268	6,3982115E-02	-,3266140	3124812	61,28234
28	1132,353	5,447560	0,	,3494359	5,7529267E-02	-,2384307	3117792	46,38803
29	1132,353	4,823017	0,	,3190411	4,7873120E-02	-,1685774	3113385	35,99463
30	1132,353	4,326763	0,	,2961054	3,2095923E-02	-,1245442	3110625	28,75944
31	1132,353	3,971398	0,	,2693306	2,3475250E-02	-9,4601750E-02	3109436	24,05685
32	1132,353	3,775262	0,	,2443057	1,9495861E-02	-7,5797305E-02	3108547	21,20149
33	1132,353	3,628867	0,	,2296128	1,6294262E-02	-6,7100967E-02	3107893	20,02748
34	1132,353	3,628867	0,	,2296128	1,6294262E-02	-6,7100967E-02	3107893	20,02748
35	1132,353	3,628867	0,	,2296128	1,6294262E-02	-6,7100967E-02	3107893	20,02748
36	1132,353	3,587094	0,	,2266256	1,8082592E-02	-6,5911571E-02	3107697	19,93189
37	1132,353	3,587094	0,	,2266256	1,8082592E-02	-6,5911571E-02	3107697	19,93189
38	1132,353	3,587094	0,	,2266256	1,8082592E-02	-6,5911571E-02	3107697	19,93189
39	1132,353	3,587094	0,	,2266256	1,8082592E-02	-6,5911570E-02	3107697	19,93189
40	1132,353	3,587094	0,	,2266256	1,8082592E-02	-6,5911570E-02	3107697	19,93189
41	1132,353	3,587094	0,	,2266256	1,8082592E-02	-6,5911570E-02	3107697	19,93189
42	1132,353	3,587094	0,	,2266256	1,8082592E-02	-6,5911569E-02	3107697	19,93189

ZOOM TO GIVEN [illegible], CORRECTED DATA

	TIME	VG77F	HGC7F	GAM7D	VI77F	RG77N	AMACH	AMASFI
1	0.	1936.000	50000.00	0.	3465.625	0.	1.999844	17302.76
2	4.000000	1944.674	49748.19	-3.617534	3472.575	1.272975	2.008804	17560.78
3	8.000000	1959.638	49054.40	-6.395942	3483.844	2.549577	2.024261	18240.38
4	12.00000	1978.367	48042.40	-8.237553	3498.939	3.831903	2.043608	19225.51
5	16.00000	1998.358	46826.63	-9.176124	3516.648	5.122532	2.064258	20407.05
6	20.00000	2015.946	45551.23	-8.850729	3534.877	6.424528	2.082426	21640.39
7	24.00000	2027.601	44411.31	-7.150568	3550.032	7.739745	2.094465	22883.94
8	28.00000	2032.317	43570.21	-4.695699	3558.543	9.066328	2.099337	23892.44
9	32.00000	2026.146	43145.88	-.8914724	3555.166	10.39831	2.092963	24357.47
10	36.00000	2007.056	43366.08	3.973966	3534.110	11.72264	2.073243	24001.41
11	40.00000	1979.098	44243.36	8.667456	3498.438	13.02423	2.044363	22842.78
12	44.00000	1940.176	45707.86	13.53489	3445.658	14.28777	2.004157	21117.39
13	48.00000	1894.174	47836.71	17.87695	3382.539	15.49932	1.956638	19059.18
14	52.00000	1842.471	50358.28	21.56978	3313.076	16.65468	1.903230	16585.78
15	56.00000	1784.380	53220.40	24.76566	3237.600	17.74901	1.843224	14306.06
16	60.00000	1721.240	56298.63	27.24122	3160.207	18.78329	1.778002	12010.77
17	64.00000	1654.015	59489.83	29.05367	3082.686	19.75977	1.708560	9978.384
18	68.00000	1583.794	62679.81	30.18492	3006.953	20.68328	1.636022	8130.366
19	72.00000	1512.048	65835.51	30.65001	2934.635	21.55883	1.561910	6467.493
20	76.00000	1441.550	68837.21	30.29438	2869.371	22.39326	1.489088	5187.330
21	80.00000	1373.261	71635.52	29.22005	2810.831	23.19440	1.418547	4187.302
22	84.00000	1308.143	74188.84	27.34746	2758.389	23.96757	1.351282	3409.670
23	88.00000	1241.103	76458.69	25.17898	2706.735	24.71623	1.282031	0.
24	92.00000	1180.040	78406.74	22.17048	2662.000	25.46265	1.218954	0.
25	96.00000	1127.350	80016.15	18.56148	2625.166	26.15108	1.164526	0.
26	100.00000	1084.191	81273.04	14.36478	2596.172	26.84557	1.119944	0.
27	104.0000	1051.958	82162.58	9.574967	2575.226	27.52982	1.086649	0.
28	108.0000	1031.966	82666.44	4.235672	2562.288	28.20706	1.065280	0.
29	108.0000	1031.966	82666.44	4.235672	2562.288	28.20706	1.065280	0.
30	110.9800	1025.459	82780.81	1.5779435E-02	2557.474	28.70888	1.058310	0.
31	110.9800	1025.459	82780.81	1.5779435E-02	2557.474	28.70888	1.058310	0.
32	110.9910	1025.448	82780.82	8.0466271E-06	2557.464	28.71074	1.058299	0.
33	110.9910	1025.448	82780.82	8.0466271E-06	2557.464	28.71074	1.058299	0.
34	110.9910	1025.448	82780.82	8.0466271E-06	2557.464	28.71074	1.058299	0.
35	110.9910	1025.448	82780.82	4.0233135E-06	2557.464	28.71074	1.058299	0.
36	110.9910	1025.448	82780.82	4.0233135E-06	2557.464	28.71074	1.058299	0.
37	110.9910	1025.448	82780.82	4.0233135E-06	2557.464	28.71074	1.058299	0.
38	110.9910	1025.448	82780.82	4.0233135E-06	2557.464	28.71074	1.058299	0.
39	110.9910	1025.448	82780.82	0.	2557.464	28.71074	1.058299	0.

TABLE V(c) Run 3

$\Delta T = 0$

$V_W = 0$

$q_f = 40$

ATOP III ATMOSPHERIC TRAJECTORY OPTIMIZATION PROGRAM VERSION 3,00 15 MAY 1972

CASE F4HA07 STAGE 1 CYCLE 15 PASS 2 PAGE 174

ZOOM TO GIVEN Q, CORRECTED DATA

	AMASS	ALPHA	TF77P	CL	CD	ANZB7G	ESPEF	DYNPP
1	1166,000	.1871379	15273.17	-8,5457642E-03	3,8502210E-02	5,0955334E-02	3473667	681,9943
2	1164,799	.6234378	15494.81	6.6615225E-03	3,8450851E-02	-,1003704	3482480	696,4580
3	1163,564	1,373297	16097.23	3,2504520E-02	3,9131185E-02	-,3779028	3489599	731,0831
4	1162,272	1,827348	16975,95	4,7947816E-02	3,9551018E-02	-,5788319	3494246	782,0868
5	1160,904	2,378819	18033,49	6,6186577E-02	4,0492630E-02	-,8495848	3495267	845,7660
6	1159,452	3,171537	19143,27	9,2110115E-02	4,1903402E-02	-1,263599	3489929	914,6640
7	1157,916	3,721249	20262,31	,1099700	4,3327059E-02	-1,605274	3477164	977,3843
8	1156,298	3,730826	21171,70	,1101965	4,3358439E-02	-1,684714	3459925	1022,271
9	1154,628	5,022642	21616,70	,1526034	4,7678489E-02	-2,353763	3433876	1036,921
10	1152,953	4,920451	21349,91	,1499035	4,7154062E-02	-2,249223	3402399	1006,806
11	1151,331	5,144164	20363,22	,1583164	4,8194368E-02	-2,216502	3374642	938,6981
12	1149,813	5,778646	18857,12	,1812891	5,1278255E-02	-2,269107	3346318	839,4650
13	1148,423	5,399023	17037,12	,1728730	4,9759846E-02	-1,870188	3324674	724,0267
14	1147,191	6,036506	14764,79	,2012544	5,3386959E-02	-1,823591	3308375	607,1955
15	1146,123	6,029942	12561,92	,2078656	5,4119644E-02	-1,541464	3294131	496,6550
16	1145,219	6,484580	10315,90	,2326610	5,8040435E-02	-1,384724	3281390	398,8826
17	1144,459	6,685609	8230,607	,2477253	5,9727882E-02	-1,168006	3269383	316,2256
18	1143,834	7,022045	6503,808	,2776723	6,4671724E-02	-1,028784	3257531	248,7744
19	1143,331	7,061791	5053,926	,2953742	6,6344244E-02	-,8573445	3246201	195,1568
20	1142,936	6,882079	3987,018	,3035947	6,5939216E-02	-,6932099	3237349	153,6945
21	1142,609	7,055061	3177,534	,3306241	6,9321497E-02	-,5986731	3229993	122,0352
22	1142,347	7,215222	2556,574	,3571096	7,2084786E-02	-,5187790	3223632	98,03093
23	1142,308	7,193627	0,	,3785871	7,3595363E-02	-,4394175	3210104	79,18241
24	1142,308	7,059665	0,	,4011669	7,4626666E-02	-,3831310	3197384	65,22942
25	1142,308	6,970999	0,	,4201471	7,5188281E-02	-,3388393	3188055	55,13491
26	1142,308	6,672042	0,	,4204500	7,2155494E-02	-,2950324	3180116	48,02715
27	1142,308	6,048013	0,	,3872972	6,3851878E-02	-,2448938	3173842	43,33674
28	1142,308	5,312139	0,	,3425506	5,5535731E-02	-,2030060	3168954	40,66004
29	1142,308	5,312139	0,	,3425506	5,5535731E-02	-,2030060	3168954	40,66004
30	1142,308	4,875534	0,	,3159321	5,1590990E-02	-,1837028	3165879	39,91178
31	1142,308	4,875534	0,	,3159321	5,1590990E-02	-,1837028	3165879	39,91178
32	1142,308	4,873927	0,	,3158327	5,1577288E-02	-,1836410	3165868	39,91096
33	1142,308	4,873927	0,	,3158327	5,1577288E-02	-,1836410	3165868	39,91096
34	1142,308	4,873927	0,	,3158327	5,1577288E-02	-,1836410	3165868	39,91096
35	1142,308	4,873926	0,	,3158327	5,1577283E-02	-,1836410	3165868	39,91096
36	1142,308	4,873926	0,	,3158327	5,1577283E-02	-,1836410	3165868	39,91096
37	1142,308	4,873926	0,	,3158327	5,1577283E-02	-,1836410	3165868	39,91096
38	1142,308	4,873926	0,	,3158327	5,1577283E-02	-,1836410	3165868	39,91096
39	1142.308	4,873926	0.	,3158327	5,1577282E-02	-,1836410	3165868	39,91096

CASE F[illegible]HA07 STAGE [illegible] CYCLE 15 PASS 3 PAGE 209

ZOOM TO GIVEN Q, CORRECTED DATA

	TIME	VG77F	HGC7F	GAM7D	VI77F	RG77N	AMACH	AMASF1
1	0,	1936,000	50000,00	0,	3465,625	0,	1,999844	17302,76
2	4,000000	1944,713	49913,76	-1,280913	3474,118	1,274023	2,008844	17412,88
3	8,000000	1956,149	49649,78	-2,601106	3484,864	2,554092	2,020657	17692,96
4	12,00000	1970,359	49201,86	-3,938887	3497,891	3,841174	2,035335	18150,25
5	16,00000	1987,297	48566,14	-5,270715	3513,162	5,136479	2,052832	18790,14
6	20,00000	2006,757	47742,23	-6,550569	3530,536	6,440973	2,072933	19614,73
7	24,00000	2028,252	46736,91	-7,729702	3549,708	7,755706	2,095138	20618,63
8	28,00000	2051,064	45565,29	-8,760208	3570,131	9,081564	2,118702	21745,04
9	32,00000	2074,404	44245,44	-9,609652	3591,236	10,41903	2,142811	23198,53
10	36,00000	2098,024	42807,01	-10,18997	3613,147	11,76907	2,167211	24938,05
11	40,00000	2120,630	41293,41	-10,40696	3634,976	13,13258	2,190562	26763,37
12	44,00000	2140,739	39761,44	-10,24642	3655,366	14,50986	2,211335	28630,94
13	48,00000	2157,051	38273,66	-9,566042	3673,359	15,90086	2,228184	30754,11
14	52,00000	2167,351	36941,20	-7,972645	3687,349	17,30507	2,238823	32660,53
15	56,00000	2168,061	35949,31	-4,833381	3693,473	18,72073	2,237494	34012,85
16	60,00000	2155,867	35571,63	9,3394516E-02	3684,439	20,14051	2,221097	34346,18
17	64,00000	2128,691	36048,16	6,526126	3651,529	21,54633	2,197851	33957,18
18	68,00000	2082,713	37578,91	14,81208	3582,017	22,90710	2,151395	31669,28
19	72,00000	2013,657	40321,26	24,44802	3463,777	24,17475	2,080061	27586,97
20	76,00000	1928,117	44153,20	33,61391	3311,644	25,30552	1,991700	22695,61
21	80,00000	1833,126	48733,91	41,21892	3149,267	26,28466	1,893577	17665,75
22	84,00000	1733,636	53705,22	46,86511	2995,254	27,12417	1,790806	13579,90
23	88,00000	1631,072	58776,30	50,67676	2857,530	27,85018	1,684860	10134,41
24	92,00000	1526,610	63745,25	52,67510	2737,513	28,48985	1,576953	7309,572
25	96,00000	1421,985	68478,59	53,69910	2635,076	29,06681	1,468878	5174,931
26	100,00000	1318,386	72891,32	53,37971	2547,845	29,59963	1,361863	3694,303
27	104,0000	1213,262	76925,09	52,00866	2470,927	30,10221	1,253292	0,
28	108,0000	1108,344	80528,80	49,68430	2402,492	30,58171	1,144894	0,
29	112,0000	1009,597	83681,97	46,39037	2345,276	31,04467	1,039983	0,
30	116,0000	918,4988	86373,41	41,98339	2296,664	31,49643	,9408870	0,
31	120,0000	837,0572	88594,73	36,32831	2261,831	31,94102	,8535673	0,
32	124,0000	767,4743	90337,47	29,26868	2235,802	32,38133	,7798458	0,
33	128,0000	713,0899	91595,14	20,82326	2213,732	32,81915	,7227471	0,
34	132,0000	677,5877	92364,70	11,16617	2201,390	33,25535	,6857023	0,
35	136,0000	664,0188	92644,56	,7502970	2196,714	33,69074	,6715938	0,
36	136,0000	664,0188	92644,56	,7502970	2196,714	33,69074	,6715938	0,
37	136,0000	664,0188	92644,56	,7502970	2196,714	33,69074	,6715938	0,
38	136,2838	663,9375	92645,80	0,	2196,673	33,72162	,6715098	0,

ORIGINAL PAGE IS OF POOR QUALITY

TABLE V(d) Run 4

$\Delta T = 10$

$V_W = 0$

ATOP III ATMOSPHERIC TRAJECTORY OPTIMIZATION PROGRAM VERSION 3,00 15 MAY 1972

CASE F4HA07   STAGE 1   CYCLE 15   PASS 3   PAGE 210

ZOOM TO GIVEN Q, CORRECTED DATA

	AMASS	ALPHD	TE77P	CL	CD	ANZ87G	ESPEF	DYNPP
1	1166,000	2,237167	16800,48	6,1949553E-02	4,0225092E-02	-,6447483	3473667	681,9943
2	1164,802	2,167630	16890,95	5,9560273E-02	4,0101561E-02	-,6298409	3487628	690,9910
3	1163,591	2,093110	17149,87	5,7001466E-02	3,9970475E-02	-,6195559	3501727	708,0266
4	1162,354	2,014513	17584,09	5,4305071E-02	3,9833707E-02	-,6138924	3515361	733,9082
5	1161,079	1,936891	18198,53	5,1612773E-02	3,9698789E-02	-,6140054	3528634	769,6346
6	1159,754	1,880927	18995,05	4,9668446E-02	3,9614656E-02	-,6283994	3541252	816,3328
7	1158,366	1,860401	19968,60	4,8923960E-02	3,9607058E-02	-,6641630	3552593	875,0072
8	1156,903	1,811110	21042,22	4,7254123E-02	3,9555635E-02	-,6952006	3561790	946,3993
9	1155,355	1,808203	22414,16	4,7114058E-02	3,9542069E-02	-,7553774	3567869	1031,160
10	1153,694	1,829695	24052,23	4,7751188E-02	3,9550149E-02	-,8384330	3571290	1129,976
11	1151,909	1,896513	25771,12	4,9797362E-02	3,9598101E-02	-,9582125	3570707	1241,211
12	1149,996	1,904782	27510,43	4,9985302E-02	3,9610920E-02	-1,054806	3564688	1361,123
13	1147,945	2,079645	29467,43	5,5390869E-02	3,9930074E-02	-1,268762	3552269	1483,967
14	1145,753	2,394065	31244,31	6,5301228E-02	4,0495692E-02	-1,599620	3532014	1596,912
15	1143,445	3,045202	32547,90	8,5965061E-02	4,1651538E-02	-2,187391	3501891	1672,605
16	1141,080	3,602866	32952,43	,1039326	4,2825542E-02	-2,644647	3463468	1678,160
17	1138,717	4,225175	32794,49	,1240864	4,4854484E-02	-3,018603	3420463	1606,248
18	1136,440	5,487864	30826,72	,1654629	4,9758417E-02	-3,575797	3372511	1430,269
19	1134,384	6,484615	27088,81	,2007044	5,4742025E-02	-3,555580	3316571	1172,465
20	1132,642	7,029663	22414,63	,2241189	5,8948743E-02	-3,034224	3272171	894,6124
21	1131,241	7,196104	17604,18	,2435028	6,1634153E-02	-2,394179	3239477	649,6182
22	1130,158	7,090281	13086,42	,2540098	6,2359571E-02	-1,761029	3220297	458,0651
23	1129,344	6,948769	9254,500	,2641864	6,2830818E-02	-1,271257	3209019	318,1811
24	1128,744	6,505293	6359,794	,2681450	6,1451376E-02	-,8900063	3201961	219,8216
25	1128,318	6,031877	4380,311	,2697828	5,9329410E-02	-,6186818	3197959	152,1337
26	1128,016	5,527733	3065,317	,2693646	5,6626866E-02	-,4294643	3195956	105,9332
27	1127,885	5,039046	0,	,2717480	5,4090226E-02	-,2977274	3190737	74,00667
28	1127,885	4,618800	0,	,2810234	5,1422333E-02	-,2158980	3183038	52,00433
29	1127,885	4,247933	0,	,2791742	4,5976889E-02	-,1519857	3178251	36,92631
30	1127,885	3,928888	0,	,2724616	3,0206554E-02	-,1064965	3175552	26,62267
31	1127,885	3,717890	0,	,2425517	1,9577549E-02	-7,0195141E-02	3174287	19,75330
32	1127,885	3,618037	0,	,2183940	1,7105314E-02	-4,8601333E-02	3173535	15,21101
33	1127,885	3,565310	0,	,2135199	1,6911192E-02	-3,8568783E-02	3173007	12,33091
34	1127,885	3,525072	0,	,2103657	1,6675563E-02	-3,3018870E-02	3172628	10,71490
35	1127,885	3,491951	0,	,2083551	1,6516011E-02	-3,0972387E-02	3172365	10,14790
36	1127,885	3,491951	0,	,2083551	1,6516011E-02	-3,0972387E-02	3172365	10,14790
37	1127,885	3,491951	0,	,2083551	1,6516011E-02	-3,0972387E-02	3172365	10,14790
38	1127,885	3,489747	0,	,2082265	1,6508486E-02	-3,0943802E-02	3172350	10,14479

ATOP III ATMOSPHERIC TRAJECTORY OPTIMIZATION PROGRAM VERSION 3,00 15 MAY 1972

CASE FUH407 STAGE 1 CYCLE 15 PASS 2 PAGE 178

ZOOM TO GIVEN Q, CORRECTED DATA

	TIME	VG77F	HGC7F	GAM7D	VI77F	RG77N	AMACH	AMASFI
1	0,	1936,000	50000,00	0,	3465,625	0,	1,999844	17302,76
2	4,000000	1944,528	49917,92	-1,217586	3473,954	1,273942	2,008653	17408,45
3	8,000000	1955,605	49667,59	-2,462564	3484,414	2,553850	2,020095	17674,40
4	12,00000	1969,256	49244,65	-3,713211	3497,018	3,840690	2,034196	18107,47
5	16,00000	1985,428	48646,90	-4,951213	3511,729	5,135511	2,050901	18709,78
6	20,00000	2003,946	47874,55	-6,147703	3528,424	6,439281	2,070030	19483,22
7	24,00000	2024,474	46932,32	-7,269025	3546,866	7,753127	2,091235	20424,79
8	28,00000	2046,416	45830,20	-8,260992	3566,644	9,077694	2,113901	21493,25
9	32,00000	2068,744	44590,25	-9,017470	3587,091	10,41387	2,136965	22781,55
10	36,00000	2091,007	43250,38	-9,465153	3608,095	11,76246	2,159962	24402,47
11	40,00000	2112,365	41852,93	-9,629162	3628,878	13,12411	2,182025	26088,82
12	44,00000	2131,445	40442,86	-9,407230	3648,381	14,49906	2,201734	27779,14
13	48,00000	2146,639	39092,87	-8,673123	3665,244	15,88715	2,217428	29587,54
14	52,00000	2156,656	37892,09	-7,188626	3678,360	17,28750	2,227776	31303,64
15	56,00000	2158,408	37001,05	-4,395954	3684,452	18,69816	2,229586	32584,53
16	60,00000	2147,635	36670,75	,3960510	3676,267	20,11245	2,218458	33072,25
17	64,00000	2122,332	37178,73	6,462013	3645,372	21,51288	2,192320	32342,75
18	68,00000	2081,734	38619,63	13,61697	3585,667	22,87396	2,150363	30172,67
19	72,00000	2021,443	41115,16	21,88446	3487,123	24,15790	2,088104	26706,17
20	76,00000	1949,302	44566,84	29,45246	3365,961	25,33188	2,013584	22325,43
21	80,00000	1870,199	48680,67	35,55183	3239,088	26,36865	1,931872	18165,96
22	84,00000	1784,542	53181,71	40,26758	3113,095	27,33417	1,843391	14332,63
23	88,00000	1694,975	57836,57	43,46322	2996,574	28,18328	1,750670	11082,50
24	92,00000	1603,441	62454,07	45,16682	2893,801	28,95053	1,656317	8392,595
25	96,00000	1511,230	66896,34	45,62147	2804,177	29,67294	1,561065	6149,965
26	100,00000	1420,083	71069,37	44,97672	2727,155	30,34833	1,466914	4526,763
27	104,0000	1331,345	74909,16	43,37730	2661,145	30,99453	1,375249	3364,241
28	108,0000	1239,529	78363,52	40,84523	2599,035	31,61913	1,280405	0,
29	112,0000	1153,346	81389,50	37,48207	2545,796	32,22631	1,191380	0,
30	116,0000	1075,416	83974,69	33,29733	2501,634	32,82084	1,107109	0,
31	120,0000	1007,238	86109,72	28,25344	2466,029	33,40610	1,032349	0,
32	124,0000	950,6490	87787,01	22,30133	2438,514	33,98498	,9710001	0,
33	128,0000	907,7810	89001,96	15,70061	2418,886	34,55944	,9249184	0,
34	132,0000	880,2321	89751,11	8,413490	2406,731	35,13115	,8954849	0,
35	136,0000	869,2578	90031,52	,7485643	2401,755	35,70142	,8838176	0,
36	136,0000	869,2578	90031,52	,7485643	2401,755	35,70142	,8838176	0,
37	136,0000	869,2578	90031,52	,7485643	2401,755	35,70142	,8838176	0,
38	136,3864	869,1034	90033,71	0,	2401,648	35,75640	,8836568	0,

TABLE V(e) Run 5

$\Delta T = 10$

$V_W = 0$

$q_f = 20$

ZOOM TO GIVEN Q, CORRECTED DATA

	AMASS	ALPHD	TE77P	CL	CD	ANZB7G	ESPEF	DYNPF
1	1166,000	2,282902	16800,48	6,3481815E-02	4,0307824E-02	-,6598221	3473667	681,9943
2	1164,802	2,222837	16886,86	6,1407307E-02	4,0201186E-02	-,6480227	3487600	690,7225
3	1163,592	2,159285	17132,66	5,9211578E-02	4,0089482E-02	-,6412854	3501230	707,0302
4	1162,357	2,091314	17542,87	5,6864628E-02	3,9971208E-02	-,6390706	3514551	731,5860
5	1161,086	2,016699	18120,72	5,4298543E-02	3,9842662E-02	-,6403048	3527492	765,2252
6	1159,766	1,955997	18867,33	5,2181814E-02	3,9739836E-02	-,6522478	3539830	808,9103
7	1158,391	1,897207	19779,59	5,0149852E-02	3,9642833E-02	-,6710206	3551162	863,6380
8	1156,944	1,877902	20802,49	4,9444117E-02	3,9618875E-02	-,7131553	3560710	930,2476
9	1155,418	1,922573	22020,12	5,0816259E-02	3,9669896E-02	-,7934787	3567134	1008,775
10	1153,789	1,954407	23547,77	5,1745750E-02	3,9712379E-02	-,8796091	3570727	1098,860
11	1152,046	1,939943	25136,59	5,1195551E-02	3,9673711E-02	-,9504967	3571059	1199,005
12	1150,185	2,054928	26729,37	5,4748309E-02	3,9867639E-02	-1,103663	3566572	1306,017
13	1148,206	2,141867	28403,56	5,7434068E-02	4,0033736E-02	-1,250959	3555985	1413,198
14	1146,101	2,445427	30004,21	6,7022001E-02	4,0581008E-02	-1,551940	3539241	1510,800
15	1143,891	2,988602	31235,64	8,4267980E-02	4,1548593E-02	-2,025987	3514582	1579,228
16	1141,618	3,882168	31788,61	,1128765	4,3741370E-02	-2,713237	3480845	1588,434
17	1139,351	4,057369	31252,65	,1189524	4,4325630E-02	-2,729031	3443037	1513,940
18	1137,184	5,224648	29346,24	,1570981	4,8492580E-02	-3,227228	3403683	1359,454
19	1135,216	6,023852	26165,42	,1855759	5,2518257E-02	-3,190228	3359602	1137,483
20	1133,518	6,174950	21963,79	,1940904	5,3220003E-02	-2,633793	3326427	896,6561
21	1132,119	6,422373	17857,92	,2113309	5,5674139E-02	-2,169152	3306428	677,8835
22	1131,003	6,538043	13869,30	,2264706	5,7678860E-02	-1,706730	3293188	497,6646
23	1130,133	6,379426	10300,73	,2319615	5,7577921E-02	-1,262100	3285417	359,3856
24	1129,464	6,076543	7385,708	,2344450	5,6736759E-02	-,9146602	3281194	257,9345
25	1128,967	5,656973	5261,021	,2342612	5,5309017E-02	-,6558228	3278636	185,3149
26	1128,602	5,214135	3789,372	,2319784	5,3474915E-02	-,4693295	3277435	134,0738
27	1128,331	4,794016	2770,261	,2294264	5,1475346E-02	-,3392788	3277079	98,10611
28	1128,292	4,426518	0,	,2295483	4,9631125E-02	-,2450153	3268484	72,12047
29	1128,292	4,127387	0,	,2378692	4,8416006E-02	-,1899653	3261171	54,04631
30	1128,292	3,859366	0,	,2444063	4,6031448E-02	-,1487967	3256127	41,27054
31	1128,292	3,654115	0,	,2433212	4,1695962E-02	-,1162984	3252658	32,44900
32	1128,292	3,591033	0,	,2462123	3,4323020E-02	-9,6826318E-02	3250290	26,54128
33	1128,292	3,550447	0,	,2476634	2,4879604E-02	-8,2649350E-02	3248858	22,75958
34	1128,292	3,514406	0,	,2428162	2,1652662E-02	-7,3315257E-02	3247903	20,60692
35	1128,292	3,485563	0,	,2372823	2,0646237E-02	-6,8881475E-02	3247164	19,81510
36	1128,292	3,485563	0,	,2372823	2,0646237E-02	-6,8881475E-02	3247164	19,81510
37	1128,292	3,485563	0,	,2372823	2,0646237E-02	-6,8881475E-02	3247164	19,81510
38	1128,292	3,483298	0,	,2370835	2,0623908E-02	-6,8791595E-02	3247099	19,80568

ATOP III ATMOSPHERIC TRAJECTORY OPTIMIZATION PROGRAM VERSION 3,00 15 MAY 1972

CASE F4HA07 STAGE 1 CYCLE 15 PASS 2 PAGE 175

ZOOM TO GIVEN Q, CORRECTED DATA

	TIME	VG77F	HGC7F	GAM7D	VI77F	RG77N	AMACH	AMASF1
1	0.	1936,000	50000,00	0,	3465,625	0,	1,999844	17302,76
2	4,000000	1949,940	49731,31	-3,871514	3477,589	1,274506	2,014243	17596,07
3	8,000000	1971,649	48965,65	-7,257977	3494,290	2,555623	2,036668	18367,69
4	12,00000	1998,684	47777,23	-9,716271	3515,697	3,840479	2,064595	19549,26
5	16,00000	2026,716	46339,33	-10,55599	3541,293	5,145346	2,093552	20973,47
6	20,00000	2050,270	44890,56	-9,621800	3567,179	6,463465	2,117882	22387,60
7	24,00000	2066,285	43665,27	-7,340063	3588,240	7,800850	2,134425	23860,04
8	28,00000	2072,727	42831,45	-4,039934	3599,643	9,153955	2,141060	24851,92
9	32,00000	2069,764	42522,09	-,2635176	3598,834	10,51391	2,138018	25207,75
10	36,00000	2055,882	42789,47	4,245462	3582,574	11,86887	2,123679	24862,83
11	40,00000	2029,652	43761,45	9,368174	3547,172	13,20142	2,096584	23654,91
12	44,00000	1991,094	45428,29	14,68888	3492,003	14,49374	2,056755	21637,42
13	48,00000	1942,899	47764,39	19,65614	3422,130	15,72730	2,006970	19327,24
14	52,00000	1890,204	50591,62	23,49640	3349,037	16,89741	1,952537	16717,36
15	56,00000	1832,021	53749,95	26,62479	3272,321	18,00432	1,892435	14209,13
16	60,00000	1767,342	57124,53	29,19796	3191,569	19,04835	1,825624	11910,76
17	64,00000	1700,053	60601,57	30,75578	3115,119	20,03297	1,756116	9822,589
18	68,00000	1631,750	64042,84	31,33952	3044,989	20,96946	1,685560	7961,762
19	72,00000	1562,481	67367,98	31,25866	2979,007	21,86436	1,614007	6336,772
20	76,00000	1493,591	70512,04	30,58465	2917,632	22,72418	1,542845	5023,498
21	80,00000	1426,592	73433,42	29,32194	2861,740	23,55338	1,473637	4050,454
22	84,00000	1361,400	76089,30	27,44153	2810,662	24,35774	1,406295	0,
23	88,00000	1293,688	78438,27	24,98471	2758,976	25,13817	1,336350	0,
24	92,00000	1233,650	80453,35	21,89660	2715,752	25,89755	1,274332	0,
25	96,00000	1182,343	82112,98	18,19633	2680,731	26,64089	1,221333	0,
26	100,00000	1140,667	83402,54	13,94917	2653,376	27,37182	1,175682	0,
27	104,0000	1109,768	84308,23	9,195674	2633,611	28,09372	1,141682	0,
28	104,0000	1090,609	84816,67	4,007688	2621,215	28,80925	1,120790	0,
29	108,0000	1090,609	84816,67	4,007688	2621,215	28,80925	1,120790	0,
30	110,9280	1084,439	84928,88	1,2457520E-02	2616,611	29,33050	1,114189	0,
31	110,9280	1084,439	84928,88	1,2457520E-02	2616,611	29,33050	1,114189	0,
32	110,9370	1084,430	84928,88	4,0233135E-06	2616,602	29,33211	1,114180	0,
33	110,9370	1084,430	84928,88	4,0233135E-06	2616,602	29,33211	1,114180	0,
34	110,9370	1084,430	84928,88	4,0233135E-06	2616,602	29,33211	1,114180	0,
35	110,9370	1084,430	84928,88	0,	2616,602	29,33211	1,114180	0,

TABLE V(f) Run 6

ATOP III ATMOSPHERIC TRAJECTORY OPTIMIZATION PROGRAM VERSION 3,00   15 MAY 1972

CASE F4HA07   STAGE 1   CYCLE 15   PASS 2   PAGE 176

ZOOM TO GIVEN Q, CORRECTED DATA

	AMASS	ALPHD	TE77P	CL	CD	ANZB7G	ESPEF	DYNPP
1	1166.000	8.3283133E-03	16800.48	-1.4715255E-02	3,8662598E-02	,1085394	3473667	681,9943
2	1164.798	,3817699	17066.49	-1.5250170E-03	3,8314403E-02	-2,1158897E-02	3492196	700,8002
3	1163.558	,6445274	17805.40	7.8605211E-03	3,8475471E-02	-,1225049	3510382	743,2208
4	1162.251	1.550259	18950.40	3.8633032E-02	3,9308531E-02	-,4922376	3526200	808,4236
5	1160.852	2.581068	20338.44	7.2590306E-02	4,0856007E-02	-,9799251	3536813	890,4631
6	1159.354	3.430516	21701.32	,1000661	4,2357566E-02	-1,464511	3538659	976,7002
7	1157.755	3.753050	23111.26	,1102876	4,3396503E-02	-1,735659	3532567	1051,933
8	1156.070	4.200969	24077.10	,1246215	4,4847028E-02	-2,050445	3519316	1101,602
9	1154.337	4.065814	24446.60	,1203524	4,4413527E-02	-2,008784	3503314	1114,841
10	1152.603	5.000566	24162.07	,1508441	4,7504013E-02	-2,444786	3483203	1065,949
11	1150.923	5.045191	23058.61	,1532168	4,7793316E-02	-2,313894	3460610	1010,302
12	1149.356	5.930571	21128.67	,1839978	5,2056844E-02	-2,466300	3436221	897,7327
13	1147.939	5.702378	18879.65	,1785783	5,0902419E-02	-2,042506	3415650	764,3950
14	1146.695	5.766891	16299.93	,1861952	5,1617099E-02	-1,761672	3404890	631,9714
15	1145.626	6.129429	13667.25	,2057867	5,4184691E-02	-1,571697	3397124	510,4365
16	1144.727	6.613717	11205.34	,2315123	5,8421121E-02	-1,399517	3388058	404,2565
17	1143.979	6.020108	8856.634	,2174182	5,5052560E-02	-1,030489	3381920	316,7890
18	1143.365	6.464708	6910.515	,2444997	5,8827363E-02	-,9041944	3377445	247,5981
19	1142.873	6.331326	5400.866	,2533040	5,9223496E-02	-,7319554	3372370	193,6856
20	1142.483	6.898581	4219.435	,2923331	6,5248390E-02	-,6630682	3366849	152,3122
21	1142.171	6.678845	3367.653	,2983697	6,4397199E-02	-,5364385	3361652	120,8676
22	1141.957	7.016726	0.	,3321080	6,9160463E-02	-,4728956	3354938	96,97024
23	1141.957	7.249146	0.	,3628242	7,2753645E-02	-,4167986	3339450	78,28092
24	1141.957	6.788522	0.	,3602983	6,9181583E-02	-,3413345	3327382	64,66026
25	1141.957	6.595964	0.	,3723580	6,8948474E-02	-,2990642	3317931	54,87394
26	1141.957	6.205772	0.	,3674297	6,5491098E-02	-,2568623	3310328	47,82123
27	1141.957	5.757967	0.	,3524088	6,1036870E-02	-,2223235	3304211	43,20112
28	1141.957	4.998925	0.	,3122277	5,4415329E-02	-,1851528	3299215	40,64641
29	1141.957	4.998925	0.	,3122277	5,4415329E-02	-,1851528	3299215	40,64641
30	1141.957	4.651630	0.	,2923878	5,1584336E-02	-,1703846	3296053	39,95700
31	1141.957	4.651630	0.	,2923878	5,1584336E-02	-,1703846	3296053	39,95700
32	1141.957	4.650560	0.	,2923229	5,1576632E-02	-,1703439	3296044	39,95636
33	1141.957	4.650560	0.	,2923229	5,1576632E-02	-,1703439	3296044	39,95636
34	1141.957	4.650560	0.	,2923229	5,1576632E-02	-,1703439	3296044	39,95636
35	1141.957	4.650560	0.	,2923228	5,1576630E-02	-,1703439	3295044	39,95636

ORIGINAL PAGE IS
OF POOR QUALITY

ATOP III ATMOSPHERIC TRAJECTORY OPTIMIZATION PROGRAM VERSION 3,00 15 MAY 1972

CASE F4HA07 STAGE 1 CYCLE 15 PASS 3 PAGE 194

ZOOM TO GIVEN Q, CORRECTED DATA

	TIME	VG77F	HGC7F	GAM70	VI77F	RG77N	AMACH	AMASF1
1	0,	2011,000	50000,00	0,	3540,625	0,	1,999844	17302,76
2	4,000000	2019,704	49913,94	-1,232081	3549,122	1,323278	2,008187	17410,30
3	8,000000	2031,167	49649,82	-2,509117	3559,930	2,652602	2,018043	17663,16
4	12,00000	2045,510	49200,68	-3,807382	3573,145	3,989100	2,029492	18129,08
5	16,00000	2062,764	48562,31	-5,101022	3588,804	5,333983	2,042542	18755,30
6	20,00000	2082,844	47733,56	-6,364476	3606,864	6,688379	2,057110	19556,35
7	24,00000	2105,491	46716,18	-7,577204	3627,133	8,053575	2,072953	20543,71
8	28,00000	2130,329	45514,90	-8,709055	3649,349	9,430542	2,089724	21705,77
9	32,00000	2156,965	44141,09	-9,699328	3673,349	10,82041	2,107089	23242,23
10	36,00000	2185,279	42616,51	-10,48325	3699,319	12,22454	2,125056	25068,57
11	40,00000	2214,218	40972,97	-10,99364	3726,550	13,64431	2,142717	27633,66
12	44,00000	2242,377	39257,13	-11,12876	3754,088	15,08118	2,164498	29289,25
13	48,00000	2267,927	37539,59	-10,71404	3780,691	16,53018	2,190661	31819,52
14	52,00000	2288,253	35920,90	-9,635105	3803,903	18,00980	2,208782	34058,16
15	56,00000	2299,348	34531,85	-7,553374	3819,870	19,50051	2,205449	34996,53
16	60,00000	2296,624	33601,51	-3,693708	3823,146	21,00364	2,192425	35525,93
17	64,00000	2277,142	33450,72	2,071074	3804,963	22,50665	2,170639	35957,25
18	68,00000	2233,651	34373,08	10,19607	3747,778	23,98176	2,137728	35080,64
19	72,00000	2162,935	36663,93	20,17111	3636,240	25,37598	2,089502	32754,35
20	76,00000	2069,514	40262,14	30,15527	3477,395	26,63404	2,007069	27227,65
21	80,00000	1963,744	44633,53	38,65504	3299,270	27,72418	1,938134	21633,24
22	84,00000	1857,309	49943,10	45,06527	3130,896	28,65646	1,864343	16632,10
23	88,00000	1752,261	55260,19	49,58597	2981,197	29,45750	1,786455	12584,00
24	92,00000	1649,030	60553,05	52,30235	2853,707	30,15856	1,703410	9482,550
25	96,00000	1545,861	65663,77	53,65212	2745,532	30,78792	1,596839	6754,164
26	100,00000	1442,739	70485,59	53,71904	2653,320	31,36729	1,490316	4767,493
27	104,0000	1340,820	74950,65	52,78367	2574,295	31,91248	1,385036	3392,667
28	108,0000	1234,459	79006,74	50,91133	2500,916	32,43325	1,275168	0,
29	112,0000	1132,217	82612,04	48,20737	2437,396	32,93547	1,168900	0,
30	116,0000	1036,396	85757,28	44,63601	2383,663	33,42431	1,064007	0,
31	120,0000	948,3931	88435,03	40,06773	2339,270	33,90373	,9674040	0,
32	124,0000	870,2873	90639,54	34,39088	2303,807	34,37677	,8837759	0,
33	128,0000	804,2250	92365,39	27,47944	2276,652	34,84586	,8138551	0,
34	132,0000	753,1760	93606,77	19,34355	2257,292	35,31245	,7603026	0,
35	136,0000	720,3317	94360,55	10,18376	2245,458	35,77760	,7260553	0,
36	140,0000	708,2304	94625,35	,4064070	2241,098	36,24193	,7134817	0,
37	140,0000	708,2304	94625,35	,4064070	2241,098	36,24193	,7134817	0,
38	140,0000	708,2304	94625,35	,4064070	2241,098	36,24193	,7134817	0,
39	140,1642	708,1984	94625,76	0,	2241,078	36,26096	,7134490	0,

TABLE V(g) Run 7

$\Delta T = 10$
$V_W = 150$
$q_f = 10$

ATOP III ATMOSPHERIC TRAJECTORY OPTIMIZATION PROGRAM VERSION 3,00 15 MAY 1972

CASE F4HA07 STAGE 1 CYCLE 15 PASS 3 PAGE 195

ZOOM TO GIVEN Q, CORRECTED DATA

	AMASS	ALPHA	TETTP	CL	CD	ANZBTG	ESPEF	DYNPP
1	1165,000	2,238868	16800,48	6,2007215E-02	4,0228205E-02	-,6453156	3621679	681,9943
2	1164,802	2,164023	16890,00	5,9443754E-02	4,0094675E-02	-,6262807	3635481	690,5336
3	1163,591	2,088139	17146,66	5,6850515E-02	3,9960753E-02	-,6164890	3651289	706,1942
4	1162,355	2,012730	17577,76	5,4276189E-02	3,9828609E-02	-,6102726	3666223	729,7413
5	1161,083	1,941909	18188,29	5,1823307E-02	3,9703984E-02	-,6106219	3681333	762,0779
6	1159,761	1,872728	18980,37	4,9441668E-02	3,9599112E-02	-,6169681	3696559	804,2513
7	1158,377	1,800574	19953,44	4,6991464E-02	3,9541160E-02	-,6275180	3711576	857,4252
8	1156,919	1,745252	21103,97	4,5133990E-02	3,9498586E-02	-,6506546	3725904	922,9109
9	1155,370	1,725600	22603,54	4,4475250E-02	3,9482472E-02	-,6971934	3739215	1002,077
10	1153,763	1,719270	24362,63	4,4260038E-02	3,9469258E-02	-,7597439	3752085	1096,348
11	1151,904	1,745815	26254,79	4,5106527E-02	3,9485896E-02	-,8507784	3763332	1205,943
12	1149,964	1,813514	28398,99	4,7242234E-02	3,9536983E-02	-,9644541	3771344	1335,949
13	1147,854	1,946360	30749,70	5,1362293E-02	3,9679770E-02	-1,184960	3774156	1485,749
14	1145,574	2,077505	32802,13	5,5431142E-02	3,9912925E-02	-1,400025	3768791	1632,169
15	1143,183	2,465504	33578,12	6,8489068E-02	4,0640832E-02	-1,825658	3749886	1735,231
16	1140,730	3,226954	34399,38	9,2370125E-02	4,1969338E-02	-2,520641	3713915	1794,568
17	1138,243	3,805039	34547,90	,1113018	4,3528697E-02	-2,991766	3664546	1771,863
18	1135,784	5,166526	34075,76	,1556982	4,8256595E-02	-3,873335	3595915	1645,405
19	1133,425	5,944015	32308,54	,1829141	5,2135086E-02	-3,903425	3513602	1409,594
20	1131,345	6,787412	27040,14	,2145827	5,7105852E-02	-3,558810	3430721	1094,651
21	1129,653	6,664424	21460,57	,2188965	5,7269759E-02	-2,723591	3363183	820,1819
22	1128,332	6,678227	16364,68	,2249027	5,8398856E-02	-2,064967	3322605	594,3229
23	1127,324	6,475942	11991,66	,2312709	5,7892262E-02	-1,465914	3302228	423,1817
24	1126,563	6,140894	8501,935	,2242361	5,6363833E-02	-1,035041	3294938	296,7508
25	1126,004	5,644868	5806,201	,2272134	5,4766744E-02	-,7083991	3292448	205,6628
26	1125,609	5,147371	3999,349	,2241508	5,2828367E-02	-,4829566	3291351	142,2969
27	1125,329	4,715276	2794,615	,2236536	5,0957145E-02	-,3356506	3291054	99,31274
28	1125,290	4,352637	0.	,2270304	4,9244854E-02	-,2336747	3282562	69,37029
29	1125,290	4,066067	0.	,2403874	4,7797091E-02	-,1747167	3275714	49,08162
30	1125,290	3,814608	0.	,2486856	4,4146206E-02	-,1286642	3271368	34,97912
31	1125,290	3,622393	0.	,2507020	3,3657994E-02	-9,4421995E-02	3268622	25,50243
32	1125,290	3,581180	0.	,2435685	2,1101207E-02	-6,8929764E-02	3267270	19,26549
33	1125,290	3,539172	0.	,2188518	1,7379402E-02	-4,8501196E-02	3266477	15,09376
34	1125,290	3,515513	0.	,2118549	1,6647548E-02	-3,8717441E-02	3265927	12,44768
35	1125,290	3,498262	0.	,2097462	1,6676754E-02	-3,3781733E-02	3265529	10,96947
36	1125,290	3,483614	0.	,2084889	1,6609331E-02	-3,2039551E-02	3265245	10,46645
37	1125,290	3,483614	0.	,2084889	1,6609331E-02	-3,2039551E-02	3265245	10,46645
38	1125,290	3,483614	0.	,2084889	1,6609331E-02	-3,2039551E-02	3265245	10,46645
39	1125,290	3,483071	0.	,2084564	1,6607381E-02	-3,2031017E-02	3265235	10,46530

ATOP III ATMOSPHERIC TRAJECTORY OPTIMIZATION PROGRAM VERSION 3.00 15 MAY 1972

CASE F4HA07 STAGE 1 CYCLE 14 PASS 2 PAGE 160

ZOOM TO GIVEN Q, CORRECTED DATA

	TIME	VG77F	HGC7F	GAM7D	VI77F	RG77N	AMACH	AMASF1
1	0.	2011.000	50000.00	0.	3540.625	0.	1.999804	17302.70
2	4.000000	2020.260	49900.64	-1.411224	3549.614	1.323439	2.008664	17423.95
3	8.000000	2032.510	49601.79	-2.809798	3561.057	2.653166	2.019079	17730.07
4	12.00000	2047.752	49104.29	-4.171790	3574.991	3.990390	2.031101	18221.77
5	16.00000	2065.887	48411.77	-5.472118	3591.389	5.336240	2.044663	18897.15
6	20.00000	2086.661	47531.79	-6.670322	3610.128	6.692166	2.059562	19750.50
7	24.00000	2109.644	46478.22	-7.726841	3630.953	8.059298	2.075455	20769.89
8	28.00000	2134.246	45270.09	-8.604663	3653.485	9.438845	2.091864	21937.71
9	32.00000	2159.974	43934.46	-9.242051	3677.516	10.83210	2.108449	23487.49
10	36.00000	2186.309	42509.37	-9.573486	3702.836	12.24042	2.124908	25195.81
11	40.00000	2211.961	41044.56	-9.526344	3728.445	13.66519	2.140214	26944.25
12	44.00000	2235.439	39603.84	-9.038502	3753.015	15.10713	2.156272	28772.75
13	48.00000	2255.156	38263.72	-8.027334	3774.987	16.56625	2.176204	30743.90
14	52.00000	2269.019	37123.82	-6.306088	3792.175	18.04124	2.189961	32415.69
15	56.00000	2274.251	36329.20	-3.511481	3801.163	19.52873	2.194614	33570.86
16	60.00000	2267.515	36086.66	.7065703	3796.056	21.02105	2.186738	33698.61
17	64.00000	2245.361	36615.30	6.169959	3768.738	22.50169	2.165421	33087.33
18	68.00000	2203.561	38075.19	13.03160	3708.998	23.94403	2.125559	30896.06
19	72.00000	2139.925	40597.55	20.81619	3609.196	25.30907	2.069659	27202.40
20	76.00000	2058.489	44087.01	28.19936	3481.986	26.56294	2.018562	22900.02
21	80.00000	1970.033	48282.67	34.39640	3345.597	27.69202	1.960764	18680.79
22	84.00000	1878.161	52902.16	39.20176	3212.638	28.70235	1.897803	14815.98
23	88.00000	1785.566	57707.99	42.50980	3090.966	29.61007	1.831410	11646.91
24	92.00000	1693.652	62511.04	44.52343	2984.508	30.43628	1.749503	9022.107
25	96.00000	1601.663	67165.59	45.13645	2892.768	31.20179	1.654481	6652.002
26	100.00000	1510.788	71564.74	44.63125	2814.171	31.92409	1.560610	4662.571
27	104.0000	1420.547	75637.68	43.16291	2745.394	32.61616	1.467392	0.
28	108.0000	1326.642	79316.85	40.80367	2680.054	33.28469	1.370391	0.
29	112.0000	1239.892	82567.07	37.66393	2625.205	33.93541	1.260184	0.
30	116.0000	1160.990	85374.23	33.78605	2579.237	34.57322	1.191792	0.
31	120.0000	1091.115	87729.64	29.17152	2541.372	35.20161	1.114604	0.
32	124.0000	1031.724	89627.24	23.82627	2511.138	35.82314	1.049560	0.
33	128.0000	984.4998	91062.60	17.78869	2488.295	36.43952	.9969045	0.
34	132.0000	951.1515	92032.59	11.16297	2472.713	37.05251	.9631837	0.
35	136.0000	933.0615	92535.29	4.127875	2464.283	37.66316	.9439125	0.
36	136.0000	933.0615	92535.29	4.127875	2464.283	37.66316	.9439125	0.
37	138.2917	929.8461	92612.32	3.1261146E-03	2462.579	38.01246	.9405143	0.
38	138.2917	929.8461	92612.32	3.1261146E-03	2462.579	38.01246	.9405143	0.
39	138.2917	929.8461	92612.32	3.1261146E-03	2462.579	38.01246	.9405143	0.
40	138.2935	929.8456	92612.32	0.	2462.578	38.01278	.9405139	0.

TABLE V(h) Run 8

ATOP III ATMOSPHERIC TRAJECTORY OPTIMIZATION PROGRAM VERSION 3,00 15 MAY 1972

CASE F4M407 STAGE 1 CYCLE 14 PASS 2 PAGE 161

ZOOM TO GIVEN Q, CORRECTED DATA

	AMASS	ALPHD	TF77P	CL	CD	ANZBTG	ESPEF	DYNPP
1	1166,000	2,067644	16800,48	5,6269958E-02	3,9918429E-02	-,5888747	3621679	681,9943
2	1164,802	2,038566	16902,89	5,5246788E-02	3,9868525E-02	-,5870723	3637181	691,3015
3	1163,589	2,006709	17192,47	5,4128385E-02	3,9814380E-02	-,5906401	3652488	708,5455
4	1162,348	1,973384	17669,38	5,2939680E-02	3,9757403E-02	-,5998383	3667740	734,2770
5	1161,067	1,940549	18331,25	5,1768778E-02	3,9702312E-02	-,6156636	3682987	769,1612
6	1159,734	1,929073	19172,05	5,1323850E-02	3,9687225E-02	-,6465926	3698090	813,9902
7	1158,335	1,916513	20179,67	5,0844794E-02	3,9670892E-02	-,6847748	3712746	869,3386
8	1156,861	1,920978	21336,80	5,0932393E-02	3,9685467E-02	-,7384358	3726454	935,7000
9	1155,294	1,954107	22844,43	5,1955328E-02	3,9742539E-02	-,8153879	3739124	1013,344
10	1153,614	2,002886	24438,92	5,3469427E-02	3,9819114E-02	-,9115785	3750921	1101,881
11	1151,813	2,085678	26176,48	5,6079053E-02	3,9957073E-02	-1,038286	3766620	1199,010
12	1149,891	2,170715	27927,75	5,8737514E-02	4,0099151E-02	-1,180769	3766871	1303,965
13	1147,835	2,291463	29773,57	6,2497811E-02	4,0303448E-02	-1,361736	3768382	1416,230
14	1145,651	2,531530	31338,61	7,0099701E-02	4,0725563E-02	-1,627295	3763361	1514,579
15	1143,369	2,979148	32441,03	8,4399222E-02	4,1524805E-02	-2,033256	3749683	1560,111
16	1141,033	3,580234	32812,22	,1037915	4,2777747E-02	-2,500910	3726843	1567,075
17	1138,713	4,075584	32147,64	,1200895	4,4414490E-02	-2,763783	3693729	1517,417
18	1136,495	5,216602	30201,41	,1577529	4,8540215E-02	-3,252839	3647341	1363,333
19	1134,482	5,913816	26743,53	,1828435	5,1980657E-02	-3,168154	3587541	1145,404
20	1132,746	6,366737	22559,44	,2001356	5,4149787E-02	-2,773326	3529931	922,0273
21	1131,313	6,506945	18336,05	,2106400	5,5822956E-02	-2,271796	3465445	711,7346
22	1130,163	6,618019	14321,66	,2224507	5,7530199E-02	-1,802609	3455742	534,5765
23	1129,256	6,483577	10911,55	,2259671	5,7441031E-02	-1,355468	3438982	395,6340
24	1128,547	6,229912	7966,672	,2263205	5,6563101E-02	-,9844546	3431721	286,9920
25	1128,010	5,772333	5666,655	,2220811	5,4711924E-02	-,6911739	3427937	205,4979
26	1127,616	5,255971	4073,108	,2166455	5,2700351E-02	-,4858441	3426056	148,2617
27	1127,368	4,804637	0,	,2127147	5,0913120E-02	-,3408485	3422901	107,8790
28	1127,368	4,418053	0,	,2112782	4,9196521E-02	-,2473513	3416405	78,94107
29	1127,368	4,120314	0,	,2129122	4,7802746E-02	-,1860332	3401999	58,99848
30	1127,368	3,860176	0,	,2221377	4,6869778E-02	-,1470302	3396084	44,70373
31	1127,368	3,661253	0,	,2302773	4,4986842E-02	-,1192201	3391876	35,06594
32	1127,368	3,604715	0,	,2377132	4,2453933E-02	-9,9863872E-02	3388612	28,48730
33	1127,368	3,560517	0,	,2422832	3,9125075E-02	-8,6143327E-02	3386556	24,13739
34	1127,368	3,526112	0,	,2452530	3,2128420E-02	-7,7396867E-02	3384921	21,46522
35	1127,368	3,498400	0,	,2451244	2,7782972E-02	-7,2522764E-02	3383756	20,14624
36	1127,368	3,498400	0,	,2451244	2,7782972E-02	-7,2522764E-02	3383756	20,14624
37	1127,368	3,484191	0,	,2440637	2,7130595E-02	-7,1427805E-02	3383193	19,93119
38	1127,368	3,484191	0,	,2440637	2,7130595E-02	-7,1427805E-02	3383193	19,93119
39	1127,368	3,484191	0,	,2440637	2,7130595E-02	-7,1427805E-02	3383193	19,93119
40	1127,368	3,484180	0,	,2440629	2,7130458E-02	-7,1427528E-02	3383193	19,93117

```
CTABLE*OCT 1[illegible]657777777777[illegible]7777,172661[illegible]777777777777     25 F4[illegible]0712  ***  96,0000   100,0000
CTABLE*OCT 17266377777777777777,17266577777777777777     27 F4HA0712  ***  104,000   108,000
CTABLE*OCT 17266777777777777777,17267177777777777777     29 F4HA0712  ***  112,000   116,000
CTABLE*OCT 17267305763102413313,60602661101400б141
```

ATOP III ATMOSPHERIC TRAJECTORY OPTIMIZATION PROGRAM VERSION 3,00 15 MAY 1972

CASE F4HA07 STAGE 1 CYCLE 15 PASS 2 PAGE 175

ZOOM TO GIVEN Q, CORRECTED DATA

	TIME	VG77F	HGC7F	GAM7D	VI77F	RG77N	AMACH	AMASF1
1	0,	2011,000	50000,00	0,	3540,625	0,	1,999844	17302,76
2	4,000000	2025,036	49685,14	-4,306667	3552,177	1,323439	2,012137	17629,56
3	8,000000	2048,150	48814,12	-7,889083	3569,392	2,652682	2,029887	18477,66
4	12,00000	2078,148	47468,43	-10,69907	3592,239	3,989181	2,051359	19774,04
5	16,00000	2111,976	45780,62	-12,32057	3620,807	5,336965	2,074131	21395,86
6	20,00000	2146,131	43925,96	-12,60724	3653,720	6,702001	2,095552	23457,27
7	24,00000	2177,304	42106,86	-11,41733	3688,536	8,090738	2,113402	25640,25
8	28,00000	2201,701	40545,54	-8,971757	3719,621	9,506560	2,125602	27496,96
9	32,00000	2215,981	39417,88	-5,502351	3740,663	10,94649	2,134876	28991,80
10	36,00000	2216,673	38903,26	-1,010742	3745,348	12,40076	2,134852	29729,98
11	40,00000	2202,888	39139,09	4,151079	3729,353	13,85254	2,121023	29360,34
12	44,00000	2174,703	40188,15	9,658415	3690,866	15,28061	2,095263	27831,63
13	48,00000	2134,152	42034,27	15,01539	3632,654	16,66331	2,070410	25537,13
14	52,00000	2085,079	44556,79	19,63154	3562,658	17,98586	2,041545	22467,20
15	56,00000	2028,678	47589,36	23,57176	3484,606	19,24198	2,007819	19487,17
16	60,00000	1968,068	50992,35	26,62368	3405,282	20,42943	1,970832	16503,22
17	64,00000	1904,711	54602,26	28,88261	3327,462	21,55464	1,931012	13821,69
18	68,00000	1837,594	58324,70	30,67[illegible]82	3248,882	22,62051	1,887041	11578,41
19	72,00000	1768,878	62070,99	31,77445	3174,026	23,63214	1,827210	9618,417
20	76,00000	1698,318	65749,47	32,21014	3102,712	24,59677	1,754323	7788,955
21	80,00000	1627,203	69290,10	31,99119	3036,073	25,52036	1,680863	6113,045
22	84,00000	1557,352	72627,43	31,11529	2975,471	26,41001	1,608708	4834,360
23	88,00000	1487,816	75715,65	29,68197	2918,615	27,27137	1,536880	0,
24	92,00000	1414,129	78501,59	27,59850	2860,946	28,10581	1,460763	0,
25	96,00000	1347,772	80948,23	24,88479	2812,300	28,91719	1,392217	0,
26	100,00000	1289,698	83030,86	21,52819	2772,451	29,71099	1,330319	0,
27	104,0000	1240,881	84727,44	17,55409	2740,925	30,49190	1,275455	0,
28	108,0000	1202,198	86019,98	13,05105	2716,993	31,26346	1,232398	0,
29	112,0000	1174,526	86895,33	8,112396	2700,180	32,02832	1,201865	0,
30	116,0000	1158,601	87342,78	2,851603	2690,132	32,78867	1,184481	0,
31	116,0000	1158,601	87342,78	2,851603	2690,132	32,78867	1,184481	0,
32	118,0995	1155,099	87403,55	9,1490148E-03	2687,452	33,18650	1,180754	0,
33	118,0995	1155,099	87403,55	9,1490148E-03	2687,452	33,18650	1,180754	0,
34	118,0995	1155,099	87403,55	9,1490148E-03	2687,452	33,18650	1,180754	0,
35	118,1062	1155,093	87403,55	4,0233135E-06	2687,446	33,18779	1,180748	0,
36	118,1062	1155,093	87403,55	4,0233135E-06	2687,446	33,18779	1,180748	0,
37	118,1062	1155,093	87403,55	4,0233135E-06	2687,446	33,18779	1,180748	0,
38	118,1062	1155,093	87403,55	4,0233135E-06	2687,446	33,18779	1,180748	0,
39	118,1062	1155,093	87403,55	0,	2687,446	33,18779	1,180748	0,

TABLE V(i) Run 9

ATOP III ATMOSPHERIC TRAJECTORY OPTIMIZATION PROGRAM VERSION 3,00 15 MAY 1972

CASE F4HA07 STAGE 1 CYCLE 15 PASS 2 PAGE 176

ZOOM TO GIVEN Q, CORRECTED DATA

	AMASS	ALPHD	TE77P	CL	CD	ANZB7G	ESPEF	DYNPP
1	1166,000	-,6520018	16800,48	-3,7172879E-02	3,9246425E-02	,3292532	3621679	681,9943
2	1164,797	,1057288	17106,75	-1,1039435E-02	3,8564850E-02	7,4890065E-02	3639978	700,8820
3	1163,553	,4170010	17937,39	5,8990596E-06	3,8268202E-02	-3,8503168E-02	3659316	743,6511
4	1162,234	1,113988	19219,07	2,3915259E-02	3,8905818E-02	-,3212709	3678343	809,9708
5	1160,814	1,851830	20829,24	4,8695960E-02	3,9588640E-02	-,6776486	3695441	897,7011
6	1159,270	2,510618	22862,82	7,0262016E-02	4,0731480E-02	-1,069650	3709048	1001,392
7	1157,573	3,186689	24986,89	9,2177782E-02	4,1923545E-02	-1,541908	3718438	1111,186
8	1155,736	3,438804	26796,59	,1002166	4,2377128E-02	-1,824390	3722150	1211,290
9	1153,784	3,831901	28249,15	,1128412	4,3654003E-02	-2,183213	3717630	1289,668
10	1151,750	4,157202	28986,13	,1233563	4,4712826E-02	-2,445195	3702745	1321,613
11	1149,703	4,447231	28686,59	,1330412	4,5670625E-02	-2,574718	3679808	1290,092
12	1147,721	4,795229	27270,46	,1450909	4,6820614E-02	-2,606517	3651584	1197,271
13	1145,873	4,918099	25051,69	,1499183	4,7136829E-02	-2,410429	3623100	1070,149
14	1144,212	4,893208	22024,52	,1500279	4,6958296E-02	-2,082073	3599994	922,1747
15	1142,763	5,296578	19043,02	,1647878	4,8892946E-02	-1,913326	3580614	771,4756
16	1141,524	5,030309	16021,01	,1586763	4,7813507E-02	-1,511315	3567659	631,6459
17	1140,475	5,545557	13198,30	,1806360	5,0686255E-02	-1,387781	3560052	510,2377
18	1139,599	5,870853	10788,82	,1970706	5,2602658E-02	-1,209211	3552640	407,3336
19	1138,871	5,934370	8617,279	,2060868	5,3628751E-02	-,9409651	3547979	319,7040
20	1138,271	6,418029	6631,321	,2330347	5,7811378E-02	-,8650351	3542467	247,2152
21	1137,792	6,382478	5121,616	,2421181	5,8359290E-02	-,6959837	3536577	191,6421
22	1137,416	6,549673	4024,113	,2635868	6,1207956E-02	-,5909882	3531191	149,6891
23	1137,163	6,779601	0,	,2883297	6,4342751E-02	-,5019606	3523193	117,6986
24	1137,163	6,709077	0,	,3031030	6,4968202E-02	-,4168999	3504521	93,25306
25	1137,163	6,376930	0,	,3048102	6,3207132E-02	-,3384304	3490345	75,37645
26	1137,163	5,942451	0,	,2978660	5,9986375E-02	-,2730610	3479668	62,31908
27	1137,163	5,398253	0,	,2842354	5,6397536E-02	-,2207480	3471571	52,86076
28	1137,163	4,904556	0,	,2708566	5,3397207E-02	-,1846117	3465196	46,43862
29	1137,163	4,403077	0,	,2511379	5,0143581E-02	-,1561265	3459990	42,39102
30	1137,163	3,951531	0,	,2293694	4,7314396E-02	-,1355603	3455558	40,32163
31	1137,163	3,951531	0,	,2293694	4,7314396E-02	-,1355603	3455558	40,32163
32	1137,163	3,758502	0,	,2191012	4,6167432E-02	-,1282912	3453428	39,95475
33	1137,163	3,758502	0,	,2191012	4,6167432E-02	-,1282912	3453428	39,95475
34	1137,163	3,758502	0,	,2191012	4,6167432E-02	-,1282912	3453428	39,95475
35	1137,163	3,757884	0,	,2190667	4,6163832E-02	-,1282696	3453421	39,95435
36	1137,163	3,757884	0,	,2190667	4,6163832E-02	-,1282696	3453421	39,95435
37	1137,163	3,757884	0,	,2190667	4,6163832E-02	-,1282696	3453421	39,95435
38	1137,163	3,757884	0,	,2190667	4,6163832E-02	-,1282696	3453421	39,95435
39	1137,163	3,757884	0,	,2190667	4,6163831E-02	-,1282696	3453421	39,95435

ZOOM TO GIVEN Q, CORRECTED DATA

	AMASS	ALPHD	TE77P	CL	CD	ANZB7G	ESPEF	DYNPP
1	1166.000	2.637038	16914.41	7.4392897E-02	4.0955382E-02	-.8406120	3660069	749.8288
2	1164.779	2.542255	16952.02	7.1263867E-02	4.0787917E-02	-.8109045	3663813	752.9513
3	1163.553	2.437492	17061.71	6.7799350E-02	4.0601013E-02	-.7814048	3667822	760.2166
4	1162.316	2.323143	17260.92	6.4015087E-02	4.0395721E-02	-.7523723	3672035	772.4580
5	1161.060	2.204270	17564.64	6.0080572E-02	4.0181032E-02	-.7256139	3676377	790.6160
6	1159.779	2.085968	17985.08	5.6492466E-02	3.9983479E-02	-.7067360	3680680	815.7032
7	1158.462	1.972258	18531.94	5.2415243E-02	3.9757069E-02	-.6856311	3684739	846.8149
8	1157.102	1.879179	19213.73	4.9371287E-02	3.9601753E-02	-.6807805	3688176	891.1969
9	1155.687	1.796929	20033.56	4.6710315E-02	3.9521135E-02	-.6847582	3690241	943.9253
10	1154.207	1.721677	20959.82	4.4310354E-02	3.9447342E-02	-.6961542	3690157	1008.068
11	1152.650	1.672001	22240.45	4.2750231E-02	3.9397505E-02	-.7247049	3687295	1064.726
12	1150.991	1.657296	23687.56	4.2301048E-02	3.9400092E-02	-.7776512	3681840	1175.040
13	1149.220	1.702157	25234.71	4.3086663E-02	3.9454515E-02	-.8721571	3672197	1278.271
14	1147.333	1.847359	26833.56	4.8101638E-02	3.9595848E-02	-1.039596	3656627	1391.106
15	1145.314	2.035164	28753.91	5.3796897E-02	3.9875125E-02	-1.253522	3634766	1506.606
16	1143.159	2.582428	30500.37	7.1003571E-02	4.0943889E-02	-1.749547	3604693	1609.789
17	1140.893	3.362471	31762.75	9.5659147E-02	4.2218674E-02	-2.426295	3564193	1669.894
18	1138.574	4.046450	32131.30	.1176147	4.4265818E-02	-2.939643	3515010	1649.622
19	1136.287	5.237033	31228.31	.1556866	4.8374200E-02	-3.584952	3457210	1523.467
20	1134.152	5.960786	28407.01	.1812761	5.2094310E-02	-3.559034	3396844	1248.104
21	1132.283	6.424831	24369.74	.1999689	5.4414427E-02	-3.116021	3347823	1029.166
22	1130.739	6.443438	19773.98	.2071619	5.5211277E-02	-2.433397	3317016	774.6735
23	1129.505	6.147371	15381.32	.2076619	5.4452292E-02	-1.782062	3302803	565.4317
24	1128.544	5.864319	11487.86	.2074985	5.3556916E-02	-1.280072	3298638	406.3067
25	1127.807	5.542200	8260.226	.2048242	5.2356495E-02	-.9024773	3298272	290.2101
26	1127.254	5.100305	5850.646	.2027333	5.1061794E-02	-.6380566	3298743	207.5101
27	1126.850	4.699219	4181.332	.2005444	4.9811669E-02	-.4539179	3299373	149.3795
28	1126.552	4.361355	3066.279	.2007354	4.8605618E-02	-.3303965	3300056	108.7373
29	1126.509	4.071613	0.	.2018218	4.7245602E-02	-.2377470	3290910	79.43853
30	1126.509	3.822800	0.	.2104778	4.6541130E-02	-.1843204	3283020	59.14640
31	1126.509	3.636276	0.	.2217204	4.5056505E-02	-.1472235	3277498	44.91962
32	1126.509	3.588744	0.	.2346769	4.2965894E-02	-.1212035	3273606	34.98669
33	1126.509	3.554038	0.	.2419172	3.9045569E-02	-.1008784	3270878	28.28783
34	1126.509	3.524029	0.	.2469170	2.8577194E-02	-8.6777199E-02	3269073	23.90871
35	1126.509	3.502136	0.	.2439769	2.3337683E-02	-7.6224104E-02	3267943	21.28063
36	1126.509	3.483659	0.	.2407743	2.1505751E-02	-7.0908427E-02	3267106	20.06780
37	1126.509	3.483659	0.	.2407743	2.1505751E-02	-7.0908427E-02	3267106	20.06780
38	1126.509	3.483659	0.	.2407743	2.1505751E-02	-7.0908427E-02	3267106	20.06780
39	1126.509	3.479571	0.	.2398857	2.1332175E-02	-7.0191782E-02	3266799	19.93909
40	1126.509	3.479571	0.	.2398857	2.1332175E-02	-7.0191782E-02	3266799	19.93909
41	1126.509	3.479571	0.	.2398857	2.1332175E-02	-7.0191782E-02	3266799	19.93909
42	1126.509	3.479571	0.	.2398857	2.1332175E-02	-7.0191782E-02	3266799	19.93909
43	1126.509	3.479571	0.	.2398857	2.1332175E-02	-7.0191782E-02	3266799	19.93909

ORIGINAL PAGE IS OF POOR QUALITY

.TABLE V(j) Run 10

ATOP III ATMOSPHERIC TRAJECTORY OPTIMIZATION PROGRAM VERSION 3,00 15 MAY 1972

CASE F4MA07 STAGE 1 CYCLE 15 PASS 2 PAGE 167

ZOOM TO GIVEN Q, CORRECTED DATA

	TIME	VG77F	HGC7F	GAM7D	VI77F	RG77N	AMACH	AMASF1
1	0.	2030,000	50000,00	0.	3559,625	0.	2,096903	17058,79
2	4,000000	2032,423	49963,01	-,5395062	3562,007	1,333838	2,099447	17701,63
3	8,000000	2036,292	49841,76	-1,185358	3565,719	2,669692	2,103403	17818,90
4	12,00000	2041,807	49620,90	-1,934872	3570,906	4,008206	2,109140	18028,33
5	16,00000	2049,153	49265,35	-2,781103	3577,695	5,350428	2,116728	18345,66
6	20,00000	2058,442	48821,43	-3,703416	3586,148	6,697003	2,126323	18784,32
7	24,00000	2069,718	48218,08	-4,688914	3596,268	8,048899	2,137971	19355,53
8	28,00000	2082,919	47465,47	-5,710224	3607,981	9,406922	2,151606	20069,61
9	32,00000	2097,709	46559,86	-6,720641	3621,001	10,77180	2,166685	20930,98
10	36,00000	2113,667	45502,71	-7,690513	3634,974	12,14393	2,183369	21939,24
11	40,00000	2130,377	44300,31	-8,577669	3649,615	13,52380	2,200630	23259,61
12	44,00000	2147,688	42967,59	-9,311132	3665,014	14,91189	2,218513	24607,11
13	48,00000	2164,433	41532,99	-9,783238	3680,387	16,30868	2,235810	26469,43
14	52,00000	2179,076	40047,78	-9,808577	3694,819	17,71475	2,250936	28188,21
15	56,00000	2190,279	38596,07	-9,196227	3707,474	19,13058	2,262499	30252,25
16	60,00000	2195,295 —	37308,50	-7,409584	3716,462	20,55631	2,267649	32100,04
17	64,00000	2189,557	36433,82	-3,659462	3716,357	21,99036	2,261762	33365,69
18	68,00000	2169,018	36295,28	2,142347	3697,017	23,42262	2,240546	33588,45
19	72,00000	2128,999	37178,74	10,07728	3643,937	24,82748	2,199207	32359,37
20	76,00000	2067,892	39305,37	19,36824	3546,540	26,16076	2,136085	29155,93
21	80,00000	1992,072	42594,05	28,31419	3416,093	27,37940	2,057765	24819,86
22	84,00000	1908,534	46739,27	35,63672	3275,065	28,46398	1,971472	20093,35
23	88,00000	1821,756	51375,39	40,91959	3101,722	29,42336	1,881832	15765,19
24	92,00000	1733,063	56179,24	44,27351	3023,572	30,28061	1,790214	12142,86
25	96,00000	1642,529	60994,71	46,01371	2920,902	31,06063	1,696635	9258,980
26	100,00000	1550,945	65614,05	46,43810	2832,115	31,78438	1,602091	6805,045
27	104,0000	1459,763	69959,56	45,78496	2755,414	32,46807	1,507902	4975,549
28	108,0000	1370,455	73967,05	44,22119	2689,107	33,12346	1,415640	3705,196
29	112,0000	1276,954	77584,73	41,78080	2625,537	33,75765	1,319064	0,
30	116,0000	1188,784	80768,65	38,54088	2570,713	34,37443	1,227986	0,
31	120,0000	1108,522	83507,50	34,53490	2524,710	34,97847	1,142300	0,
32	124,0000	1037,487	85794,20	29,74312	2486,890	35,57292	1,064045	0,
33	128,0000	977,3683	87623,46	24,14174	2456,989	36,16035	,9986256	0,
34	132,0000	930,1573	88990,94	17,77008	2434,853	36,74295	,9477383	0,
35	136,0000	897,7125	89893,52	10,73925	2420,311	37,32224	,9130043	0,
36	140,0000	881,3253	90328,44	3,259852	2412,986	37,89960	,8955485	0,
37	140,0000	881,3253	90328,44	3,259852	2412,986	37,89960	,8955485	0,
38	140,0000	881,3253	90328,44	3,259852	2412,986	37,89960	,8955485	0,
39	141,7081	879,4378	90371,24	4,0233135E-06	2412,007	38,14579	,8935531	0,
40	141,7081	879,4378	90371,24	4,0233135E-06	2412,007	38,14579	,8935531	0,
41	141,7081	879,4378	90371,24	4,0233135E-06	2412,007	38,14579	,8935531	0,
42	141,7081	879,4378	90371,24	4,0233135E-06	2412,007	38,14579	,8935531	0,
43	141,7081	879,4378	90371,24	0,	2412,007	38,14579	,8935531	0,

ORIGINAL PAGE IS OF POOR QUALITY

ATOP III ATMOSPHERIC TRAJECTORY OPTIMIZATION PROGRAM VERSION 3.00 15 MAY 1972

CASE F4HA07 STAGE 1 CYCLE 15 PASS 2 PAGE 169

ZOOM TO GIVEN Q, CORRECTED DATA

TIME	VG77F	HGC7F	GAM7D	VI77F	RG77N	AMACH	AMASF1
0.	2105.000	50000.00	0.	3634.625	0.	2.096943	17658.79
4.000000	2110.433	49888.51	-1.513895	3639.741	1.383819	2.101720	17773.90
8.000000	2119.132	49554.46	-3.005950	3647.502	2.771427	2.108205	18087.51
12.00000	2130.982	49002.04	-4.429686	3657.874	4.163952	2.116316	18603.59
16.00000	2145.733	48241.78	-5.751591	3670.731	5.562685	2.125876	19313.49
20.00000	2162.987	47288.06	-6.923581	3685.875	6.968834	2.136583	20204.96
24.00000	2182.137	46164.35	-7.904371	3702.930	8.383850	2.147978	21257.05
28.00000	2202.474	44897.61	-8.663000	3721.416	9.808782	2.159509	22470.92
32.00000	2223.583	43525.06	-9.118949	3741.267	11.24492	2.170980	24100.78
36.00000	2244.565	42098.53	-9.176352	3761.956	12.69387	2.181782	25600.45
40.00000	2264.028	40683.57	-8.815931	3782.177	14.15678	2.190927	27476.90
44.00000	2280.543	39348.20	-7.984036	3800.509	15.63378	2.202409	29235.64
48.00000	2291.900	38187.39	-6.433037	3814.886	17.12426	2.213577	30691.49
52.00000	2295.523	37348.95	-3.890354	3822.110	18.62561	2.216657	32097.94
56.00000	2288.395	37016.52	-9.6720455E-03	3817.074	20.13116	2.208914	32585.01
60.00000	2266.728	37413.10	5.180488	3771.704	21.62679	2.187209	31993.25
64.00000	2229.370	38687.36	11.24027	3740.336	23.08912	2.150713	30076.19
68.00000	2174.830	40887.42	17.76006	3660.754	24.49019	2.106019	27053.19
72.00000	2102.443	43974.23	24.64467	3550.079	25.80073	2.059584	23227.38
76.00000	2019.272	47824.00	30.82498	3423.592	26.99721	2.005438	19267.76
80.00000	1931.758	52166.06	35.73390	3296.904	28.08114	1.946518	15592.82
84.00000	1840.014	56786.56	39.67372	3171.903	29.05979	1.881597	12364.77
88.00000	1747.568	61506.89	42.41149	3057.097	29.94655	1.805219	9726.029
92.00000	1655.137	66166.00	43.79247	2956.473	30.76035	1.709718	7549.808
96.00000	1563.572	70634.41	43.94660	2869.923	31.52045	1.615134	5300.713
100.00000	1474.163	74822.31	43.04694	2796.089	32.24211	1.522776	3938.516
104.0000	1380.120	78657.09	41.15860	2726.542	32.93579	1.425632	0.
108.0000	1291.216	82080.62	38.43184	2667.064	33.60763	1.333797	0.
112.0000	1209.853	85072.34	34.93068	2617.413	34.26407	1.242675	0.
116.0000	1136.932	87619.32	30.69607	2576.225	34.90947	1.161069	0.
120.0000	1073.788	89713.12	25.73479	2542.913	35.54672	1.092479	0.
124.0000	1021.963	91347.52	20.07444	2517.078	36.17825	1.036320	0.
128.0000	983.0703	92518.20	13.79705	2498.455	36.80559	.9945369	0.
132.0000	958.5966	93222.40	7.046352	2486.917	37.43010	.9684126	0.
136.0000	949.5333	93458.63	3.0133277E-02	2482.327	38.05293	.9568015	0.
136.0000	949.5333	93458.63	3.0133277E-02	2482.327	38.05293	.9568015	0.
136.0000	949.5333	93458.63	3.0133277E-02	2482.327	38.05293	.9568015	0.

TABLE V(k) Run 11

136.0171	949.5282	93458.63	0.	2482.323	38.05559	.9567964	0.

ZOOM TO GIVEN Q, CORRECTED DATA

TIME	VG77F	HGC7F	GAM7D	VI77F	RG77N	AMACH	AMASF1
0.	2105.000	50000.00	0.	3634.625	0.	2.096943	17658.79
4.000000	2110.433	49888.51	-1.513895	3639.741	1.383819	2.101720	17773.90
8.000000	2119.132	49554.46	-3.005950	3647.502	2.771427	2.108205	18087.51
12.00000	2130.982	49002.04	-4.429686	3657.874	4.163952	2.116316	18603.59
16.00000	2145.733	48241.78	-5.751591	3670.731	5.562685	2.125876	19313.49
20.00000	2162.987	47288.06	-6.923581	3685.875	6.968834	2.136583	20204.96
24.00000	2182.137	46164.35	-7.904371	3702.930	8.383850	2.147978	21257.05
28.00000	2202.474	44897.61	-8.663000	3721.416	9.808782	2.159509	22470.92
32.00000	2223.583	43525.06	-9.118949	3741.267	11.24492	2.170980	24104.78
36.00000	2244.565	42098.53	-9.176352	3761.956	12.69387	2.181782	25600.45
40.00000	2264.028	40683.57	-8.815931	3782.177	14.15678	2.190927	27476.90
44.00000	2280.543	39348.20	-7.984036	3800.509	15.63378	2.202409	29235.64
48.00000	2291.900	38187.39	-6.433037	3814.886	17.12426	2.213577	30691.49
52.00000	2295.523	37348.95	-3.890354	3822.110	18.62561	2.216657	32097.94
56.00000	2288.395	37016.52	-9.6720455E-03	3817.074	20.13116	2.208914	32585.01
60.00000	2266.728	37413.10	5.180488	3771.704	21.62679	2.187209	31993.25
64.00000	2228.970	38687.36	11.24027	3740.336	23.08912	2.150713	30076.19
68.00000	2174.830	40887.42	17.76006	3660.754	24.49019	2.106019	27053.19
72.00000	2102.443	43974.23	24.64467	3550.079	25.80073	2.059584	23227.38
76.00000	2019.272	47824.00	30.82498	3423.592	26.99721	2.005438	19267.76
80.00000	1931.759	52166.06	35.73390	3296.904	28.08114	1.946518	15592.82
84.00000	1840.014	56786.56	39.67372	3171.903	29.05979	1.881597	12364.77
88.00000	1747.568	61506.89	42.41149	3057.097	29.94655	1.805219	9726.029
92.00000	1655.137	66166.00	43.79247	2956.473	30.76035	1.709718	7549.808
96.00000	1563.572	70634.41	43.94060	2869.923	31.52045	1.615134	5360.713
100.0000	1474.163	74822.31	43.04694	2796.089	32.24211	1.522776	3938.516
104.0000	1380.120	78657.09	41.15860	2726.542	32.93579	1.425632	0.
108.0000	1291.216	82080.62	38.43184	2667.064	33.60763	1.333797	0.
112.0000	1209.853	85072.34	34.93068	2617.413	34.26407	1.242675	0.
116.0000	1136.932	87619.32	30.69607	2576.225	34.90947	1.161069	0.
120.0000	1073.788	89713.12	25.73479	2542.913	35.54672	1.092479	0.
124.0000	1021.963	91347.52	20.07444	2517.078	36.17825	1.036320	0.
128.0000	983.0703	92518.20	13.79705	2498.455	36.80559	.9945369	0.
132.0000	958.5986	93222.40	7.046352	2486.917	37.43010	.9684126	0.
136.0000	949.5333	93458.63	3.0133277E-02	2482.327	38.05293	.9568015	0.
136.0000	949.5333	93458.63	3.0133277E-02	2482.327	38.05293	.9568015	0.
136.0000	949.5333	93458.63	3.0133277E-02	2482.327	38.05293	.9568015	0.

TABLE V(k) Run 11

136.0171	949.5282	93458.63	0.	2482.323	38.05559	.9567964	0.

ZOOM TO GIVEN Q, CORRECTED DATA

	AMASS	ALPHD	TE77P	CL	CD	ANZB7G	ESPEF	DYNPP
1	1166.000	1.793388	16914.41	4.6712645E-02	3.9546321E-02	-.5411262	3815131	749.8288
2	1164.777	1.778724	17020.20	4.6223133E-02	3.9533560E-02	-.5416030	3823032	757.2767
3	1163.540	1.760137	17324.41	4.5801902E-02	3.9519171E-02	-.5494536	3830795	774.2306
4	1162.274	1.780677	17830.32	4.6266340E-02	3.9528931E-02	-.5743307	3838383	801.0917
5	1160.966	1.776746	18527.65	4.6125032E-02	3.9521151E-02	-.5997019	3845712	836.2872
6	1159.602	1.820222	19402.61	4.7513762E-02	3.9555752E-02	-.6522684	3852504	886.2848
7	1158.171	1.834601	20433.24	4.7951558E-02	3.9563453E-02	-.7020173	3858309	945.2451
8	1156.662	1.880515	21619.20	4.9389916E-02	3.9599114E-02	-.7754966	3862526	1015.129
9	1155.054	1.968234	23204.50	5.1620211E-02	3.9712483E-02	-.8766961	3865490	1095.601
10	1153.331	2.076628	24850.16	5.5553654E-02	3.9916266E-02	-1.013531	3866682	1184.727
11	1151.491	2.139179	26482.10	5.7508566E-02	4.0022746E-02	-1.131313	3865633	1278.469
12	1149.535	2.285467	28156.69	6.2117728E-02	4.0281002E-02	-1.313006	3860560	1377.159
13	1147.457	2.547779	29698.76	7.0405256E-02	4.0756272E-02	-1.582704	3849549	1470.517
14	1145.278	2.942287	30852.79	8.2952184E-02	4.1461980E-02	-1.930291	3831030	1535.174
15	1143.040	3.560870	31381.45	.1027989	4.2695401E-02	-2.412725	3804091	1548.932
16	1140.802	4.106357	30939.92	.1205982	4.4088072E-02	-2.719178	3767399	1496.070
17	1138.651	4.701850	29246.71	.1403942	4.6450818E-02	-2.877646	3723190	1355.468
18	1136.676	5.356706	26439.69	.1630299	4.9282758E-02	-2.883272	3674160	1169.770
19	1134.933	6.375951	22743.68	.1982961	5.4182041E-02	-2.890913	3617793	965.0743
20	1133.469	6.332866	18822.25	.1997036	5.3978027E-02	-2.299460	3569050	761.0550
21	1132.273	6.795673	15096.06	.2223114	5.8056918E-02	-1.959752	3534415	582.5225
22	1131.314	7.120465	11658.90	.2424899	6.1269056E-02	-1.601054	3508387	430.4193
23	1130.553	7.013427	8746.943	.2491242	6.1453274E-02	-1.207839	3492627	320.5798
24	1129.964	6.680838	6261.876	.2489777	5.9958072E-02	-.8659705	3483288	230.1769
25	1129.528	6.186472	4487.974	.2469790	5.8099592E-02	-.6165522	3477702	165.9472
26	1129.209	5.594177	3267.844	.2384164	5.5320115E-02	-.4342619	3474660	120.7855
27	1129.163	5.066835	0.	.2332415	5.2889834E-02	-.3048329	3461931	86.16519
28	1129.163	4.638154	0.	.2290400	5.0637487E-02	-.2222127	3451560	65.54617
29	1129.163	4.288877	0.	.2328020	4.9167798E-02	-.1696480	3444460	49.36862
30	1129.163	3.985212	0.	.2374735	4.7237464E-02	-.1341523	3439429	38.28027
31	1129.163	3.754081	0.	.2408437	4.5063299E-02	-.1090439	3435609	30.72455
32	1129.163	3.667286	0.	.2435703	4.1998090E-02	-9.1931944E-02	3433140	25.64160
33	1129.163	3.598426	0.	.2452880	3.6575058E-02	-8.0726982E-02	3431127	22.38265
34	1129.163	3.546799	0.	.2458034	3.3495112E-02	-7.4175100E-02	3429608	20.55115
35	1129.163	3.499413	0.	.2442015	3.0927663E-02	-7.1417214E-02	3428419	19.92969
36	1129.163	3.499413	0.	.2442015	3.0927663E-02	-7.1417214E-02	3428419	19.92969
37	1129.163	3.499413	0.	.2442015	3.0927663E-02	-7.1417214E-02	3428419	19.92969
38	1129.163	3.499228	0.	.2441906	3.0925405E-02	-7.1413216E-02	3428414	19.92947

CASE F4HA07 STAGE 1 CYCLE 15 PASS 2 PAGE 171

ZOOM TO GIVEN Q, CORRECTED DATA

TIME	VG77F	HGC7F	GAM7D	VI77F	RG77N	AMACH	AMASF1
0.	2030.000	50000.00	0.	3559.625	0.	2.096943	17058.79
4.000000	2034.163	49951.64	-.7028796	3563.719	1.334403	2.101244	17715.76
8.000000	2040.061	49794.59	-1.523548	3569.362	2.671869	2.107336	17667.44
12.00000	2047.834	49513.28	-2.430539	3576.636	4.013365	2.115300	18135.62
16.00000	2057.540	49095.97	-3.408727	3585.547	5.359618	2.125391	18531.89
20.00000	2069.149	48531.30	-4.442974	3596.015	6.711514	2.137374	19067.63
24.00000	2082.536	47811.76	-5.502018	3607.936	8.069698	2.151211	19750.93
28.00000	2097.490	46933.64	-6.549764	3621.115	9.434814	2.166659	20586.42
32.00000	2113.513	45901.23	-7.509018	3635.222	10.80735	2.183210	21570.94
36.00000	2129.862	44732.00	-8.292351	3649.785	12.18778	2.200098	22754.03
40.00000	2146.082	43457.01	-8.778064	3664.708	13.57660	2.216853	24235.68
44.00000	2160.958	42127.42	-8.871375	3679.281	14.97452	2.232220	25776.07
48.00000	2172.652	40823.79	-8.300561	3692.196	16.38220	2.244300	27289.44
52.00000	2178.949	39660.66	-6.913264	3701.282	17.79932	2.250804	28732.57
56.00000	2177.821	38790.79	-4.271361	3704.133	19.22393	2.249639	29986.08
60.00000	2165.627	38460.63	.2731763	3694.401	20.65023	2.237043	30475.22
64.00000	2140.323	38941.05	6.248363	3663.840	22.06283	2.210905	29812.39
68.00000	2099.638	40307.64	13.41249	3604.351	23.43600	2.168878	27600.66
72.00000	2044.133	42832.86	21.18350	3513.630	24.73518	2.111543	24785.28
76.00000	1975.770	46213.30	28.51502	3398.936	25.93294	2.040925	20560.52
80.00000	1898.480	50290.85	34.81065	3273.021	27.01446	1.961086	16957.83
84.00000	1816.155	54792.18	39.53052	3150.482	27.98457	1.876040	13417.68
88.00000	1730.792	59461.77	42.55852	3037.644	28.86108	1.787866	10503.92
92.00000	1643.097	64101.08	44.08992	2942.019	29.66521	1.697281	8020.534
96.00000	1554.268	68569.86	44.39358	2856.618	30.41564	1.605523	5912.044
100.00000	1466.018	72774.37	43.66989	2782.381	31.12690	1.514363	4369.797
104.0000	1378.057	76650.86	42.03585	2716.602	31.81018	1.423502	0.
108.0000	1286.094	80134.78	39.51875	2653.301	32.47057	1.328506	0.
112.0000	1201.544	83192.56	36.22315	2600.179	33.11331	1.238971	0.
116.0000	1125.212	85812.00	32.18513	2555.809	33.74298	1.153973	0.
120.0000	1058.397	87985.06	27.38997	2519.636	34.36298	1.080617	0.
124.0000	1002.656	89705.41	21.84537	2491.273	34.97589	1.020125	0.
128.0000	959.7002	90968.63	15.61995	2470.422	35.58364	.9739268	0.
132.0000	931.2488	91771.96	8.844555	2457.022	36.18800	.9435247	0.
136.0000	918.3514	92113.55	1.720374	2450.789	36.79035	.9298182	0.
136.0000	918.3514	92113.55	1.720374	2450.789	36.79035	.9298182	0.
136.0000	918.3514	92113.55	1.720374	2450.789	36.79035	.9298182	0.

TABLE V(ℓ) Run 12

136.9532	917.6340	92126.69	4.0233135E-06	2450.331	36.93368	.9290674	0.
136.9532	917.6340	92126.69	4.0233135E-06	2450.331	36.93368	.9290674	0.
136.9532	917.6340	92126.69	4.0233135E-06	2450.331	36.93368	.9290674	0.
136.9532	917.6340	92126.69	4.0233135E-06	2450.331	36.93368	.9290674	0.
136.9532	917.6340	92126.69	0.	2450.331	36.93368	.9290674	0.

ZOOM TO GIVEN Q, CORRECTED DATA

AMASS	ALPHD	TE77P	CL	CD	ANZB7G	ESPEF	DYNPP
1000.000	2.197682	16914.41	5.9993900E-02	4.0177837E-02	-.7984830	3660069	749.8288
998.7789	2.098515	16961.68	5.6719230E-02	4.0002508E-02	-.7628319	3666989	754.6515
997.5506	2.001089	17100.70	5.3498919E-02	3.9826521E-02	-.7322593	3674002	764.7571
996.3080	1.919376	17353.21	5.0792778E-02	3.9676907E-02	-.7128308	3680933	781.0359
995.0425	1.817265	17729.72	4.7441038E-02	3.9558192E-02	-.6891576	3687567	804.3547
993.7448	1.731049	18240.30	4.4634694E-02	3.9474822E-02	-.6768614	3693519	835.7237
992.4051	1.644957	18891.36	4.1867356E-02	3.9391801E-02	-.6689838	3698408	876.2300
991.0130	1.580909	19685.82	3.9843041E-02	3.9328941E-02	-.6761773	3701690	927.0003
989.5579	1.561939	20619.52	3.9275025E-02	3.9306417E-02	-.7119245	3702531	988.6812
988.0294	1.570308	21739.98	3.9572330E-02	3.9308103E-02	-.7701891	3699957	1062.032
986.4072	1.627817	23130.41	4.1386944E-02	3.9372785E-02	-.8672490	3693994	1146.117
984.6801	1.754385	24573.67	4.5292016E-02	3.9497362E-02	-1.020448	3683637	1238.422
982.8469	1.969011	25991.90	5.1832393E-02	3.9746914E-02	-1.248298	3667403	1332.479
980.9130	2.204587	27301.49	5.9214822E-02	4.0166834E-02	-1.509036	3644001	1416.965
978.8820	2.730367	28581.23	7.5851643E-02	4.1097331E-02	-1.997400	3613789	1475.703
976.7884	3.478832	29137.83	9.9726564E-02	4.2421731E-02	-2.621743	3576772	1482.478
974.6991	3.831879	28664.77	.1114158	4.3580293E-02	-2.796057	3537623	1415.165
972.7023	4.780331	26903.14	.1423417	4.6673826E-02	-3.202855	3496684	1271.902
970.8794	5.207797	24135.88	.1579818	4.8545309E-02	-2.997224	3460502	1071.345
969.3045	5.840421	20371.34	.1817202	5.1607212E-02	-2.740016	3430641	851.3772
967.9974	6.057445	16536.36	.1953581	5.2981796E-02	-2.239025	3410992	646.7553
966.9476	5.930660	12823.30	.2004900	5.2997217E-02	-1.696414	3401340	477.2499
966.1217	5.700379	9630.428	.2013714	5.2412024E-02	-1.238344	3398420	340.7291
965.4820	5.437694	6954.758	.2004277	5.1625582E-02	-.8897722	3397875	250.3561
965.0042	5.082528	5006.178	.2013840	5.0887231E-02	-.6455305	3397707	180.9649
964.6527	4.715315	3647.208	.2002331	4.9830581E-02	-.4667843	3397782	131.7193
964.4297	4.377142	0.	.2001712	4.8641418E-02	-.3358943	3395544	96.73097
964.4297	4.090015	0.	.2012948	4.7334135E-02	-.2488082	3383370	71.35059
964.4297	3.869819	0.	.2102208	4.6723556E-02	-.1950559	3374970	53.64061
964.4297	3.671184	0.	.2208392	4.5355487E-02	-.1568127	3369031	41.11605
964.4297	3.522965	0.	.2282050	4.3294563E-02	-.1281940	3364780	32.57021
964.4297	3.507515	0.	.2359187	4.0220423E-02	-.1089139	3361714	26.79910
964.4297	3.495758	0.	.2418039	3.4519643E-02	-9.5829051E-02	3359479	23.04472
964.4297	3.486054	0.	.2443219	2.7646412E-02	-8.7427818E-02	3357956	20.84529
964.4297	3.476809	0.	.2430886	2.5299038E-02	-8.3119877E-02	3356818	19.92979
964.4297	3.476809	0.	.2430886	2.5299038E-02	-8.3119877E-02	3356818	19.92979
964.4297	3.476809	0.	.2430886	2.5299038E-02	-8.3119877E-02	3356818	19.92979
964.4297	3.474622	0.	.2429114	2.5161713E-02	-8.2872755E-02	3356575	19.88565
964.4297	3.474622	0.	.2429114	2.5161713E-02	-8.2872755E-02	3356575	19.88565
964.4297	3.474622	0.	.2429114	2.5161713E-02	-8.2872755E-02	3356575	19.88565
964.4297	3.474622	0.	.2429114	2.5161713E-02	-8.2872755E-02	3356575	19.88565
964.4297	3.474622	0.	.2429114	2.5161713E-02	-8.2872755E-02	3356575	19.88565

REFERENCES

1. Hague, D. S. : Three-Degree-of-Freedom Problem Optimization Formulation - Analytical Development. Part I, vol. 3, FDL-TDR-64-1, McDonnell-Douglas Corporation, October 1964.

2. Mobley, R. L. and Vorwald, R. R.: Three-Degree-of-Freedom Optimization Formulation - User's Manual, Part II, vol. 3, FDL-TDR-64-1, McDonnell-Douglas Corporation, October 1964.

3. Brown, Robert C.; Brulle, R. V.; Combs, A. E.; and Griffin, G.D.: Six-Degree-of-Freedom Flight Path Study Generalized Computer Program. Part I, vol. 1, FDL-TDR-64-1, McDonnell-Douglas Corporation, October 1964.

4. Seubert, F. W. and Usher, Newell E.: Six-Degree-of-Freedom Flight Path Study Generalized Computer Program - User's Manual. Part II, WADD Technical Report 60-781, McDonnell-Douglas Corporation, May 1961.

5. Landgraf, S. K.: Some Practical Applications of Performance Optimization Techniques to High-Performance Aircraft. AIAA Paper 64-288, July 1964.

6. Hague, D. S.: An Outline and Operating Instructions for the Steepest-Descent Trajectory Optimization Program - STOP. Aerodynamics Methods Note 1, McDonnell-Douglas Corporation, March 11, 1963.

7. Hague, D. S.; Geib, Ken; Ballew, L.; and Witherspoon, J.: Two Vehicle Optimization - Theoretical Outline and Program User's Manual. Report B983, McDonnell-Douglas Corporation 1965.

8. Hague, D. S.: The Optimization of Multiple-Arc Trajectories by the Steepest-Descent Method. Recent Advances in Optimization Techniques. Lavi and Vogl, ed., John Wiley, 1966, pp. 489-517.

9. Hague, D. S. and Glatt, C. R.: Study of Navigation and Guidance of Launch Vehicles Having Cruise Capability. vol. 2, Boeing Document D2-113016-5, The Boeing Company, April 1967.

10. Retka, J.; Harder, D.; Hague, D. S.; Glatt, C. R.; Seavoy, T.; and Minden, D.: Study of Navigation and Guidance of Launch Vehicles Having Cruise Capability. vol. 4, Boeing Document D2-113016-7, April 1967.

11. Stein, H.; Mathews, M. L.; and Frenck, J. W.: STOP - A Computer Program for Supersonic Transport Trajectory Optimization. NASA CR-793, May 1967.

12. Petersen, L. D.: Trajectory Optimization by the Method of Steepest Descent. vol. 1, AFFDL-TR-67-108, April 1968.

13. Moulton, Forest R.: Methods of Exterior Ballistics. Dover, New York.

14. Goldstein, H.: Classical Mechanics, Edison Wesley, 1950.

15. Minzner, R. A. and Ripley, W. S.: The ARDC Model Atmosphere. AFCRC-TN-56-204, United States Air Force, Cambridge Research Center, December 1956.

16. Champion, K. S. W.; Minzner, R. A.; and Pond, H. T.: The ARDC Model Atmosphere, 1959. AFCRC-TR-59-267, United States Air Force, Cambridge Research Center, August 1959.

17. Anon.: U. S. Standard Atmosphere, 1962. U. S. Government Printing Office, 1962.

18. Heiskanen, W. and Meinesz, Vening: The Earth and Its Gravity Field. McGraw-Hill Book Company, 1958.

19. Jeffreys, H: The Earth. Fourth ed., Cambridge University Press, 1959.

20. O'Keefe, J. A.; Eckels, A; and Squires, R. K.: Vanguard Measurements Give Pear Shaped Component of Earth's Figure. Science, vol. 129, p 565.

21. Cahill, R.; and Body, W.: F4H-1 Airplane Time-to-Climb Records Documentation Report. McDonnell Report 8847, June 1962.

22. ———.: Group Weight Statement, F4H-1 Aircraft, June 1960.

23. ———.: Verbal Communication from Edwards AFB to Mr. William Page of NASA Ames Research Center, 1975.

24. Hague, D. S.; Jones, R. T.; and Glatt, C. R.: Combat Optimization and Analysis Program--COAP, AFFDL-TR-71-52, May 1971.

25. Hague, D. S.; Glatt, C. R.; and Jones, R. T.: Integration of Aerospace Vehicle Performance and Design Optimization. AIAA Paper No. 72-948, 1972.

26. Johnson, David T.: Evaluation of Energy Maneuverability Procedures in Aircraft Flight Path Optimization and Performance Estimation. AFFDL-TR-72-58, Wright-Patterson AFB, Ohio November 1972.

27. Rutowski, E. R.: "Energy Approach to the General Aircraft Performance Problem," Journal of Aeronautical Sciences. March 1954.

28. Lush, K. J.: A Review of the Problem of Choosing a Climb Technique for High Performance Aircraft, British Aeronautical Research Council Report No. 2557, 1951.

29. Smith, Major, R. J., "The Day the Eagle Streaked," Air Force Magazine, July 1975, p. 33.

30. Freeburg, D. H., McDonnell Douglas Company, letter to A. P. Margozzi, NASA Ames Research Center, "J79-GE-15 Engine Performance for NASA Study of F4-C Zoom Climb Maneuver", 18 June 1975.

APPENDIX A

PAST COMPARISONS BETWEEN PREDICTED OPTIMAL PATHS AND ACTUAL FLIGHTS PATHS FLOWS

The success of the variational steepest-descent method in solution of aircraft performance optimization problems is evident from the strong support given to this technique by a series of contracts let by leading Government research centers concerned with this area. The reason for this support is clear when performance gains obtained are examined. Figure 1 presents the 1962 time-to-climb record flights of the McDonnell F-4B aircraft. Figure 2 illustrates how closely these paths follow the minimum time ascent paths predicted by the References 1 and 2 program. Figure 3 provides a comparison between flight handbook performance estimates, a minimum time climb obtained by the References 7 and 8 program, and an attempt by Marine Col. Yunck to fly the predicted optimum.

The predicted optimal path and the path flown by Col. Yunck both produce a 23 percent improvement in aircraft performance over the flight handbook. During the Cuban crisis of the early sixties, results of this type were produced routinely from the References 1 and 2 program to aid in Air Force readiness studies. It should be noted that unlike optimization studies in other technology fields, these performance gains are obtained without vehicle modification. To obtain these performance gains while retaining flight handbook methods would have required a 23 per cent increase in aircraft design capability, several years' effort and several billion dollars to replace an existing fleet of aircraft which could achieve this capability simply by being flown in the optimum manner. This one example serves as a lasting example of:

1) The high cost associated with an oversimplified approach to performance optimization; and

2) The insignificant computational cost of adequate performance optimization studies for production aircraft when compared to the resulting payoff.

Further details of these F-4B performance optimization studies may be obtained from Reference 5.

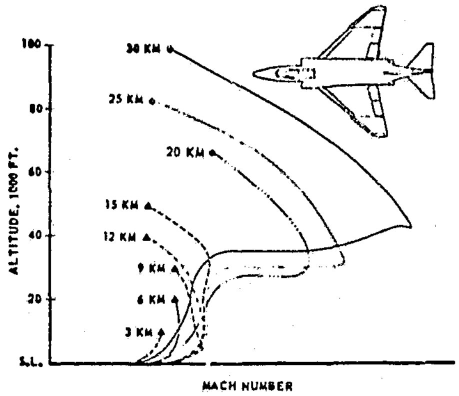

FIGURE 1. F-4B TIME-TO-CLIMB RECORD FLIGHTS

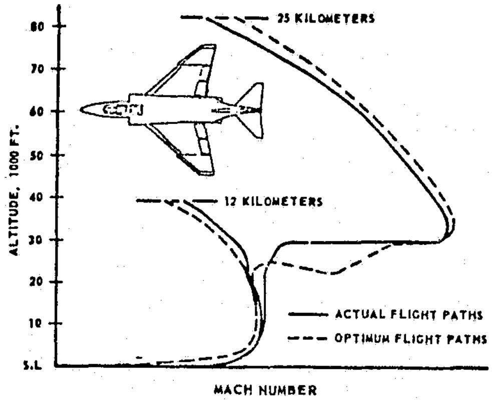

FIGURE 2. COMPARISON OF ACTUAL AND CALCULATED OPTIMUM FLIGHT PATHS FOR TWO F-4B TIME-TO-CLIMB RECORD FLIGHTS

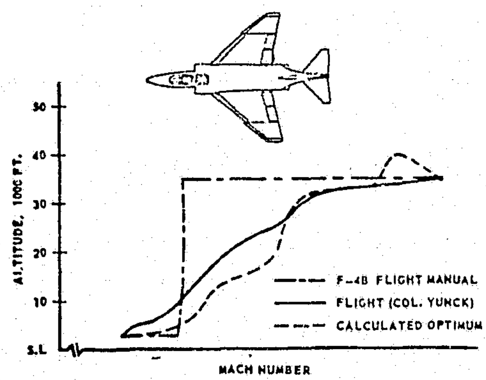

FIGURE 3. FLIGHT PATH COMPARISON